Journal of the OPTICAL SOCIETY *of* AMERICA

VOLUME 38
No. 10

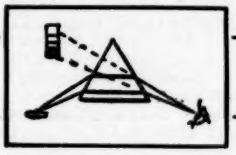

OCTOBER
1948

Comparative Survey of Some Possible Systems of Polorized Headlights . . . . . B. H. BILLINGS AND E. H. LAND 819

Physics Abstracts 829

Effect of Spectral Quality of Light on Visual Performance and Fatigue . . . . . ERNST SIMONSON AND JOSEF BROSEK 830

Erratum: Some Considerations of the Effect of Radiation on the Performance of Liquid Fuel Rockets . . . . . S. S. PENNER AND S. WEINBAUM 840

Effect of High Index Glasses on the Field Characteristics of Photographic Objectives . . . . . G. H. AKLIN 841

Infra-Red Sensitivity of Superconducting Bolometers . . . . . NELSON FUSON 845

In Defense of Beer's Law . . . . . ARTHUR C. HARDY AND F. MANSFIELD YOUNG 854

Syntheses of Spectral-Distribution Curves . . . . . W. L. BREWER AND F. R. HOLLY, JR. 858

Book Review 874

Recording Photometer and Its Use in Studies of Cathode-Ray Screen Displays . . . . . FERDINAND HAMBURGER, JR. AND ELLWOOD J. KING 875

Measurement of the Velocity of Light by Signals Sent in One Direction . . HERBERT E. IVES 879

Empirical Relationships between the Partial Dispersions of the Ordinary Types of Optical Glasses . . . . . D. H. RANK 885

Visibility of Stars in the Daylight Sky . . . . . R. TOUSEY AND E. O. HULBURT 886

Published monthly
at Prince and Lemon Sts., Lancaster, Pa.
by the
AMERICAN INSTITUTE OF PHYSICS
Incorporated
57 East 55 Street, New York 22, New York
FOR AND UNDER THE EDITORIAL SUPERVISION OF THE
OPTICAL SOCIETY OF AMERICA

THE OPTICAL SOCIETY OF AMERICA

Officers of the Society

RUDOLF KINGSLAKE, *President*
Eastman Kodak Company
Rochester, New York

WILLIAM F. MEGGERS, *Vice President*
National Bureau of Standards
Washington 25, D. C.

ARTHUR C. HARDY, *Secretary*
Massachusetts Institute of Technology
Cambridge 39, Massachusetts

W. W. GRAEPER, *Treasurer*
Bausch & Lomb Optical Company
Rochester 2, New York

The Board of Directors consists of the above officers; the Editor of the Journal; the Past President; and five directors-at-large.

G. R. HARRISON, *Editor and Past President*
Massachusetts Institute of Technology
Cambridge 39, Massachusetts

Directors-at-Large

FRANK BENFORD
General Electric Company
Schenectady, New York

F. M. BISHOP
Eastman Kodak Company
Rochester 4, New York

WALLACE R. BRODE
Ohio State University
Columbus 10, Ohio

A. H. BENNETT
American Optical Company
Buffalo 11, New York

E. H. LAND
Polaroid Corporation
Cambridge, Massachusetts

Local Sections

STANLEY S. BALLARD, *Secretary for the Local Sections*

Rochester Section

JOHN H. MCLEOD, *President*
HARRY D. POLSTER, *Vice President*
JAMES R. BENFORD, *Secretary*
LUVILLE T. STEADMAN, *Treasurer*

Detroit Section

DAVID L. FRY, *Chairman*
KARL W. BEYER, *Vice Chairman*
DANIEL L. HARMON, *Secretary*
W. R. O'NEILL, *Treasurer*

Niagara Frontier Section

GALEN PORTER, *President*
LELAND E. HAVENS, *Secretary*
CLAIR M. BIRDSALL, *Treasurer*

Ohio Valley Section

M. E. MERCHANT, *Chairman*
J. F. WOODRUFF, *Chairman-elect*
C. S. MILLS, *Secretary-Treasurer*

Patrons

AMERICAN OPTICAL COMPANY — BAUSCH & LOMB OPTICAL COMPANY
EASTMAN KODAK COMPANY

Corporation Members

ALLIED CHEMICAL AND DYE CORPORATION, NATIONAL ANILINE DIVISION, Buffalo, New York
AMERICAN CYSTOSCOPE MAKERS, INC., New York, New York
AMERICAN OPTICAL COMPANY, Southbridge, Massachusetts
ARGUS, INCORPORATED, Ann Arbor, Michigan
BAUSCH & LOMB OPTICAL COMPANY, Rochester, New York
BELL & HOWELL COMPANY, Chicago, Illinois
BELL TELEPHONE LABORATORIES, INC., New York, New York
CENTURY LIGHTING, INC., New York, New York
CORNING GLASS WORKS, Corning, New York
R. R. DONNELLEY & SONS COMPANY, Chicago, Illinois
E. I. DUPONT DE NEMOURS & COMPANY, INC., Chemical Department, Experimental Station, Wilmington, Delaware
EASTMAN KODAK COMPANY, Rochester, New York
EDMUND SALVAGE COMPANY, Oaklyn-Audubon, New Jersey
FAIRCHILD AVIATION CORPORATION, Jamaica, New York
FARRAND OPTICAL COMPANY, INC., New York, New York
FISH-SCHURMAN CORPORATION, New York, New York
GAERTNER SCIENTIFIC CORPORATION, Chicago, Illinois
W. & L. E. GURLEY, Troy, New York
INTERCHEMICAL CORPORATION, New York, New York
KEUFFEL & ESSER COMPANY, Hoboken, New Jersey
KOLLSMAN INSTRUMENT DIVISION OF SQUARE D COMPANY, Elmhurst, New York
NATIONAL CARBON COMPANY, Cleveland, Ohio
NATIONAL TECHNICAL LABORATORIES, South Pasadena, California
PERKIN-ELMER CORPORATION, Glenbrook, Connecticut
POLAROID CORPORATION, Cambridge, Massachusetts
PORTMAN MACHINE TOOL COMPANY, New Rochelle, New York
SIMPSON OPTICAL MANUFACTURING COMPANY, Chicago, Illinois
SOCONY-VACUUM LABORATORIES, Paulsboro, New Jersey
ARTHUR H. THOMAS COMPANY, Philadelphia, Pennsylvania
UNIVIS LENS COMPANY, Dayton, Ohio
ZENITH OPTICAL COMPANY, Huntington, West Virginia

THE OPTICAL SOCIETY OF AMERICA was organized in 1916 "*to increase and diffuse the knowledge of optics in all its branches, pure and applied, to promote the mutual interests of investigators of optical problems, of designers, manufacturers and users of optical instruments and apparatus of all kinds and to encourage cooperation among them.*" It aims to serve the interests of all who are engaged in any branch of optics from fundamental research to the manufacture of optical goods.

MEMBERSHIP

Regular Members: "Any person who has contributed materially to the advancement of optics is eligible for regular membership."

Associate Members: "Any person who is interested in optics is eligible for associate membership."

Corporate Members: "Any corporation desirous of encouraging the work of the Society is eligible for corporation membership."

Patrons: The payment, within any one year, of $1000 or more toward the expenses of the Society by any corporation or individual entitles such corporation or individual to the rank of patron.

The Society cordially invites to membership all who are interested in any branch of optics, either in research, in instruction, in optical or illuminating engineering, in the manufacture and distribution of optical goods of all kinds, or in physiological and medical optics.

ANNUAL DUES

Regular members, $8.50; Associate members, $6.00; Corporate members, $50.00. These dues include subscription to the Society's official journal, the *Journal of the Optical Society of America.*

CHANGES OF ADDRESS

All changes of address of members of the Optical Society of America should be communicated to the Secretary, Professor Arthur C. Hardy, Massachusetts Institute of Technology, Cambridge 39, Massachusetts.

Journal of the
OPTICAL SOCIETY
of AMERICA

VOLUME 38, NUMBER 10 OCTOBER, 1948

A Comparative Survey of Some Possible Systems of Polarized Headlights

B. H. BILLINGS* AND E. H. LAND
Research Laboratory, Polaroid Corporation, Cambridge, Massachusetts

(Received May 5, 1948)

In a polarizing headlight system polarizers are placed on automobile headlights and in a viewer before the eyes of automobile drivers. These polarizers are so oriented that the viewer is crossed with the headlights of an approaching car. This blocks most of the light from approaching headlights. A polarizing system has other features which make it different from a non-polarizing system. The amount of the polarized component of the reflected light from an object illuminated by a car's headlights which is transmitted back through the viewer in the same car depends on the type and orientation of the polarizers. Thus objects have different brightness depending on the polarizing system being used. Similarly, the contrast between objects and their background will be different for different polarizing systems. In this paper some basic matrices of an optical calculus are derived. This calculus is then used to show the orientation of the headlights and viewer polarizers for all possible polarizing systems. For each of these systems the relative brightness of a specularly reflecting object is determined. Finally, equations are derived for the contrast of various types of objects with their background and a few special cases are calculated.

INTRODUCTION

THE use of polarizers for avoiding glare in automobile headlight systems has been known for some time. One of the first proposals was made by Short[1] in 1921. His scheme involved vertical and horizontal polarizers. With this system only the depolarized reflected component of the light from a driver's headlight is transmitted through his own analyzer. In the system proposed by Chubb[2] and by Land,[3] the windshield polarizer and headlight polarizers on a given car were parallel and at 45°. Both the depolarized and the polarized components were thus reflected back through the windshield.

This system was modified by Cooke[4] to include 1/4λ-plates in order to make circular polarizers.

There is a brief discussion of elliptical polarizers for headlights in a paper by Christoph and Neugebauer[5] but this was in connection with the use of non-achromatic phase plates for making circular polarizers. Although there have been several papers[6] which have discussed polarization

* Now with Baird Associates, Inc., Cambridge, Massachusetts.

[1] F. Short, U. S. Patent 1,734,022, filed September 26, 1921.

[2] L. W. Chubb, U. S. Patent, 2,087,795, filed July 29, 1920.

[3] E. H. Land, U. S. Patent, 2,031,045, filed January 16, 1933.

[4] A. G. Cooke, British Patent 365,507, filed June 9, 1931.

[5] W. Christoph and H. E. J. Neugebauer, Zeits. f. Physik **20**, 257 (1939).

[6] L. W. Chubb, "Polarized Light for Motor Vehicle Lighting," I. E. S. Trans. **32**, 505 (1937); E. H. Land, "Polaroid and the Headlight Problem," J. Frank. Inst. **224**, 269 (1937); A. Gamble, "La lumière Polarisée son emploi dans les Projecteurs D'Automobiles," Bull. de la Société française des Électriciens **7**, 511 (1937); Henry T. Gibbs, "Polarized Light for Motor Vehicles," J. Frank. Inst. **228**, 719 (1939); Val Roper and K. D. Scott, "Seeing with Polarized Headlamps," I. E. S. Trans. **36**, 1205 (1941); E. H. Land, "Polarized Light in the Transportation Industries," The Michigan-Life Conference on New Technologies in Transportation (University of Michigan Official Publications) **42**, 151 (1940); H. Sauer, "Polarisiertes Licht

systems for night driving, they have invariably been concerned with one of the specific systems described above.

There are, however, an infinite number of polarized headlight systems all of which provide extinction of the approaching headlight. The headlight polarizer can be selected to produce any desired state of polarization. It can give linear polarized light inclined at any angle to the vertical. It can give elliptically polarized light with any desired value for the eccentricity of the ellipse and with the ellipse major axis inclined at any angle to the vertical. For each of these choices of headlight polarizers there is, of course, a viewer polarizer which will give extinction.

However, there are other important properties of a headlight polarizing system besides the property of extinction. The brightness of a given object and its contrast with its background may be different when viewed with different polarizing systems. The viewer may be able to eliminate a large fraction of horizontally polarized light which can be considered to be the major part of daytime reflected glare. The systems described above behave very differently with respect to these properties.

In order to determine this behavior it is necessary to describe the windshield polarizer orientation which corresponds to a given headlight polarizer orientation. This relationship may be visualized as follows: The axis of the windshield polarizer in an opposing car is at right angles to the headlight polarizer axis. In any given case the orientation of the windshield polarizer is then determined by a 180° rotation of this axis about the vertical. The windshield axis will then be in the same quadrant as the headlight axis and the angle between the windshield polarizer axis and the vertical will be the same as the angle between the headlight polarizer axis and the horizontal. This can be expressed mathematically as

$$\alpha+\beta=90°,$$

where α is the angle of the headlight polarizer from the vertical and β is the angle of the viewer polarizer both measured as seen from inside the car measured clockwise.

With knowledge of the angle of the headlight and viewer polarizer it is possible to calculate the apparent brightness of an object illuminated by the headlight. When the headlight and viewer polarizer are at 45° to the vertical the brightness is a maximum. At angles closer to the vertical or horizontal the brightness is less and is a minimum when the headlight polarizer is vertical or horizontal.

For any of these possible linear systems the transmission for horizontally polarized light can be calculated. The vertical viewer polarizer gives the best protection against daytime glare although it is poorest from the point of view of object brightness at night.

Although these various factors are not so spectacular as the reduction of the intensity of the opposing headlight by a factor of several thousand, they can nevertheless be important in particular cases. For example, some dark objects which have zero contrast with their background in the present non-polarizing system may have contrast as high as 50 percent in a system with linear polarizers at 45°. On the other hand some objects may have finite contrast in the non-polarizing system and have zero contrast in the 45° system. Also, the brightness of some objects may be zero in a 90° system whereas the same object would be quite bright in a 45° system.

In this paper the various possible polarized headlight systems will be discussed and their behavior as far as contrast, object brightness, and reduction of daytime glare are concerned.

The discussion will be theoretical in that it is based on perfect polarizers which are perfectly aligned. While the effects on the system of imperfect polarizers, misalignments, windshield tilt, etc., have also been carefully considered, we shall not attempt to treat such important practical details here.

THE MUELLER MATRICES

To discuss the various types of headlight systems, an optical calculus will be used which was developed by Perrin[7] and Soleillet[8] and put in matrix form by Mueller.[9] Its relationship to the optical calculus of R. Clark Jones[10] has been presented in a recent paper. This calculus has the

in der Kraftfahrzeug-Beleuchtung," Zeits. VDI **82**, 201 (1938).

[7] F. Perrin, J. Chem. Phys. **10**, 415 (1942).
[8] Paul Soleillet, Ann. de physique **12**, 23 (1929).
[9] H. Mueller, M.I.T. Course (8.26), Spring 1945.
[10] R. Clark Jones, J. Opt. Soc. Am. **37**, 107 (1947).

advantage that both polarizing and depolarizing systems can be represented. Totally polarized monochromatic light requires three parameters to represent its essential characteristics. Any three parameters could, of course, be used, but the most familiar ones are the amplitudes and phase difference of two linear components at right angles. The optical calculus uses in place of these three quantities the combination

$$\begin{aligned} M &= A_x^2 - A_y^2, \\ C &= 2A_xA_y\cos\phi, \\ S &= 2A_xA_y\sin\phi, \end{aligned} \tag{1}$$

where A_x and A_y are the amplitudes of the components along the x and y axes and ϕ is the phase difference between the components.

It has been shown by Soleillet[8] that if a fourth variable I, the intensity of the light is added to the three variables above a linear relation can be written between the four components of the light going into an instrument and the four components of the light going out. These relationships can be written for depolarizing as well as polarizing systems. For totally polarized light in a non-depolarizing system only three of the variables are independent and we can write the equation

$$I^2 = M^2 + C^2 + S^2.$$

Since the equations connecting the incident and emergent light are all linear in I, M, C and S, the technique developed by Mueller can be used and the light can be represented as a vector in I, M, C, S space and the instrument as a matrix operating on the vector.

The Mueller matrices associated with an elementary instrument such as a wave plate at an arbitrary angle will be developed first. The product of the elementary matrices of a complex system will then give the matrix of the whole system.

The matrix of most of the elementary instruments can be written down from familiar relationships. For a partial polarizer whose axes are parallel to the x and y axes:

$$A_x' = P_xA_x \quad \text{and} \quad A_y' = P_yA_y \tag{2}$$

where A_x and A_y are the x and y components of the light going into the polarizer, P_x and P_y are the transmission factors of the polarizers and A_x' and A_y' are the x and y components of light coming out of the polarizer.

In terms of the Perrin components, the x and y amplitudes can be written

$$A_x^2 = \tfrac{1}{2}(I+M), \quad A_y^2 = \tfrac{1}{2}(I-M). \tag{3}$$

From this equation and Eq. (1)

$$M' = \tfrac{1}{2}P_x^2(I+M) - \tfrac{1}{2}P_y^2(I-M), \tag{4}$$

where again primed components refer to light after it has gone through the polarizer. Similarly,

$$I' = \tfrac{1}{2}P_x^2(I+M) + \tfrac{1}{2}P_y^2(I-M). \tag{5}$$

$$C' = P_xP_yC, \quad S' = P_xP_yS. \tag{6}$$

The matrix for a partial polarizer with the axes in the x and y direction then becomes

$$\mathbf{P}_h = \tfrac{1}{2}\begin{vmatrix} P_x^2+P_y^2 & P_x^2-P_y^2 & 0 & 0 \\ P_x^2-P_y^2 & P_x^2+P_y^2 & 0 & 0 \\ 0 & 0 & 2P_xP_y & 0 \\ 0 & 0 & 0 & 2P_xP_y \end{vmatrix}. \tag{7}$$

This discussion will be limited to perfect polarizers, i.e., $P_x=1$ and $P_y=0$.

The matrix now becomes:

$$\mathbf{P}_h = \tfrac{1}{2}\begin{vmatrix} 1 & 1 & 0 & 0 \\ 1 & 1 & 0 & 0 \\ 0 & 0 & 0 & 0 \\ 0 & 0 & 0 & 0 \end{vmatrix}. \tag{8}$$

In order to describe the behavior of a polarizer at any angle α the matrix (8) must be transformed to arbitrary coordinate axes. This is done by the transformation equation.

$$\mathbf{P}(\alpha) = \mathbf{T}(-2\alpha)\mathbf{P}_h\mathbf{T}(2\alpha) \tag{9}$$

where $\mathbf{T}(2\alpha)$ can be written

$$\mathbf{T}(2\alpha) = \begin{vmatrix} 1 & 0 & 0 & 0 \\ 0 & \cos 2\alpha & -\sin 2\alpha & 0 \\ 0 & \sin 2\alpha & \cos 2\alpha & 0 \\ 0 & 0 & 0 & 1 \end{vmatrix}. \tag{10}$$

This is the matrix of a rotator, which is defined as an element which exhibits pure optical activity. α is defined as the angle which the polarizer transmission axis makes with the x axis. For the polarizing elements on an automobile the sign of α will be considered as positive if from the point of view of the car driver the angle is measured in a clockwise direction from the x axis.

Equation (9) can be expanded to give

$$\mathbf{P}(\alpha)=\tfrac{1}{2}\begin{vmatrix} 1 & \cos 2\alpha & \sin 2\alpha & 0 \\ \cos 2\alpha & \cos^2 2\alpha & \sin 2\alpha \cos 2\alpha & 0 \\ \sin 2\alpha & \sin 2\alpha \cos 2\alpha & \sin^2 2\alpha & 0 \\ 0 & 0 & 0 & 0 \end{vmatrix}. \quad (11)$$

Similarly a matrix can be constructed for a wave plate of retardation δ. For a wave plate with axes parallel to the reference axes, this becomes:

$$\mathbf{R}(\delta)=\begin{vmatrix} 1 & 0 & 0 & 0 \\ 0 & 1 & 0 & 0 \\ 0 & 0 & \cos\delta & -\sin\delta \\ 0 & 0 & \sin\delta & \cos\delta \end{vmatrix}. \quad (12)$$

With these matrices the various properties of any optical system and, in particular, the properties of a polarized headlight system can be calculated.

One of the first problems is the determination of the vector for completely unpolarized light. This can be accomplished with the phenomenological approach used by Perrin.[7] The action of a perfect polarizer on a general light vector (I, M, C, S) is represented by the equation

$$\mathbf{P}\begin{bmatrix} I \\ M \\ C \\ S \end{bmatrix}=\begin{bmatrix} I' \\ — \\ — \\ — \end{bmatrix} \quad (13)$$

which can be expanded to give

$$I'=\tfrac{1}{2}(I+M\cos 2\theta+C\sin 2\theta), \quad (14)$$

where θ is the angle of the polarizer to some predetermined axes.

In an actual measurement finite lengths of time are taken so that Eq. (14) should be rewritten

$$\bar{I}'=\tfrac{1}{2}[\bar{I}+\bar{M}\cos 2\theta+\bar{C}\sin 2\theta], \quad (15)$$

where

$$\bar{I}=\frac{1}{T}\int_0^T I dt \quad (16)$$

and T is the duration of the measurement. In order for I' to be independent of θ, as it is when the vector represents natural light, we must have $\bar{M}=\bar{C}=0$.

Similarly, the equation for light going through a quarter wave plate and a polarizer can be written

$$\bar{I}'=\tfrac{1}{2}[\bar{I}-\bar{M}\cos 2\theta-\bar{S}\sin 2\theta]. \quad (17)$$

Again I' is independent of θ and therefore $\bar{S}=0$. These same conclusions would have been reached by simply defining natural light as light which is unaffected by passing through any rotor or wave plate. In any case, the vector for natural light of unit intensity can be written

$$\begin{bmatrix} I \\ 0 \\ 0 \\ 0 \end{bmatrix}. \quad (18)$$

LINEAR HEADLIGHT SYSTEM

In the general headlight system a series of linear polarizers and possibly retardation sheets are placed over all automobile headlights. The corresponding analyzer is placed before the automobile driver's eyes. We shall refer the axes of the various elements to the vertical. The elements on opposing cars will be reversed in order and rotated 180° about a vertical axis. If the axis of the viewer polarizer in a car is at $+15°$, the viewer polarizer in an opposing car must be at $-15°$.

The headlight polarizer will be represented by $\mathbf{P}_h(\epsilon)$ and the analyzer by $\mathbf{P}_w(\alpha)$ where ϵ and α are the angles of the axes with the vertical. The positive sign will be taken if the angles are measured in a clockwise direction from the vertical as viewed by a person inside the car. The corresponding retardation plates are $\mathbf{R}_h(\gamma, \delta)$ and $\mathbf{R}_w(\beta, \delta)$ where β and γ are the angles of the retardation axes with the vertical and δ is the retardation. Instead of beginning with the completely general case, we shall consider first the behavior of a system which employs only linear polarizers.

The positions of the polarizers on the headlight and windshield which will give extinction can be obtained from the equation

$$\mathbf{P}_w(\alpha)\mathbf{P}_h(-\epsilon)\begin{bmatrix} I \\ 0 \\ 0 \\ 0 \end{bmatrix}=\begin{bmatrix} 0 \\ — \\ — \\ — \end{bmatrix}. \quad (19)$$

The expansion of these matrices gives

$$\tfrac{1}{4}[1+\cos 2(\alpha+\epsilon)]=0. \quad (20)$$

From this we can get the relationship

$$\alpha+\epsilon=\pm\frac{\pi}{2}. \tag{21}$$

This shows the possible arrangements of the polarizers in the headlight system. The equation says that on any car the angle of the headlight polarizer axis from the vertical is the same as the angle of the analyzer axis from the horizontal. This relationship was more simply deduced in the first part of this paper. For each of these possible arrangements, we can compute the transmission of the polarized or specular component of the light which is directly reflected back through the system. This can be done with the equation

$$I=\tfrac{1}{4}[1+\cos 2(\alpha-\epsilon)]. \tag{22}$$

If this result is combined with Eq. (20) a formula is obtained which holds only for those systems which give extinction. This can be written

$$I=\tfrac{1}{4}[1-\cos 4\epsilon]. \tag{23}$$

For the horizontal glare factor

$$\mathbf{P}_w(\alpha)\begin{bmatrix}1\\-1\\0\\0\end{bmatrix}=\begin{bmatrix}I\\-\\-\\-\end{bmatrix} \tag{24}$$

which can be expanded to give

$$I=\sin^2\alpha. \tag{25}$$

These curves are plotted in Fig. 1.

The contrast calculations are slightly more involved. The amount of light from the headlight reflected from an object back through the analyzer depends on the total reflectivity of the object and the amount by which the original percent polarization of the incident light is changed. An investigation of the polarized and unpolarized components reflected from various surfaces has been carried out by Lawrence.[11] If both of these quantities are known, a reflectivity matrix can be calculated which will show the behavior of the object in any headlight system. To simplify the calculation of this matrix, we will assume that the object is isotropic. This means that the change in percent polarization of light incident on this object is the same no matter what is the vibration direction of the light.

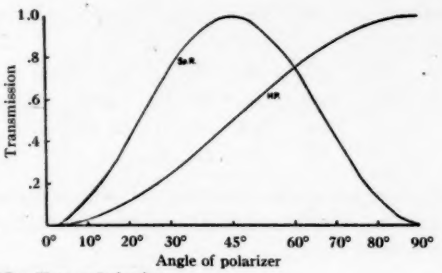

FIG. 1. The relative amount of light from a polarizing headlight reflected specularly back through the automobile viewer and the amount of horizontally polarized light (daytime glare) transmitted by the automobile viewer as a function of the angle which the viewer axis is rotated from the vertical.

For most obstacles on the road this assumption is probably adequate. For certain road surfaces it may be dubious. This assumption of isotropy means that for all orientations the values of the elements in the reflection matrix are identical. This fact can be expressed in the equation

$$\mathbf{T}(2\theta)\varrho\mathbf{T}(-2\theta)=\varrho \tag{26}$$

where ϱ is the reflectivity matrix and $\mathbf{T}(2\theta)$ is the matrix of a rotator defined by Eq. (10). This equation is of exactly the same type as those used for finding the number of independent constants associated with a physical property of a crystal. In the case of a crystal, the angle θ depends on its symmetry. The solution of this equation can be written

$$\varrho=\begin{vmatrix}\rho_{11}&0&0&\rho_{14}\\0&\rho_{22}&\rho_{23}&0\\0&-\rho_{23}&\rho_{22}&0\\\rho_{14}&0&0&\rho_{44}\end{vmatrix}. \tag{27}$$

To find the significance of these remaining elements, we let the matrix, operate on various kinds of light. For example, in the case of unpolarized light

$$\begin{vmatrix}\rho_{11}&0&0&\rho_{14}\\0&\rho_{22}&\rho_{23}&0\\0&-\rho_{23}&\rho_{22}&0\\\rho_{14}&0&0&\rho_{44}\end{vmatrix}\begin{vmatrix}1\\0\\0\\0\end{vmatrix}=\begin{vmatrix}\rho_{11}\\0\\0\\\rho_{14}\end{vmatrix}. \tag{28}$$

ρ_{11} thus turns out to be the natural reflectivity of the object and, also, since the object does not

[11] Jacques Lawrence, J. Opt. Soc. Am. **31**, 9 (1941).

polarize $\rho_{14}=0$. With horizontal linearly polarized light

$$\begin{vmatrix} \rho_{11} & 0 & 0 & 0 \\ 0 & \rho_{22} & \rho_{23} & 0 \\ 0 & -\rho_{23} & \rho_{22} & 0 \\ 0 & 0 & 0 & \rho_{44} \end{vmatrix} \begin{vmatrix} 1 \\ 1 \\ 0 \\ 0 \end{vmatrix} = \begin{vmatrix} \rho_{11} \\ \rho_{22} \\ -\rho_{23} \\ 0 \end{vmatrix}. \tag{29}$$

Since the vibration direction of the polarized component of reflected light must be the same as the incident light

$$\rho_{23}=0. \tag{30}$$

Finally, with elliptically polarized light at 45°:

$$\begin{vmatrix} \rho_{11} & 0 & 0 & 0 \\ 0 & \rho_{22} & 0 & 0 \\ 0 & 0 & \rho_{22} & 0 \\ 0 & 0 & 0 & \rho_{44} \end{vmatrix} \begin{vmatrix} 1 \\ 0 \\ .7 \\ .7 \end{vmatrix} = \begin{vmatrix} \rho \\ 0 \\ .7\rho_{22} \\ .7\rho_{44} \end{vmatrix}. \tag{31}$$

Since again the polarized portion of the light must maintain its same vibration direction

$$\rho_{44}=\rho_{22}. \tag{32}$$

The elements ρ_{22} are the intensities of the polarized component. We will assume that the light from the automobile headlight is completely polarized. In this case

$$\rho_{22}=\rho_{11}P, \tag{33}$$

where P is the fractional polarization of the reflected light. ρ_{11} can now be replaced with the symbol ρ and the general matrix becomes

$$\varrho=\rho\begin{vmatrix} 1 & 0 & 0 & 0 \\ 0 & P & 0 & 0 \\ 0 & 0 & P & 0 \\ 0 & 0 & 0 & P \end{vmatrix}. \tag{34}$$

With this matrix it is now possible to calculate the contrasts between different objects in different headlight systems. The contrast will be defined as

$$\frac{dI}{I}=\frac{I\text{ object}-I\text{ background}}{I\text{ object}}. \tag{35}$$

When the background intensity is greater, it will be defined as

$$\frac{dI}{I}=\frac{I\text{ background}-I\text{ object}}{I\text{ background}}. \tag{36}$$

Consider first the contrast in a linearly polarized system. The headlight polarizer is at an angle ϵ and the windshield polarizer at an angle α. The intensity of the reflected light can be written

$$\mathbf{P}_w(\alpha)\varrho\mathbf{P}_h(\epsilon)\begin{bmatrix} 1 \\ 0 \\ 0 \\ 0 \end{bmatrix}=\begin{bmatrix} I \\ — \\ — \\ — \end{bmatrix}. \tag{37}$$

The contrast calculated from this equation is

$$\frac{dI}{I}=\frac{\rho_0[1+P_0\cos\ (\alpha-\epsilon)]-\rho_b[1+P_b\cos 2(\alpha-\epsilon)]}{\rho_0[1+P_0\cos 2(\alpha-\epsilon)]}, \tag{38}$$

where the subscript 0 refers to the object and the subscript b to the background. This contrast is to be compared with the contrast in an unpolarized system which can be written

$$\frac{dI}{I}=\frac{\rho_0-\rho_b}{\rho_0}. \tag{39}$$

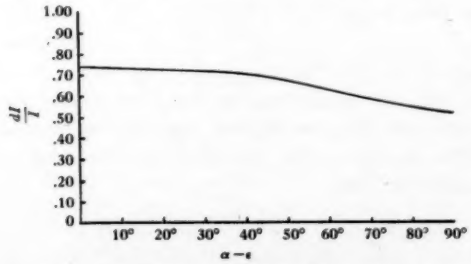

Object reflectivity = 2.6% % polarization = 58
Road reflectivity = 0.81% % polarization = 35

FIG. 2. Contrast of a coat of 2.6% reflectivity and 58% polarization against a macadam road of 0.81% reflectivity and 35% polarization plotted against the difference between the headlight polarizer angle and the viewer angle.

For a headlight or viewer polarizer angle of 22½°, Eq. (38) shows that the contrast is the same as the contrast in an unpolarized light system.

One of the most interesting things which is apparent from these last equations is the extreme change in contrast which is possible in going to a polarized light system.

Consider an object which reflects all of the light and is superimposed on a field which also reflects all the light. Suppose, furthermore, that half the light from the object remains polarized,

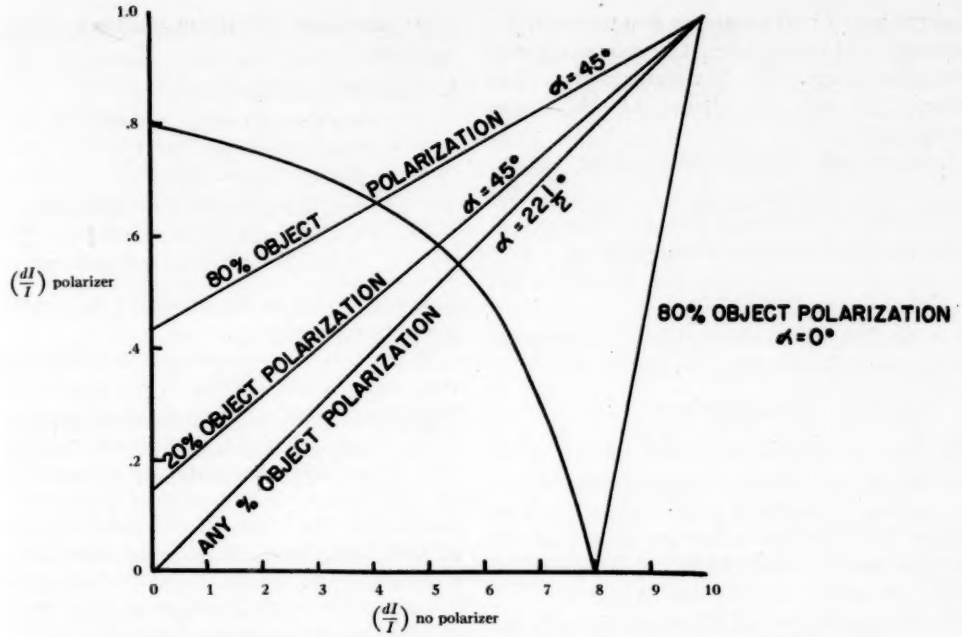

FIG. 3. The natural light contrast of an object of 5% reflectivity against various backgrounds plotted against the contrast in various linearly polarized headlight systems. [0% polarization of background; .05 = object reflectivity.]

whereas only a quarter of the field light is polarized. In this case the contrast is zero in unpolarized light. For a system with polarizers at 45° the contrast becomes

$$\left(\frac{dI}{I}\right)_{45} = \frac{1}{6}. \tag{40}$$

This contrast change is particularly spectacular when actually demonstrated in a driving test. Systems of this type were proposed for *IFF* during the war.

In order to see what contrast conditions are met in practice and thus to examine the differences in behavior of various headlight systems, it is necessary to reduce field brightness measurements to a form suitable for use in the equations.

Two measurements are necessary: (1) the brightness when illuminated with linearly polarized light from a headlight and viewed through a parallel polarizer; (2) the brightness when illuminated with linearly polarized light from a headlight and viewed with a crossed polarizer.

The equations connecting these two measurements with the polarization and reflectivity of the object can be written

$$\mathbf{P}_v\rho\mathbf{P}_v\begin{bmatrix} I_0 \\ 0 \\ 0 \\ 0 \end{bmatrix} = \begin{bmatrix} I_{vv} \\ — \\ — \\ — \end{bmatrix}, \quad \mathbf{P}_v\rho\mathbf{P}_h\begin{bmatrix} I_0 \\ 0 \\ 0 \\ 0 \end{bmatrix} = \begin{bmatrix} I_{vh} \\ — \\ — \\ — \end{bmatrix}. \tag{41}$$

These can be condensed to

$$\frac{I_{vv}}{I_0} = \frac{\rho}{4}(1+P), \quad \frac{I_{vh}}{I_0} = \frac{\rho}{4}(1-P). \tag{42}$$

To illustrate the way the contrast varies in a typical situation a set of measurements were made by Mr. Dexter Cooper of these laboratories. The measurements were made with a polarized headlight system illuminating a man standing on a bituminous macadam road:

Measurement I.
Man's coat at 100 feet from headlights
$I_{vv} = 0.30$ foot lambert
$I_{vh} = 0.08$ foot lambert
Reflectance = 2.6% = ρ
Bituminous macadam road next to coat:
$I_{vv} = 0.08$ foot lambert.
Measurement II.
Bituminous macadam road next to coat:
$I_{vv} = 0.028$ foot lambert
$I_{vh} = 0.0135$ foot lambert.

The first set of measurements was made with a Luckiesh brightness meter. The second set were made photographically. The photographic measurement is not so reliable as the meter measurement.

From the coat measurements and Eq. (42)

$$P_c = 0.58.$$

From the second road measurement:

$$P_r = 0.35.$$

From the first road measurement and the value for the coat reflectivity:

$$\rho_r = 0.81 \text{ percent.}$$

In Fig. 2 is shown a plot of the contrast of the coat against the road for a linear headlight system. In Fig. 3 is shown a plot of the contrast changes of a 5-percent reflectivity object against a road of varying reflectivities.

The data can be summarized as follows:

1. The largest part of the polarized reflected component reaches the driver's eyes in the 45° case. In other words, for the 45° case objects are brighter.
2. The most contrast is obtained for a non-depolarizing target with the 45° case.
3. For the 22½° case half the polarized reflected component reaches the driver's eyes.
4. The natural light contrast of objects is preserved in a 22½° system.

ELLIPTICAL SYSTEMS

The most general headlight system will consist of linear polarizers and retardation sheets so arranged as to give elliptically polarized light.

The Extinction Condition

In the general case exactly the same computations can be made as in the linear case. We are interested, first in the positions of the polarizers and retardation plates on our windshield and headlights which will give extinction. These can be obtained from the equation:

$$\mathbf{P}_w(\alpha)\mathbf{R}_w(\beta,\delta_1)\mathbf{R}_h(-\gamma,\delta_2)\mathbf{P}_h(-\epsilon)\begin{bmatrix}1\\0\\0\\0\end{bmatrix}=\begin{bmatrix}0\\-\\-\\-\end{bmatrix}. \quad (43)$$

The expansion of these matrices gives the equation:

$$\begin{aligned}&1+\sin 2(\beta+\alpha)\sin 2(\beta+\gamma)\\&\quad\times\cos 2(\gamma-\epsilon)\cos\delta_2(1-\cos\delta_1)\\&\quad+\cos 2(\beta+\alpha)\cos 2(\beta+\gamma)\\&\quad\times\cos 2(\gamma-\epsilon)(1-\cos\delta_1)\\&\quad+\sin 2(\beta+\alpha)\sin 2(\beta+\epsilon)\cos\delta_1\cos\delta_2\\&\quad+\sin 2(\beta+\alpha)\sin 2(\gamma-\epsilon)\sin\delta_1\sin\delta_2\\&\quad+\cos 2(\beta+\alpha)\cos 2(\beta+\epsilon)\cos\delta_1=0. \quad (44)\end{aligned}$$

This equation must be satisfied if the headlights are to be extinguished.

If the two wave plates are dissimilar and if their axes are not parallel to the polarizer axes, the polarizer axes' positions for extinction are not independent of δ_1 and δ_2 the value of the retardations. Since most wave plates are non-achromatic, the retardation δ is a function of frequency. This means that the value of the polarizer and retardation sheet extinction angles will be different for different frequencies. In other words all colors will not be extinguished simultaneously. If $\delta_1=\delta_2$, Eq. (44) can be rewritten

$$\begin{aligned}&1+\sin 2(\alpha-\beta)\sin 2(\gamma-\epsilon)[2\cos^2(\beta+\gamma)\cos^2\delta-1]\\&\quad+\cos 2(\alpha-\beta)\cos 2(\gamma-\epsilon)\cos 2(\beta+\gamma)\\&\quad-\sin 2(\beta+\gamma)\sin 2(\alpha-\beta-\gamma+\epsilon)\cos\delta=0. \quad (45)\end{aligned}$$

The real, non-trivial solution of this equation is given by the relationship

$$\begin{aligned}&\alpha-\beta=\gamma-\epsilon\\&\beta+\gamma=\pm\frac{\pi}{2} \quad (46)\\&\alpha+\epsilon=\pm\frac{\pi}{2}.\end{aligned}$$

This solution is particularly interesting as it does not involve δ. It shows that the system is "achromatized." In other words, if the light is extinguished for one color, it is extinguished for all colors.

In case the retardation δ is higher than one wave, we begin to get color in the specularly reflected component. In other words, the achromatization of the system does not extend beyond the headlight extinction. This color represents a loss of light. In the extreme case where δ is very large, the system will act for the polarized component of reflected light as though a 50 percent

isotropic absorber were over both the headlight and the windshield. Because of this large light loss, we shall limit the discussion to low-order retardation plates.

Except for the extinction conditions a fixed value can be assigned to the retardation of a low-order plate and its variation with color ignored. By stipulating achromatism in the extinction Eq. (44) can be considerably simplified. A still further simplification can be made if we can show that all possible systems with different values for the retardation can be reproduced with a single value of δ.

Comparison between Elliptical Systems with Quarter-Wave Plates and Systems with Other Fractional Wave Plates

Any kind of elliptically polarized light can be produced with a quarter-wave plate and a linear polarizer. We need to show that the combination will behave the same for all the characteristics of an automobile system: day glare, polarized or specular reflection, etc., as the elliptical polarizer made of a retardation sheet other than a quarter wave.

In order to compare the $1/4\lambda$ system with the general system, one must know first the relationship between wave plate axes and polarizer axes in the two cases to produce elliptical light of identical shape and orientation. To do this we set up the relationship

$$\mathbf{Q}\left(\frac{\pi}{2}\right)\begin{bmatrix}1\\0\\0\\0\end{bmatrix}=\begin{bmatrix}I\\M\\C\\S\end{bmatrix}=\mathbf{Q}(\lambda)\begin{bmatrix}1\\0\\0\\0\end{bmatrix}, \qquad (47)$$

where $\mathbf{Q}(\pi/2)$ is the matrix, $\mathbf{R}(\pi/2, \beta)\mathbf{P}(\alpha)$, of a polarizer followed by a quarter-wave plate, and $Q(\lambda)$ is the matrix of a polarizer followed by a wave plate of any retardation.

From this matrix equation we get

$$\begin{vmatrix}q_{(\pi/2)11}\\q_{(\pi/2)21}\\q_{(\pi/2)31}\\q_{(\pi/2)41}\end{vmatrix}=\begin{vmatrix}q_{\lambda 11}\\q_{\lambda 21}\\q_{\lambda 31}\\q_{\lambda 41}\end{vmatrix} \qquad (48)$$

which says simply that the elements in the first column in both matrices must be equal for them to have exactly the same effect on natural light.

It must now be demonstrated that with the two different elements arranged as analyzers in automobile windshields, the transmitted intensity is the same for any given kind of polarized light. In this case the retardation sheet comes first, and the matrix of the system is different. From the Rayleigh reciprocity law it can be shown that in this reverse instrument the elements of the first row have the same numerical value as the elements in the first column of the direct instrument. We can write

$$\mathbf{Q}^*=\begin{vmatrix}q_{11} & q_{21} & -q_{31} & q_{41}\\ — & — & — & —\\ — & — & — & —\\ — & — & — & —\end{vmatrix}, \qquad (49)$$

where Q^* is the matrix of the retardation sheet and polarizer in reverse order. We want to show that

$$\mathbf{Q}^*\left(\frac{\pi}{2}\right)\begin{bmatrix}I\\M\\C\\S\end{bmatrix}=\mathbf{Q}^*(\lambda)\begin{bmatrix}I\\M\\C\\S\end{bmatrix}=\begin{bmatrix}I'\\—\\—\\—\end{bmatrix}. \qquad (50)$$

Since the first column of the two direct matrices are the same, the first row of the two reverse matrices will also be the same, and the intensities of the light transmitted through the $\frac{1}{4}$-wave plate combination or the general retardation combination will be exactly the same.

It is thus apparent that a $\frac{1}{4}$-wave plate can be substituted for any other wave plate in the

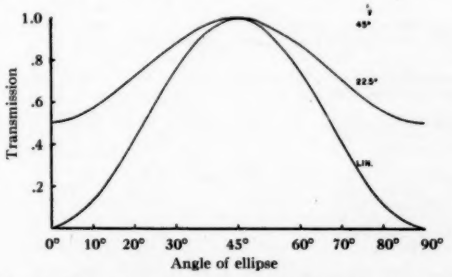

FIG. 4. The effect of ellipse orientation on the relative amount of light from headlights reflected specularly back through the viewer for elliptical systems in which the quarter-wave plate is at 45°, 22½° and 0° to the polarizer axis.

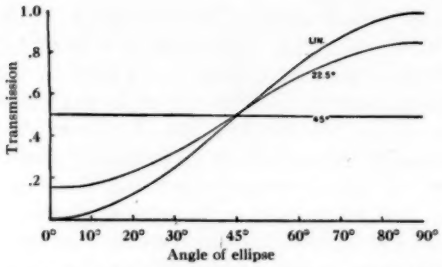

FIG. 5. The effect of ellipse orientation on the relative amount of horizontally polarized light transmitted by the viewer for elliptical systems in which the quarter-wave plate is at 45°, 22½° and 0° to the polarizer axis.

mathematical analysis. If, however, a given kind of elliptical light should prove desirable, we will not be restricted to the use of a ¼-wave plate in order to obtain this elliptical light.

Since a quarter-wave sheet will do what any other retardation sheet will do, the main part of the following discussion will be limited to combinations of polarizers and quarter-wave plates.

A quarter-wave plate has the further advantage that when combined with a polarizer the plate axis coincides with the axis of the elliptical light which it produces.

Equation (46) shows the possible arrangements of the polarizers in the headlight system. For each of these possible arrangements we can compute the transmission of polarized reflected light from the driver's headlights back through his own windshield. This can be done with the

TABLE I. Characteristics of various headlight systems including system with 50 percent neutral filters over headlights and windshields.

Light produced by windshield polarizer	Vertical linear	45° linear	22½° linear	Circular	22½° ellipse at 45°	22½° ellipse at 22½°	50% isotropic windshield
Transmission of horizontally polarized light	0	50	15	50	50	25	50
Transmission of specularly reflected light from headlights	0	100	50	100	100	75	50
Contrast of 7% reflectivity object against 3% reflectivity background. Object 25% depolarized. Background 50% depolarized	14	63	57	63	63	61	57
Contrast of 7% reflectivity object against 3% reflectivity background. Object 25% depolarized. Background 30% depolarized	49	58	57	58	58	58	57

matrix equation:

$$\mathbf{P}_w(\alpha)\mathbf{R}_w\left(\beta,\frac{\pi}{2}\right)\mathbf{R}_h\left(\gamma,\frac{\pi}{2}\right)\mathbf{P}_h(\epsilon)\begin{bmatrix}1\\0\\0\\0\end{bmatrix}=\begin{bmatrix}I\\-\\-\\-\end{bmatrix}. \quad (51)$$

Here we have let $\delta=\pi/2$ as the arguments above show this system is sufficiently general. From this we get the equation

$$I=\tfrac{1}{4}[1+\cos2(\alpha-\beta)\cos2(\gamma-\epsilon)\cos2(\beta-\gamma)+\sin2(\alpha-\beta)\sin2(\gamma-\epsilon)]. \quad (52)$$

This result can be combined with Eq. (46) to give a formula which holds only for those systems which give extinction. This new equation can be written

$$I=\tfrac{1}{2}[1-\cos^2 2\gamma\cos^2 2(\gamma-\epsilon)]. \quad (53)$$

In Fig. 4 are shown curves of the intensity for various retardation plate angles and polarizer angles. From these curves it is apparent that various combinations differ widely with respect to their transmission of reflected light. The case $\gamma-\epsilon=45°$ represents circularly polarized light. Rotation of the headlight around an axis normal to the polarizer has no effect on the reflected light getting back through the windshield. When $\gamma-\epsilon=22\frac{1}{2}°$, the light is elliptically polarized and the transmission of the reflected light becomes a function of the position of the headlight polarized axes.

The amount of horizontally polarized light transmitted by the analyzer can be determined from the matrix equation

$$\mathbf{P}_\epsilon\mathbf{R}_\gamma\begin{bmatrix}1\\-1\\0\\0\end{bmatrix}=\begin{bmatrix}I\\-\\-\\-\end{bmatrix}. \quad (54)$$

This equation can be expanded to give

$$I=\tfrac{1}{2}[1-\cos2\gamma\cos2(\gamma-\epsilon)]. \quad (55)$$

A plot of this equation is shown in Fig. 5 for various orientations of the analyzer. Here again it is apparent that the various systems behave quite differently with respect to this factor. In a completely determined system we could consider

Figs. 4 and 5 and find the "best" polarizing system for headlights.

This, of course, is calculated with the assumption of equal weights for the direct reflected factor and the horizontal glare factor which is something which can only be determined experimentally.

The calculation of contrast in elliptical systems is exactly the same as in linear systems. The reflected light is represented by the matrix equation

$$\mathbf{P}_w(\alpha)\mathbf{R}\left(\beta,\frac{\pi}{2}\right)\varrho\mathbf{R}\left(\gamma,\frac{\pi}{2}\right)\mathbf{P}_h(\epsilon)\begin{bmatrix}I\\0\\0\\0\end{bmatrix}=\begin{bmatrix}I\\-\\-\\-\end{bmatrix}. \quad (56)$$

From this we get the contrast equation

$$\frac{dI}{I}=\frac{\rho_i-\rho_0+(\rho_iP_i-\rho_0P_0)[\cos^2 2(\alpha-\beta)\cos 2(\beta-\gamma)+\sin^2 2(\alpha-\beta)]}{\rho_i\{1+P_i[\cos^2 2(\alpha-\beta)\cos 2(\beta-\gamma)+\sin^2 2(\alpha-\beta)]\}}. \quad (57)$$

The behavior of this equation is exactly the same as the equation for contrast in linear systems.

In order to show the difference between the various headlight systems, the material presented in the graphs has been summarized in Table I at the end of this section. One of the most interesting systems is that in which the viewer has a quarter-wave plate at 22½° to a polarizer at 0°. This gives elliptically polarized light with the ellipse axis at 22½° and with an ellipticity of 22½°. The ellipticity is defined as $\tan^{-1}(b/a)$ where a and b are the major and minor axes of the ellipse. This system is also included in the table.

From the data in this paper it is apparent that ideally there are several equally useful polarizing headlight systems. For its current performance demonstrations, Polaroid Corporation is using with satisfactory results, linear polarizers at an inclination not shown in the table, namely, the viewer polarizer axis is inclined −35° from the vertical, this angle representing a counterclockwise rotation of his viewer as seen by the driver behind it.

In conclusion the authors wish to express appreciation to the members of the Polaroid Corporation for many helpful suggestions.

Physics Abstracts

For many years the dues of the American Physical Society have included a subscription to Physics Abstracts, published by the Institute of Electrical Engineers of London. There has been, however, no convenient method by which persons not members of the A.P.S. could receive this publication. The Optical Society of America has now instituted an arrangement under which any O.S.A. member can receive Physics Abstracts at an annual subscription price of $4.50. All correspondence in this connection should be addressed to the American Institute of Physics, 57 East 55th Street, New York 22, New York.

The Effect of Spectral Quality of Light on Visual Performance and Fatigue*

ERNST SIMONSON AND JOSEF BROZEK**
The Laboratory of Physiological Hygiene, University of Minnesota, Minneapolis, Minnesota

(Received May 10, 1948)

There is a large but inconclusive amount of literature on the effects of the color of light on single visual functions, such as visual acuity. The amount of dependable information on the effects of the spectral quality of illumination on work performance is negligible. It was the purpose of the present study to investigate this problem. The work test involved recognition of very fine details (letters) and was designed to reproduce the essential features of conveyor inspection. The standard duration of work was 2 hours. Output, results of a large array of tests of visual functions, subjective reactions (complaints), and subjective preferences were considered as criteria in judging the relative superiority or inferiority of the three illuminants compared (ordinary inside frosted lamps; "natural white" lamps with a white, slightly bluish coating; and Verd-A-Ray lamps having a greenish coating). The illumination intensity (5 ft.-c, 100 ft.-c, and 300 ft.-c) on the work place was made identical for all three lamps. Statistically significant differences between the illuminants were established with reference to a number of criteria of performance and fatigue. The differences were, in general, in favor of the illuminant with greenish coating. The present study used commercially available illuminants. Further systematic studies designed to determine the optimal spectral characteristics of light are needed.

INTRODUCTION

THE intensity and the distribution of light on the work place are well established as factors affecting visual performance. In defining the physical characteristics of a light source the spectral quality (color) of the light cannot be neglected. Is it of consequence for visual performance and fatigue?

The Illuminating Engineering Society[1] devoted to color only six lines in their recommendations for industrial lighting, stating that color has little effect upon clearness and quickness of seeing. The statement was supported by reference to Woodside and Reinhardt[2] and Luckiesh and Moss,[3] although the latter authors had found with the sodium vapor lamp a significantly faster recognition time for small objects and high contrast than with the tungsten filament lamp.

This may serve to illustrate the existing state of confusion in the appreciation of the importance of the spectral quality of light. Contradictory claims have been made for a variety of visual functions, for instance, for the effect of color on threshold acuity. Superiority of white light was claimed by Ferree and Rand[4] and Hartridge,[5] while Bouma[6] and Arndt[7] reported that the visual acuity was poorest with white light. All authors who compared sodium lamps with incandescent tungsten lamps (Weigel,[8] Klein,[9] Arndt,[10] and Luckiesh and Moss[10a]) found that the visual acuity was better with the sodium lamps. This is consistent with findings that the acuity was best with yellow (Bouma,[6] Arndt[7]), or yellow-green light (Luckiesh,[10b] Korff-Petersen and Ogata[11]). A number of authors agree that the

* Aided by a research grant from the Verd-A-Ray Corporation, Toledo, Ohio.

** With the assistance of W. J. Bushard and H. G. Peterson of the Division of Ophthalmology, University of Minnesota, School of Medicine, J. C. Franklin, and A. Butler.

[1] Illuminating Engineering Society, *American Recommended Practice of Industrial Lighting* (New York, 1942), p. 51.

[2] C. C. Woodside and H. Reinhardt, "Comparison of the light from high intensity mercury vapor lamps and incandescent filament lamps for visual tasks," Trans. Illum. Eng. Soc. **32**, 365 (1937).

[3] M. Luckiesh and F. K. Moss, "Seeing in tungsten, mercury and sodium light," Trans. Illum. Eng. Soc. **31**, 655 (1936).

[4] C. E. Ferree and G. Rand, "Visibility of objects as affected by color and composition of light," Personnel J. **9**, 475 (1931).

[5] H. Hartridge, "The visual perception of fine detail," Phil. Trans. Roy. Soc. London. Series **B232**, 519 (1947).

[6] P. G. Bouma, "Sehschärfe und Wahrnehmungsgeschwindigkeit bei der Strassenbeleuchtung," Philips Tech. Rundschau **1**, 215 (1936).

[7] W. Arndt, "Sieht man bei farbigem Licht besser?," Zeits. tech. Physik **15**, 296 (1934).

[8] R. C. Weigel, "Untersuchungen über die Sehfähigkeit im Natrium—und Quecksilberlicht, insbesondere bei der Strassenbeleuchtung," Licht **5**, 211 (1935).

[9] C. C. Klein, "Sieht man bei farbigem Licht besser?," Licht **5**, 31 (1934).

[10] W. Arndt, "Ueber das Sehen bei Natriumdampf—und Glühlampenlicht," Licht **3**, 213 (1933).

[10a] M. Luckiesh and F. K. Moss, "Visual acuity and sodium vapor light," J. Franklin Inst. **215**, 401 (1933).

[10b] M. Luckiesh, "The influence of spectral character of light on the effectiveness of illumination," Trans. Illum. Eng. Soc. **7**, 135 (1912).

[11] A. Korff-Petersen and M. Ogata, "Der Einfluss verschiedenfarbigen Lichts auf die Genauigkeit und die

visual acuity is poorest with blue light (Ferree and Rand,[4] Ruffer,[12] Korff-Petersen,[11] Hartridge[5]), but Arndt[10] and Weigel[8] found the visual acuity better with mercury lamps than with ordinary tungsten filament lamps, although the mercury lamp light is more blue.

A similar discrepancy was observed with reference to the speed of discrimination of details. This function was poorest with blue light (Ferree and Rand,[4] at lower illumination; Ruffer[12]), and yet the mercury lamp (Arndt[7]) and the daylight Mazda C lamp (Tang[13]) were reported to be superior to ordinary incandescent lamps. In general, yellow light (including the light produced by the sodium lamps) compares favorably with other colors or ordinary tungsten filament bulbs (Ruffer,[12] Korff-Petersen,[11] Arndt,[7] Klein[9]), although at very low illumination (0.3 ft.-c) daylight might be superior (Ferree and Rand[4]).

Abstract laboratory experiments on the effect of color on visual acuity and speed of discrimination have only limited practical implications for making recommendations concerning the use of colored light in industry because they disregard the complexity of visual functions involved in the majority of industrial jobs in which vision plays a role. In view of this situation, investigations of color effects on work performance and functionally defined fatigue are much needed. Few such studies have been reported.

In investigating various color mixtures from red-yellow to bluish-green Ferree and Rand[14] studied the effect of 3 hours of reading on the power to sustain clear vision (appearance of blurring during fixation of a letter). The physiological components of this function are not fully clear and the use of the method for the study of visual fatigue is questionable. Ruffer[12] found the deterioration in 50 consecutive acuity readings to be most pronounced with red and least pronounced with yellow; from this short test no conclusions on possible color effects in sustained work performance can be made. Fernberger, Viteles and Carlson[15] found the blue Daylight Mazda Lamp C2 superior to ordinary tungsten filament lamps in inspection of white flannel cloth, consisting in recognition and removal of all dark hairs. Output in placing blocks on a table was studied by Pierce and Weinland.[16] Next to white light, the performance was best with yellow and green, poorest with yellow amber, and in between with red, orange, and blue. This haphazard order can only be explained by the fact that the work task required little, if any, visual effort.

The complexity of the general problem should be recognized. Color might affect visual performance in three ways: (1) through a direct effect on fundamental visual functions, (2) through interaction within the central nervous system, the light acting as afferent stimulus, and (3) through more remote, but not less important, motivational effects. Allen and Schwartz[17] have demonstrated that light of one (monochromatic) color might stimulate or inhibit the perception of another color so that in any spectral mixture complicated interactions will result which cannot be predicted from investigations on monochromatic stimuli; Mandelbaum and Mintz's[18] results are also of interest in this respect. Little work has been reported on the action of visual stimuli on other functions of the central nervous system. Bourguignon and Monnier[19] found that green light had a calming and red light an irritating effect on spastic muscles. The concomitant changes of the chronaxie can be only explained by interaction between the optical and the motor centers, which in turn affect the peripheral chronaxie. Although muscle spasm is an abnormal condition, there is every reason to believe that

Schnelligkeit des Erkennens von Druckzeichen," Arch. Hyg. Infekt. Krankh. **105**, 27 (1925).

[12] W. Ruffer, "Über die Beeinflussung menschlicher Leistungen durch farbiges Licht," Ind. Psychotech. **5**, 161 (1928).

[13] K. Y. Tang, "Visual performance under daylight, incandescent, mercury vapor and their mixtures," Trans. Illum. Eng. Soc. **26**, 258 (1931).

[14] C. E. Ferree and G. Rand, "Some experiments on the eye with different illuminants," Trans. Illum. Eng. Soc. **13**, 50 (1918).

[15] S. W. Fernberger, M. S. Viteles, and W. R. Carlson, "The effect of changes in quality of illumination upon visual perception," J. App. Psychol. **18**, 611 (1934).

[16] D. H. Pierce and I. D. Weinland, "The effect of color on workmen," Personnel J. **13**, 34 (1934).

[17] F. Allen and M. Schwartz, "The effect of stimulation of the senses of vision, hearing, taste and smell upon the sensibility of the organs of vision," J. Gen. Physiol. **24**, 105 (1940).

[18] J. Mandelbaum and E. U. Mintz, "The sensitivities of the color receptors as measured by dark adaptation," Am. J. Ophthalmol. **24**, 1241 (1941).

[19] G. Bourguignon and M. Monnier, "Les variations de la chronaxie sous l'influence des éclairages colorés dans le torticolis spasmodique," Comptes Rendus Acad. **203**, 347 (1936).

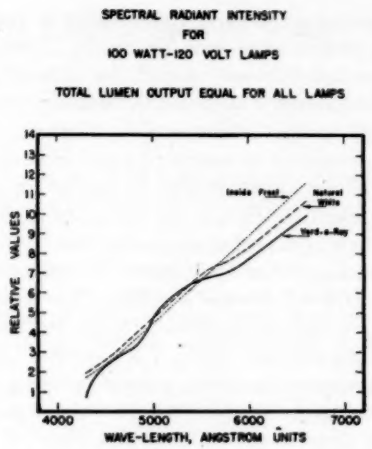

FIG. 1. Spectral radiant intensity of inside frosted (Fr), Natural White (NW) and Verd-A-Ray lamps (VR), measured at equal illumination intensity at the plane of the photometer.

some interaction between optical and motor centers might take place also under normal conditions and affect motor coordination (skill).

An analysis of the existent literature leads to the conclusion that there is little definitive knowledge on the effects of color on visual work or visual fatigue. It appears that further progress depends on the development of suitable work tasks, involving a considerable degree of visual strain over a period of several hours so that the experimental situation would be comparable to actual conditions in industry. In addition to work performance the involvement of visual functions should be investigated by means of a large battery of tests, made immediately before and after the work. Also, the subjective aspects of visual strain should not be neglected. The work task developed for the purposes of the present study reproduces the job of inspection of objects, transported on a conveyor. We believe that this work test meets the methodological requirements demanded from a "job miniature situation" designed for laboratory investigations on work performance and fatigue.

The purpose of the present experimental series was to investigate several commercially introduced illuminants, characterized by different spectral distributions, rather than to study the effect of pure spectral colors.

WORK CONDITIONS

The Work Test

The work test has been described in detail elsewhere.[20] The visual task consisted in the recognition of small letters, copied down by the subjects. The writing was done without visual control. The same dull white paper was used on the belt transporting the letters and the field surrounding the screen. The six subjects were seated in standard booths. The experiments were performed in an air-conditioned room at moderate room temperature.

Evaluation of Performance

The performance was evaluated in terms of correctly recognized letters out of a sample of 200 letters, corresponding to a time interval of 6 minutes. Three such work samples were evaluated. The first sample was taken 5 minutes after the start of the work, a second sample at the midpoint (after 1 hour of work), and the third sample near the end (after 2 hours). The subjects had the impression that the whole 2-hour performance was evaluated.

The average of the three samples gives the "average performance score." In addition, the difference between the first and the third sample ("performance drop") and the difference between the highest and lowest value of the three samples ("performance range") was calculated. The latter is an index of the intra-individual variability during the task. The "performance drop" served as one of the indices of fatigue.

Illuminants

Three different illuminants (ordinary inside frosted lamps, "Fr"; natural white lamps, "NW"; and Verd-A-Ray lamps, "VR") were used at three levels of illumination (5, 100, and 300 ft.-c). The lamps were mounted in shielded boxes. The illumination level was varied by using lamps of different wattage (40, 100 and 200 Watts). The finer adjustment was obtained by placing diaphragms with multiple perforations in front of the lamp and by slight variations of the distance between the lamps and the screen.

[20] J. Brozek, E. Simonson, and A. Keys, "A work test for quantitative study of visual performance and fatigue," J. App. Psychol. 31, 519 (1947).

The "Natural White" are lamps with a white, slightly bluish coating; the "Verd-A-Ray" lamps have a definitely greenish coating. The illuminants differ in lumen output, surface brightness distribution, and spectral quality of the light. The regulation of the illumination on the screen by means of diaphragms with multiple perforations eliminated lumen output and surface brightness distribution as experimental variables. All lamps were compared at the same illumination level on the screen. Consequently, any consistent differences in visual performance or associated changes in visual functions must be due to the differences in spectral distribution. It deserves emphasis that the color differences between the three illuminants are comparatively small, and clearly recognizable only when the lamps are viewed simultaneously. The light from all illuminants is essentially mixed white light.

A physical description of the spectral characteristics of the light emitted by the three lamps is given in Figs. 1 and 2 and Table I. Figure 1 shows the radiant energy for the different wave-lengths; the values were expressed in relative units. The total illumination intensity of the 3 lamps at the level of the photo-cell was made identical. This condition corresponds to our testing situation. It can be seen that the blue radiation of NW lamps is higher and that of VR lamps is lower compared to Fr lamps. The red radiation is smaller in both NW and VR lamps than it is in Fr lamps, but the reduction is more pronounced in VR lamps. Between 5000 and 5400A, in the green part of the spectrum, the radiation of the VR lamp is highest. The last 2 columns of Table I show the radiation of NW and VR lamps in percentage of Fr lamps.

The physiological utilization of the radiant energy depends on the light sensitivity of the human eye to the different wave-lengths. The utilizable spectral energy for the three illuminants was calculated, multiplying the values of Fig. 1 by the coefficients of relative light sensitivity (column 2, Table I). The results are given in columns 3–5, Table I. From these values, the relative distribution of the utilizable energy was calculated in percentages of the maximum for each illuminant (see Fig. 2).

The characterization of the lamps in terms of physiologically utilizable energy minimizes the differences between illuminants at the extreme ends of the spectrum. In regard to the middle part, between 5000 and 6200A, from which by far the greatest proportion of utilizable energy is derived, the curves of all three illuminants are displaced to the right from the light sensitivity curve of the human eye. This displacement is most pronounced in Fr lamps and least pronounced in VR lamps. In other words, the distribution of utilizable energy of VR lamps follows the light sensitivity curve somewhat more closely than the curves of NW and Fr lamps.

TABLE I. Emission of spectral energy for the frosted (Fr), "natural white" (NW), and Verd-A-Ray (VR) lamps, in terms of utilizable spectral energy, and emission of NW and VR lamps in percentage of Fr lamps.

Wave-length angstrom units	Relative average light sensitivity of human retina	Utilizable energy			Percent of Fr	
		Fr	NW	VR	NW	VR
4300	0.01	0.02	0.02	0.01	111	43
4400	0.02	0.04	0.05	0.03	112	88
4600	0.07	0.19	0.21	0.19	109	98
4800	0.14	0.50	0.53	0.45	107	90
5000	0.32	1.42	1.45	1.51	106	106
5200	0.70	3.72	3.92	4.05	105	109
5400	0.95	5.85	6.12	6.12	105	105
5500	1.00	6.58	6.90	6.64	105	101
5600	0.99	7.08	7.24	6.80	102	96
5700	0.95	7.12	7.12	6.53	100	92
5800	0.87	6.96	6.70	6.18	96	89
6000	0.63	5.61	5.22	4.85	93	87
6200	0.37	3.62	3.35	3.13	92	86
6300	0.25	2.56	2.35	2.20	92	86
6400	0.17	1.81	1.67	1.55	92	86
6600	0.06	0.70	0.64	0.60	92	85

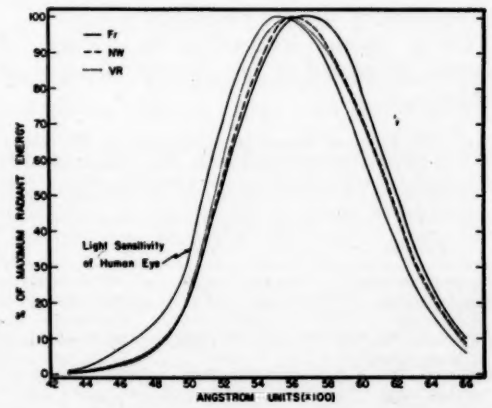

FIG. 2. Utilizable radiant energy of Fr, NW, and VR lamps at different wave-lengths, calculated from the average light sensitivity of the human retina.

TABLE II. Effect of three different illuminants (Fr, NW, VR) on visual performance, blinking rate, and questionnaire score during visual work at three levels of illumination. Mean values of 12 determinations. Negative values indicate deterioration.

Function	Level of illumination: 5 ft.-c Fr	5 ft.-c NW	5 ft.-c VR	100 ft.-c Fr	100 ft.-c NW	100 ft.-c VR	300 ft.-c Fr	300 ft.-c NW	300 ft.-c VR	Units
Questionnaire score	10.3	7.0	8.1	7.8	7.3	8.0	9.7	7.9	7.2	Total score
Performance average	164.8	166.1	171.3	187.8	190.1	189.9	187.8	189.4	186.7	Number of correct letters
Performance drop	−13.2	−15.2	−13.8	−8.6	−5.8	−6.0	−9.7	−8.6	−14.3	Number of correct letters
Performance range	25.9	24.9	16.8	10.9	9.1	7.5	11.8	11.3	15.8	Number of correct letters
Blinking rate average	9.76	9.95	9.59	5.39	6.26	5.75	8.09	8.48	8.39	Blinks per minute
Blinking rate difference	−2.19	−1.92	1.63	0.13	0.08	−1.64	−1.96	0.94	−1.15	Blinks per minute

SCORING OF THE TESTS AND RATINGS

The blinking rate was measured at the start, midpoint, and end of 2 hours of visual work. The blinks were counted for periods of 5 minutes and the scores represent the rate per min. The results were calculated and expressed as "average blinking rate" (mean of the measurements for the 3 periods) and "blinking rate difference" (change from the first to the last period).

Before the start and at the end of the visual work a battery of tests was applied, subdivided into 4 groups, and spaced in intervals of 5 minutes. A description of the methods has been given in a preceding communication to which the reader may refer.[21] The scores for the visual tests are defined as follows:

Recognition time = the time from exposure to recognition for the smallest visible stimulus.

Flicker fusion frequency = the number of flashes per second at the moment of apparent fusion.

Abduction power, adduction power, and vertical divergence = value of the interposed prism strength at the moment of diplopia.

Accommodation near point = distance from the eye, in cm, at which the letters start to blur.

Convergence near point = distance, in cm of a 2 mm target from the bridge of the nose to the point of diplopia.

Ophthalmograph-movement phase = average duration of repeated movements between 2 fixation points, in 1/100 sec.

Ophthalmograph-angular velocity = ratio of the "movement phase" over the distance of movement, in arbitrary units.

Ophthalmograph-fixation phase = time of eye movement used for fixation, during one eye-movement cycle, in 1/100 sec.

Ophthalmograph-extent of movement during fixation = amplitude of corrective movements during fixation, in arbitrary units.

Ophthalmograph-discrepancy = difference be-

TABLE III. Effect of three different illuminants (Fr, NW, VR) on the change (d) of retinal functions during visual work at three levels of illumination. Mean values of 12 determinations. Negative values indicate deterioration.

Function	Level of illumination: 5 ft.-c Fr	5 ft.-c NW	5 ft.-c VR	100 ft.-c Fr	100 ft.-c NW	100 ft.-c VR	300 ft.-c Fr	300 ft.-c NW	300 ft.-c VR	Units
Recognition time	−3.50	−6.04	−1.54	−2.29	−2.29	1.29	−0.9	−1.8	2.3	Seconds
Flicker fusion frequency	−1.00	−1.42	−0.36	−1.33	−1.52	0.13	−1.46	−1.93	−0.07	Flashes per second
Brightness discrimination—green	−0.24	0.26	0.14	−0.16	−0.07	−0.16	−0.15	−0.03	−0.09	Arbitrary Units
Brightness discrimination—red	−0.37	0.03	−0.28	−0.17	−0.03	0.11	−0.06	−0.13	0.32	Arbitrary Units

[21] E. Simonson and J. Brozek, "The effect of illumination intensity on visual work and fatigue," J. Opt. Soc. Am. 38, 384 (1948).

TABLE IV. Effect of three different illuminants (Fr, NW, VR) on the change (d) of several ophthalmological routine tests during visual work at three levels of illumination. Mean values of 12 determinations. Negative values indicate deterioration.

Function	Level of illumination: 5 ft.-c Fr	5 ft.-c NW	5 ft.-c VR	100 ft.-c Fr	100 ft.-c NW	100 ft.-c VR	300 ft.-c Fr	300 ft.-c NW	300 ft.-c VR	Units
Abduction power	−0.35	0.11	−0.09	−0.14	−0.32	−0.21	0.26	−0.03	0.06	Diopters
Adduction power	1.10	2.48	0.47	−0.48	1.66	1.47	−0.08	0.76	1.78	Diopters
Vertical divergence	0.08	0.04	−0.10	−0.02	0.11	−0.20	0.03	−0.11	0.03	Diopters
Accommodation near point	0.11	−0.03	−0.51	0.41	0.58	−0.07	−0.10	−0.09	0.15	Centimeters
Convergence near point	0.18	0.05	−0.48	−0.23	−0.12	−0.17	−0.08	−0.08	−0.29	Centimeters

tween actual distance of the fixated points and the true distance of the targets.

Brightness discrimination = difference between the standard and matched brightness value, in arbitrary units.

After completing the test battery, the subjects recorded their subjective reactions in each experimental session by means of a standardized questionnaire containing 10 items, such as smarting sensation in eyes and blurring of letters. The items were rated on a 5-point scale, ranging from "0" (absent) to "4" (extreme), and the score was calculated as the added sum of the 10 items.

In comparing 2 periods (e.g., before and after work) the biological direction of fatigue (deterioration) is indicated by the "−" sign, the direction of improvement by the "+" sign. Similarly, in comparing 2 illuminants, e.g., VR *versus* NW, the sign of the difference indicates the relative superiority (+) or inferiority (−) of the first illuminant as compared with the second illuminant. In other words, the direction as indicated by the "+" or "−" signs does not coincide with an increase or decrease of the actual score; for instance, an increase of the f.f.f. would indicate a physiological improvement (+), an increase of the recognition time would indicate a physiological deterioration (−). In a former communication (21), the "desirable" direction of the score was listed for all items.

In contrast to the questionnaire score, based on the negative impressions (complaints) produced by the visual strain, the preference scores represent a positive approach to the problem. The illumination levels (5, 50, 100, and 300 ft.-c) were identical for the 3 illuminants. The lamps were, as usual, concealed. The subjects entered the booths at random order; the time for inspection was not limited. They marked the most preferred illuminant as "1", the least preferred illuminant as "3"; thus the smaller score indicates a greater preference. The subjective preference scores were determined after the completion of the experimental series, i.e., after the subjects had worked for 3 months at frequent intervals (3 times a week) with one or the other illuminant.

SUBJECTS

The subjects were six men in their twenties who had served in the laboratory for some time as full-time experimental subjects. They were physically, mentally, and ophthalmologically normal. Their diet and daily routine and work were known, and any major interference from personal habits or accidental stresses could be excluded for the three months of the experiment. It may deserve emphasis that the subjects were completely disinterested in the specific results of these studies. They had previously demonstrated their willingness to do their best under conditions of

TABLE V. Effect of three different illuminants (Fr, NW, VR) on the changes (d) of ophthalmographic functions during visual work at 5 foot-candles. Mean values of 12 determinations. Negative values indicate deterioration.

Function	Fr	NW	VR
Movement phase, in 1/100 sec.	0.14	−0.73	−0.87
Angular velocity, arbitrary units	0.24	−0.58	−0.52
No. of movements, cycles per sec.	−0.26	−0.10	−0.19
Fixation phase, in 1/100 sec.	−1.64	−0.67	−1.09
Extent of movement during fixation phase, arbitrary units	−0.22	−0.62	−0.52
Discrepancy between fixation point and target, arbitrary units	0.26	−1.47	−0.15

TABLE VI. Average change of recognition time, flicker fusion frequency, and adduction power resulting from visual work under each illuminant (Fr, NW, VR), all illumination levels combined.

Function	Illuminant Fr $\bar{d}$	Fr F	NW $\bar{d}$	NW F	VR $\bar{d}$	VR F	Units
Recognition time	−2.24	12.61**	−3.36	17.61**	0.68	0.66	Seconds
Flicker fusion frequency	−1.3	34.08**	−1.6	67.92**	−0.1	0.48	Flashes per second
Adduction power	0.18	0.17	1.63	5.70*	1.24	5.02*	Diopters

$\bar{d}$=the mean difference between 36 pairs of measurements made before and after visual work under the illuminant indicated. Negative $\bar{d}$'s express deterioration.

F expresses the statistical significance of the mean changes ($\bar{d}$).

* F at 5 percent of significance is 4.13.

** F at 1 percent of significance is 7.44.

severe hardships and stress such as working under high temperature, several days of sleeplessness, or acute starvation. This was true also for the present series. In spite of the disinterestedness of the subjects, special precautions were taken to eliminate factors which have marred the results of many of the previous studies on illumination. The subjects were trained in the experimental procedures before the start of the experimental work proper. They were not aware of the specific factors investigated in a particular testing session. They worked in individual booths and the lamps were concealed. Furthermore, to preclude any subtle effects of suggestion, the four experimenters who applied the visual tests did not know with which lamp a particular subject was working on any given experimental day. The schedule was entirely in the hands of the assistant (A.B.), who was in charge of the work test. Only after the end of the experiments were the results decoded. Thus, the danger of the results being influenced by an uncontrolled change in attitude or motivation was eliminated; we tried rigorously to safeguard objectivity in collecting and evaluating the results.

TABLE VII. Mean differences ($\bar{\Delta}$) between three illuminants (Fr, NW, VR) at three levels of illumination, and their statistical significance.

Function	(F-test) Compared illuminants Fr:NW $\bar{\Delta}$	Fr:NW F	Fr:VR $\bar{\Delta}$	Fr:VR F	NW:VR $\bar{\Delta}$	NW:VR F	Level of illumination
Recognition time	2.5	1.90	−2.0	0.96	−4.5	5.86*	5 ft.-c
Flicker fusion frequency	0.4	0.65	−0.6	1.39	−1.1	3.16	5 ft.-c
Adduction power	−1.4	0.50	0.6	0.23	2.0	1.23	5 ft.-c
Performance average	−1.3	0.27	−6.5	6.46*	−5.2	2.84	5 ft.-c
Performance range	−1.0	0.50	−9.1	5.19*	−8.1	5.90*	5 ft.-c
Velocity	0.83	5.84*	0.76	2.26	−0.06	0.02	5 ft.-c
Average deviation	1.8	6.68*	0.4	0.64	−1.3	3.74	5 ft.-c
Recognition time	0.0	0.0	−3.6	8.48*	−3.6	8.19*	100 ft.-c
Flicker fusion frequency	0.2	0.27	−1.5	9.78**	−1.6	24.02**	100 ft.-c
Adduction power	−2.1	3.18	−1.9	1.69	0.2	0.01	100 ft.-c
Recognition time	0.9	0.35	−3.2	2.29	−4.1	3.11	300 ft.-c
Flicker fusion frequency	0.5	1.11	−1.4	10.76**	−1.9	19.92**	300 ft.-c
Adduction power	−0.8	0.97	−1.8	4.76	−1.0	0.92	300 ft.-c

Negative $\bar{\Delta}$'s indicate the relative inferiority, the positive Δ's a relative superiority of the first of the two illuminants compared.

F expresses the statistical significance of the mean differences ($\bar{\Delta}$) between the two compared illuminants.

* F at 5 percent of significance is 4.84.

** F at 1 percent of significance is 9.65.

Experimental Design and Statistical Evaluation

The three types of lamps were investigated at 5, 100, and 300 ft.-c. On each experimental day, all 3 illuminants were used at a given illumination level, 2 subjects working with each lamp. The subject pairs and illuminants were rotated in consecutive experiments. Each combination of subject pairs and illuminants was repeated twice. Thus, the scores obtained at each level of illumination are based on 12 observations for each illuminant.

In all functions except the average performance score and the average blinking rate, we are concerned with the differences between scores obtained before and after the visual work, or in the beginning and at the end. Therefore, for the purpose of condensation only these mean changes ($\bar{d}$) and not the absolute figures, are given in the tables. The differences ($\bar{\Delta}$) between the means ($\bar{d}$) were computed for pairs of illuminants.

For calculation of the statistical significance of the mean differences ($\bar{\Delta}$) between the illuminants the F-test was applied, using scores obtained by individual subjects under 2 illuminants as paired variates. When the calculations of significance were repeated by submitting the scores to a more elaborate analysis of variance, the results agreed with those obtained by the technique described above.

RESULTS

Tables II–V summarize the results obtained for the various visual functions. Out of the numerous

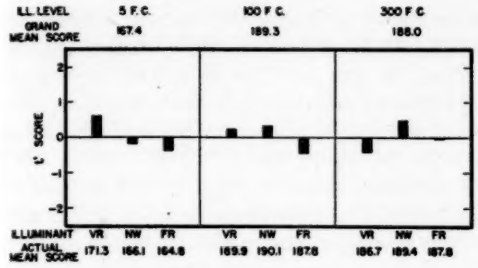

FIG. 3. Performance average.

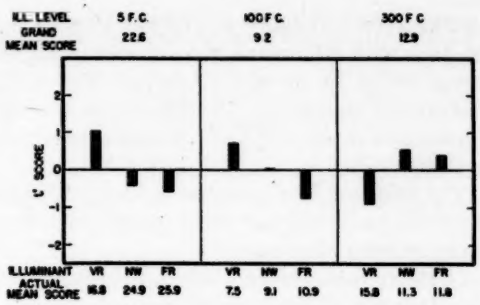

FIG. 4. Performance range.

functions investigated, comparatively few (average performance, performance drop, performance range, average blinking rate, recognition time for threshold size stimuli, f.f.f., questionnaire score) were sensitive to visual strain, as was discussed in the preceding communication.[21] Those functions which were inert, i.e., which failed to respond to the strain of the visual work or to differences in the illumination level, were also less likely to respond to comparatively slight variations in spectral distribution. This was actually the case.

In order to investigate the statistical significance of the fatigue effects in flicker fusion frequency (f.f.f.), recognition time, and adduction power, all three illumination levels were pooled. These functions indicated similar trends at all illumination levels (see Tables III and IV). Table VI shows that there is a highly significant over-all fatigue trend in the recognition time and f.f.f. both with Fr and NW lamps, while there is no significant deterioration with VR lamps. There was a significant "improvement" of the adduction power (probably caused by a temporary eye muscle adaptation) with NW and VR lamps and no such trend with Fr lamps.

Table VII shows the mean differences ($\bar{\Delta}$) between illuminants and their statistical significance. Only those functions with significant fatigue or illumination-level trends were included, except for angular velocity and average deviation of eye movements which were added because they differentiated significantly between two illuminants; the ophthalmographic functions were analyzed only for the 5-ft.-c level.

For the graphic presentation a new procedure was used, described elsewhere.[21] The differences between the illuminants are always referred to the mean score obtained for all three lamps. The deviations from the grand mean are expressed in terms of the average standard deviation of the mean differences ($\bar{\Delta}$). Consequently, both the absolute magnitude of the differences between illuminants and the variability of individual responses is taken into account. This procedure makes it possible to compare the effects of the 3 illuminants on various visual functions, as all differences are expressed in comparable units. The magnitude of the positive t'-scores indicates the relative superiority, of the negative t'-scores the relative inferiority, of the particular illuminant with reference to the particular function. The values were designated as t'-scores because of their fundamental relationship and similarity to the t-tests of significance of the differences between 2 means. For convenience the actual scores were included in the figures.

Figure 3 shows the values for the average performance. At the 5-ft.-c level, the performance with VR lamps is better than with NW or Fr lamps; the difference between the extremes (VR *versus* Fr) was statistically significant (see Table VII). At 100 and 300 ft.-c, there was no significant difference between the illuminants with reference to the performance score. The performance drop obtained as a difference between the performance score at the start and the end of the work period showed a significant fatigue decrement but did not differentiate significantly between the three illuminants.

The performance range (Fig. 4), obtained as the difference between the highest and lowest performance score during the work test, was found to be an important index for visual strain.[21] An increased performance range indicates in the present experiment a deterioration. At 5 ft.-c, the

performance variability was largest with Fr and smallest with VR lamps, the superiority of VR lamps *versus* Fr as well as *versus* NW being statistically significant. The differences between illuminants at 100 and 300 ft.-c were statistically not significant.

The blinking rate (average or change during the work task) did not show significant differences between illuminants.

Of the retinal functions tested, the recognition time for threshold size stimuli deteriorated most with NW lamps and least with VR lamps. The superiority of VR lamps *versus* NW lamps was significant at 100 ft.-c and at 5 ft.-c; at 100 ft.-c there was also a significant superiority of VR *versus* Fr lamps. The differences between Fr and NW lamps were not significant at any illumination level (Table VII, Fig. 5). The brightness discrimination did not show any significant differentiation between illuminants. The fusion frequency of flicker (f.f.f.) deteriorated most with NW lamps and least with VR lamps at all 3 illumination levels, the difference of VR both *versus* NW and Fr being highly significant at 100 and 300 ft.-c. The difference between NW and Fr lamps was statistically not significant (Fig. 6).

The ophthalmological routine tests failed to reveal any significant differences between illuminants. The deterioration of the velocity and the average deviation of eye movements from the target was significantly greater with NW lamps than with Fr lamps; the differences between illuminants in other ophthalmographic functions were statistically not significant.

The f.f.f. showed the same direction of differences between illuminants at all illumination levels and the differences were statistically significant at 100 and 300 ft.-c. On pooling the values for all 3 illumination levels the superiority of VR *versus* Fr lamps as well as *versus* NW lamps becomes highly significant (Table VIII), while the difference between Fr and NW remains insignificant. The differences between illuminants with reference to the questionnaire scores were not significant at any single level of illumination. Using the procedure of pooling illumination levels, the inferiority of Fr lamps *versus* NW and VR lamps became statistically significant.

Table IX shows subjective preferences at four illumination levels. There was no significant difference between Fr and NW lamps whereas the subjective preference for VR *versus* Fr or NW was statistically highly significant.

Discussion

The results indicate that, as a rule, the visual functions found to be sensitive to visual strain resulting from prolonged work at different levels of illumination intensity also differentiated between the illuminants. In the present experimental arrangement the differences between illuminants in regard to the illumination intensity were eliminated and the differences in brightness distribution minimized. Therefore, the differences in the spectral distribution remain as the only experimental variable.

We tried to eliminate, as far as possible, the more remote effect of color on the central nervous system and believe that the differentiation between illuminants in our series is due mainly to

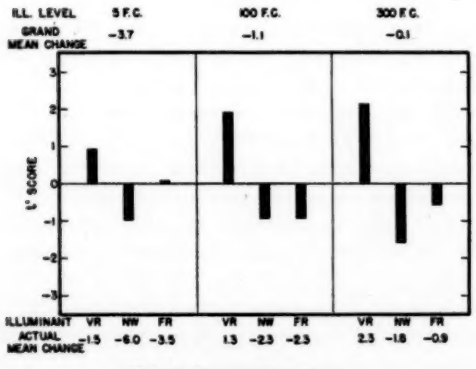

FIG. 5. Recognition time.

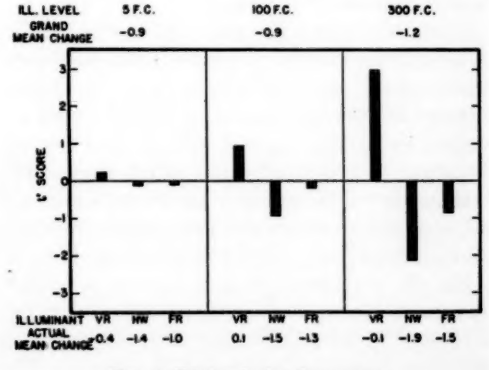

FIG. 6. Flicker fusion frequency.

the more direct action on visual functions; changes of motivation or emotion played only a secondary role, if any.

The differentiation between the illuminants is in general in favor of VR lamps, these lamps being superior to either NW or Fr lamps. The differences between Fr and NW lamps were statistically not significant except for maximum velocity and deviations of voluntary eye movements ophthalmographically recorded, which showed a significant superiority of Fr lamps.

At the present time, no definite explanation of our results can be given. However, several alternative suggestions may be offered:

(1) The relative superiority of VR lamps is due to the reduction of blue radiation. This would explain satisfactorily the difference between VR and Fr or NW lamps. The spectral difference between Fr and NW lamps might have been too small to show up in the results, but a tendency to some inferiority of NW lamps compared with Fr lamps was observed; this would agree with the above hypothesis.

(2) The relative superiority of VR lamps is due to the greater reduction in the red part of the spectrum. This would not explain the absence of differentiation between NW and Fr lamps. However, it is possible that there is a critical level for physiological effects of the reduction in red radiation, which is exceeded in VR but not in NW lamps. Such a critical level has been shown to exist for injury produced by heat radiation,[22] though on a much higher level of intensity. Since only a small part of the spectral radiation is absorbed as energy utilizable for vision, the greater part is absorbed as heat but it is not probable that heat effects could account for the differences between illuminants. The evidence for heat injury is almost exclusively histological or clinical yet a heat effect on visual performance or visual fatigue, on a much lower level of radiation intensity, is not impossible. However, in the case of heat effects, the superiority of VR lamps should increase with the illumination level. This is not the case as far as the performance indexes are concerned; only the f.f.f. fatigue decrement could be interpreted in this way.

[22] F. H. Verhoeff and L. Bell, "The pathological effects of radiant energy on the eye," Proc. Am. Acad. Arts and Sci. 51, 630 (1916).

TABLE VIII. Mean differences in flicker fusion frequency and questionnaire score between illuminants (Fr, NW, VR), all illumination levels combined, and their statistical significance (F-test).

	Compared illuminants						
	Fr:NW		Fr:VR		NW:VR		
Function	$\bar{\Delta}$	F	$\bar{\Delta}$	F	$\bar{\Delta}$	F	Units
Flicker fusion frequency	0.36	2.03	−1.16	17.73**	−1.52	32.97**	Flashes per second
Questionnaire score	−1.8	5.90*	−1.5	4.51*	0.3	0.19	Arbitrary units

Negative $\bar{\Delta}$'s indicate greater deterioration at the first of the two compared illuminants.

F expresses the statistical significance of the mean difference ($\bar{\Delta}$) between the two compared illuminants.

* F at 5 percent of significance is 4.13.

** F at 1 percent of significance is 7.44.

(3) If the distribution curve for the utilizable energy (Fig. 2) is used as a basis for explanation, the differences in the blue and red ends are minimized, whereas the differences in the middle part of the spectrum become more prominent and could be conceived as the basis for the observed physiological differences. The dislocation of the curves with reference to the spectral sensitivity curve of the human eye is greatest for the frosted lamps. On the basis of this hypothesis, the superiority relationship VR > NW > Fr should be expected, while the actual situation was VR > NW = Fr. It also should be noted that the sensitivity curve of the human eye is a curve of threshold values, while the actual visual performance is done at values many times higher.

It seems that hypothesis (1) is the most satisfactory at the present time, although it is quite possible that several factors are involved. The situation is complicated by possible inhibitory or facilitative effects between various wave-lengths.[17]

When we started the experiments we expected that the differences between the illuminants—if any—would be greatest at the lowest illumination level (5 ft.-c) because the visual strain is greatest

TABLE IX. Subjective preference scores (average values of 6 subjects).

Illumination level, in ft.-c	VR	Fr	NW
5	1.17	2.50	2.33
50	1.33	2.33	2.33
100	1.25	2.33	2.42
300	1.42	2.17	2.42
Mean of all illumination levels	1.29	2.33	2.37

under this condition. However, this was the case only for the average performance and the performance range. In the f.f.f., the differences between VR and Fr or NW lamps were more marked at 100 and 300 ft.-c than at 5 ft.-c. The statistical significance of the differences in the recognition time is greatest at the 100-ft.-c level. In this connection it is interesting to note that several other authors[4, 6, 7] had found that the color effects on visual acuity or recognition speed increased with the level of illumination.

In our experimental arrangement the three illuminants were compared at the same illumination level on the screen with the letters. For practical applications it would be important to know whether a comparison of the illuminants on an equal wattage basis might change the differentiation between illuminants. Undoubtedly, the lamps would be replaced or interchanged on such basis in the practical use, although this is not a rational approach to secure optimum illumination conditions on the working place. No direct answer can be given on the basis of the present work but the speculation can be carried on a reasonably safe ground. The lumen output of VR and NW lamps corresponds to about 85 and 84 percent of the lumen output of Fr lamps. The differences obtained for the central beam are greater (about 20 to 25 percent), caused by the more even brightness distribution on the surface of VR and NW lamps. The difference between the illumination levels obtained with VR and NW lamps of equal wattage is negligible. Therefore, the question narrows down to differences between VR and Fr lamps. A 25 percent difference in the illumination level is probably too small to affect the direction of the differences between the VR and Fr lamps in regard to the retinal functions (f.f.f. and recognition time) or subjective preference score. The work performance averages show no significant differences between 50 and 300 ft.-c, neither are there significant differences between illuminants. The question of the relative importance of spectral quality *versus* intensity of light may be more relevant for the low levels of illumination, where the performance improves noticeably as the illumination increases.

It is interesting to note that the subjective preference scores correspond to the objective findings. The same observation was made in regard to the illumination level.[21] Although the subjective responses alone should not be used to replace objective evidence, the relative comfort and preference constitute a valuable index which cannot be ignored in the integrative analysis of conditions of illumination. It appears worth while to investigate illuminants with other spectral distributions than those of the 3 illuminants used in this study. At present no statement can be made as to whether the spectral distribution of VR lamps is actually the optimum attainable.

ACKNOWLEDGMENT

We wish to thank Mr. Levi, Director of Research, Verd-A-Ray Corporation, Toledo, Ohio for the measurements of the spectral radiant intensity of the lamps.

Erratum: Some Considerations of the Effect of Radiation on the Performance of Liquid Fuel Rockets

[J. Opt. Soc. Am. **38**, 599 (1948)]

S. S. PENNER AND S. WEINBAUM
Jet Propulsion Laboratory, California Institute of Technology, Pasadena, California

THE factor 6 in Eqs. (11), (12), and (13) should be replaced by 4 in order to allow for the fact that the mean path length through a sphere approaches the value $2\delta/3$ as the product $k\rho\delta$ approaches zero.[1]

The statement that the evaluation of the mean radiant intensities was carried out by an approximate procedure was inadvertently omitted. The approximation involved in the present treatment is of the same order as the approximation involved in the mean path method of Hottel.[2] The rigorous treatment requires integration over solid angles and has been given by Schmidt[3] for a stationary point at the center of the base of a finite cylinder.

[1] H. C. Hottel, Trans. A. I. Chem. Eng. **19**, 173 (1927).
[2] H. C. Hottel and R. B. Egbert, Trans. A.S.M.E. **63**, 297 (1941).
[3] E. Schmidt, Zeits. V. D. I. **77**, 1162 (1933).

JOURNAL OF THE OPTICAL SOCIETY OF AMERICA VOLUME 38, NUMBER 10 OCTOBER, 1948

The Effect of High Index Glasses on the Field Characteristics of Photographic Objectives

G. H. AKLIN
Eastman Kodak Company, Rochester 4, New York

(Received May 10, 1948)

Improving field characteristics of photographic objectives has always been the concern of the lens designer. Progress has followed the introduction of glasses with high index and low dispersion. These new glasses have been used in the collective lenses in such a manner as to increase the index difference between collective and dispersive elements. This has the effect of basically moving both tangential and sagittal focal points closer to the focal plane throughout the zonal portions of the field, improving Petzval sum, and increasing covering power. Variations of zonal corrections and covering power with these basically improved characteristics are discussed.

The high index glasses disclosed in U. S. Reissue 21,175 (Morey) and in the more recent patents by DePaolis and Eberlin have been used in a number of lens systems. Comparative examples are shown to illustrate the extent to which Petzval sum is improved and/or covering power is increased with the use of these glasses.

MARKED improvements in field characteristics of photographic objectives have followed the introduction from time to time of glasses with higher indices and relatively low dispersion. Each time one of these glasses has been made available, it has resulted in a series of new lens formulae; often many optical design inventions are made, and we find the developments charted in the patent literature. These new glasses have been used in the collective components, so that the total effect has been to raise their indices as compared with those of the dispersive components. This is the established procedure toward basically improving field characteristics. It might be added here that a glass having relatively higher dispersion for its index, to be used in the negative components, would be another step in the desired direction as it would permit use of crown glasses whose index is high but whose dispersion is high also.

In designing a lens system, there is obtained a certain balance of dispersions and focal lengths of the individual elements for achromatization. Changes made in index or dispersion must be done in such a manner as to maintain this balance. As any increase in index made in a collective element to improve the field generally carries along with it a change in dispersion, there must be made such a change in a negative element that will compensate for it, and at the same time bring about the increased index difference that is desired.

In most lens systems the residual astigmatism is so adjusted that the primary and secondary (or tangential and sagittal) focal points are in the most favorable position for the best available imagery on the focal plane. Field curves here are more or less standard; that is, in the zonal portions the secondary remains farther inward than the primary, they form a node at a certain obliquity, and then proceed to separate rapidly at the larger angles, until the secondary has moved so far backward and the primary so far inward that the image forming quality has disappeared. Regardless of this adjustment, it is the object of all designers to improve field characteristics by attaining to some degree the following results:

1. A shift of both tangential and sagittal focal points closer to the focal plane, giving reduced astigmatism.

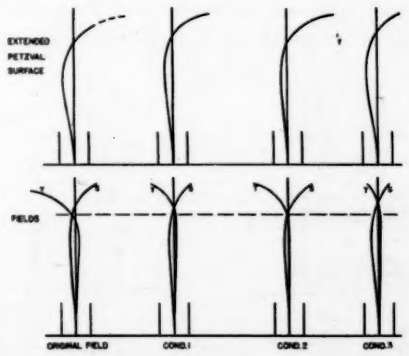

FIG. 1.

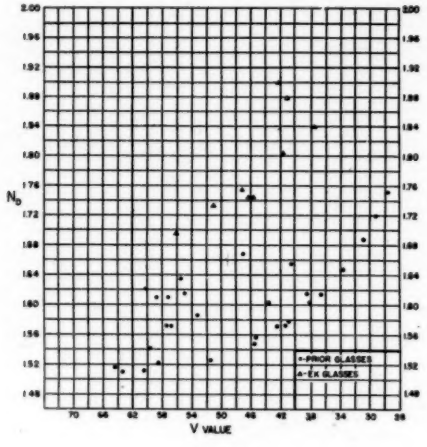

FIG. 2.

2. An increase in the angle at which the node occurs, thus increasing the covering power of the lens system.

The Petzval sum, which in most systems is a positive quantity, is a criterion for judging how the Petzval surface starts out from the lens axis. An improvement in or diminishing of the Petzval sum is generally taken to mean an improvement in zonal field characteristics, but tells us nothing of covering power. If we wish to diminish this sum by a strengthening of surface powers alone, we know then that our zonal images will move closer to the focal plane, but that also the angle at which the node occurs will diminish, sacrificing covering power for an improved zone.

However, experience has taught us that when we diminish the Petzval sum by increasing the above-mentioned index difference and maintaining surface powers, zonal characteristics are improved, covering power is increased, and the amount of improvement is more or less dependent on the amount of this increase. Variations of field improvements will be discussed in a following paragraph.

It must be said, however, that different lens types react differently to these glass changes, as do different systems of the same type, the relative powers of the individual elements being more or less different from one another. We therefore must expect different types of results in making certain index changes, depending on the type of system. For example, if we have two lenses of the *H*-type (of which the Tessar is a well-known example), but one with the arrangement of the two rear components reversed from the other, and then make the same increase in index in the collective element of this component, we can certainly expect an improvement in the field characteristics, but the amount of improvement will not be the same. Therefore each type or system is more or less a problem in itself.

From the above comments, field improvements are then obtained under the following conditions:

1. An improvement in zonal characteristics or improvement in Petzval sum, and an increase in covering power. This, as stated, is obtained by increasing the index of the collective components as compared with dispersive, and maintaining surface powers or component focal lengths.

2. A further reduction in the amount of astigmatism throughout the zonal portion of the field, maintaining the node point at the original obliquity. This would be the result of strengthening surface powers along with the index change. The Petzval sum here would be diminished further as compared with condition 1.

3. An increase in covering power over the amount gained in condition 1, maintaining the original zonal characteristics that were considered passable before any glass changes were made. This would be the result of weakening surface powers along with the index difference increase, maintaining substantially the original Petzval sum.

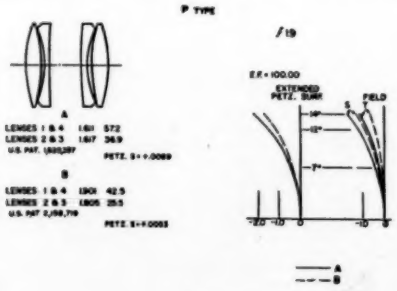

FIG. 3.

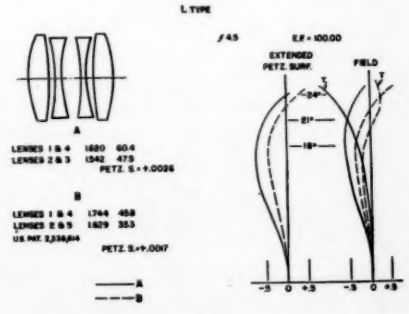

FIG. 4

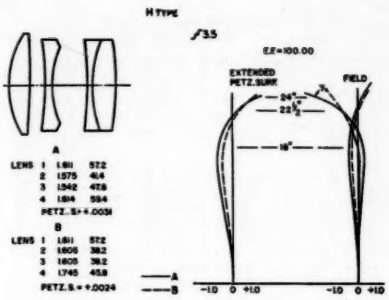

FIG. 5.

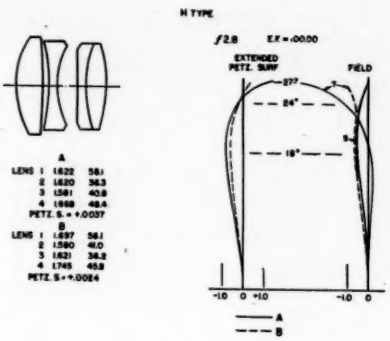

FIG. 7.

In order to compare fields of the different systems more readily, all the following figures include an "extended Petzval surface." This can be defined as the locus of points situated 3 times as far from the tangential image-surface as from the sagittal. It, of course, becomes the same as the true Petzval surface in the neighborhood of the lens axis, but in the outer parts of the field it has a double curvature and may be considered as representing the field characteristics of the lens system.

Figure 1 illustrates the above three conditions and demonstrates the relative change in the extended Petzval surface.

Covering power is a function of the flatness of the tangential and sagittal curves and not necessarily dependent on a node point. If, as shown in a number of the following examples, the tangential and sagittal curves are close to each other for some distance out from the axis, the proximity of these two curves to one another and their distance from the focal plane will be the deciding factor on covering power. Also, when surface powers are strengthened along with an increase in index difference (condition 2), the flattened character of the new tangential and sagittal curves, as compared with the original, allows for a covering power increase, although the new node point may be at a considerably smaller angle.

The high index glasses as disclosed in patents by Morey, DePaolis, and Eberlin* have been used in a number of lens systems. Along with these, glass changes were made in the negative elements so as to obtain the increase in index difference as described above. Field improvements in these different lens systems vary in character, depending on whether or not any additional surface power changes were made with index changes. That is, some examples show only zonal improvements, while others show a combination of zonal and covering power changes.

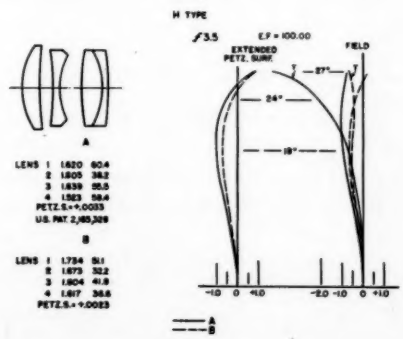

FIG. 6.

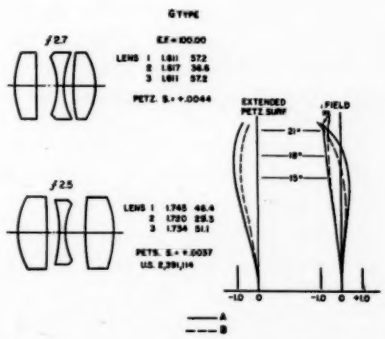

FIG. 8.

* U. S. Reissue 21, 175 (Mory); U. S. 2,241,249 Eberlin and DePaolis; U. S. 2,434,149 DePaolis.

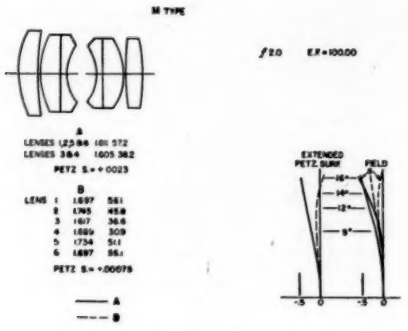

FIG. 9.

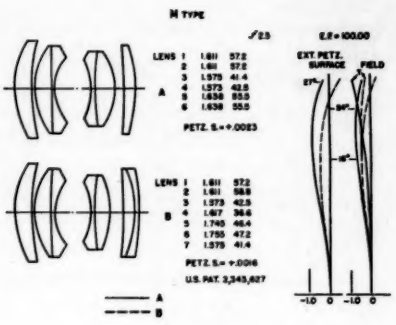

FIG. 10.

Figure 2 shows the position of the new glasses on the regular index and dispersion chart.

The following figures all show comparable lens systems, one using prior glasses and another in which new glasses have been introduced. The comparative examples to be shown are according to the lens classification as given by R. Kingslake in the May 1946 issue of the Journal of the Optical Society of America.

Figure 3 shows comparative systems of the *P*-type; Fig. 4 shows comparative systems of the *L*-type; Fig. 5 shows comparative systems of the *H*-type (f:3.5); Fig. 6 shows comparative systems of the *H*-type but reversed rear (f:3.5); Fig. 7 shows comparative systems of the *H*-type (f:2.8); Fig. 8 shows comparative systems of the *G*-type; Fig. 9 shows comparative systems of the *M*-type (narrow field); Fig. 10 shows comparative systems of the *M*-type (wider field).

It will be noted that in all of the new formulae the greatest change occurs in the shape of the tangential curve, tending to approach the shape of the sagittal. If now along with this we could have some way of rapidly flattening the sagittal, then we would really overcome the astigmatic differences in our fields.

We have chosen to discuss only field characteristics here, as these improvements appear to be the most important effect of using the new glasses. However, it may be said that spherical aberration has tended to improve also, but in most lens systems the axial aberrations are satisfactory and definitely better than the field images which have given the lens designer the greatest concern. If some manner of rapidly improving the sagittal field were obtained, then we might possibly encounter the problem of keeping the axial images looking as good as the field images.

Although there are other lens types using the new glasses that have excellent field characteristics, they have not been discussed here, as no strictly comparable examples using the prior glasses were available.

In conclusion, I should like to express my thanks to those of my colleagues who have given their helpful ideas in the preparation of this paper.

JOURNAL OF THE OPTICAL SOCIETY OF AMERICA VOLUME 38, NUMBER 10 OCTOBER, 1948

The Infra-Red Sensitivity of Superconducting Bolometers

NELSON FUSON
Johns Hopkins University, Baltimore, Maryland
(Received May 10, 1948)

Columbium nitride superconducting bolometers have been studied for sensitivity when irradiated with a wide band of modulated infra-red radiation of about 0.1 microwatt/mm² intensity. The bolometer response was amplified by means of a matching input transformer and wide-band amplifier. Time constants for different bolometers ranging from 0.7 to 17.0 milliseconds were observed. Comparisons are given between these superconducting bolometers and other infra-red detectors described in the literature on the basis of reference conditions suggested by Jones (reference 1). Of the 25 superconducting bolometers studied in detail the 9 most sensitive had figures of merit ranging from 14.0 to 1.3.

INTRODUCTION

A SUPERCONDUCTOR is a substance which when cooled through a small temperature interval around a critical low temperature loses its normal resistance characteristics and has zero resistance. If the temperature of such a material can be maintained at the point where it is halfway between its normal resistance state and its zero resistance or superconducting state, it will have, for small temperature changes within the transition interval, a high rate of change of resistance with temperature. During the past few years two types of bolometers making use of this property of high dR/dT have been developed, one using tantalum,[2] and another, columbium nitride.[3,4] The former requires the use of liquid helium to reach its transition temperature. The transition temperature of the latter, around 15°K, falls just slightly above the triple point of hydrogen, making the transition temperature easier to reach and the temperature control problem simpler to solve. All the bolometers described in this paper are of the latter type.

BOLOMETER CONSTRUCTION

The method of bolometer construction outlined by Milton[4] was followed in the main, although the type of bolometer base was altered in order to permit insertion of the bolometer into the optical path of an infra-red spectrometer. As may be seen in Fig. 1, the bolometer consists of a strip of columbium nitride (CbN) 5 mm by 0.5 mm in area, and either 0.006 mm or 0.025 mm thick, fastened to a $\frac{1}{8}$-inch copper rod base with Bakelite lacquer so that it is electrically insulated from, but thermally in fairly good contact with, the base. Fine copper lead wires, soldered to the copper-plated ends of the CbN strip, enable it to be included in the electric circuit.

The bolometers range widely in size. Usually about half the over-all length is taken up with the solder connections to the lead wires at each end, so, on the average, the bolometer receiving area is about 2.5×0.5 mm². The brittleness of the CbN often limits the size and regularity of the flake which can be cut out of the ribbon stock. Some difficulty has been encountered in making bolometers with receiving areas which are 4 mm or greater in length while at the same time no wider than 0.5 mm.

An attempt was made to correlate the thickness of the Bakelite layer separating the CbN flake from the copper base with the time constant of the corresponding bolometer. Since the insulating layer is applied with a brush and since the CbN flake is not always flat, precise measurements of the Bakelite thickness were not justified. The correlation is very approximate and may be summed up as follows: for a "thin" coating of the lacquer (*ca.* 0.025 mm) the bolometer time constant will range from 0.7 to 4.0 milliseconds; for a "thick" coating (*ca.* 0.12 mm) the time constant will fall between 4.0 and 20 milliseconds.

[1] R. Clark Jones, J. Opt. Soc. Am. **37**, 888 (1947).
[2] D. H. Andrews, W. F. Brucksch, Jr., W. T. Ziegler, and E. R. Blanchard, Rev. Sci. Inst. **13**, 281 (1942).
[3] D. H. Andrews, R. M. Milton, and W. DeSorbo, J. Opt. Soc. Am. **36**, 518 (1946); D. H. Andrews, Phys. Soc. Cambridge Conference Report, p. 56 (1947).
[4] R. M. Milton, Chem. Rev. **39**, 419 (1946).

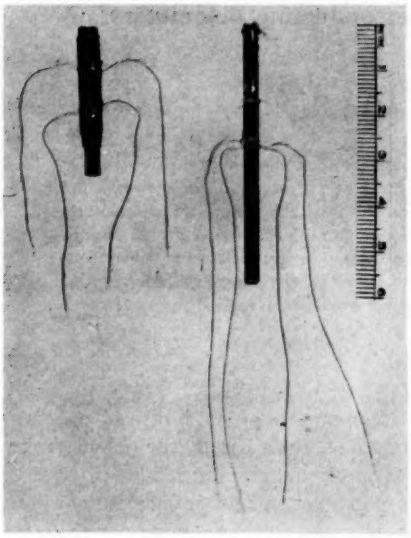

FIG. 1. Superconducting bolometers. The short thick base type, which represents a transition from the cup-shaped bases previously made, is being replaced by the long slim base for use in spectrometers.

EQUIPMENT

Figure 2 is a block diagram of the equipment used in the tests to be discussed. The infra-red source was an oxidized iron plate, heated to a temperature of 100°C by a Nichrome heater, its temperature being measured by a Chromel-Alumel thermocouple. The radiation modulator was an aluminum disk slotted in such a way that the opaque portions were equal to the apertures. This disk, rotated on the armature shaft of a synchronous motor, interrupted the radiation at 360 c.p.s. The wave form was approximately a square wave. The aperture which defined the size of the radiation source as seen by the bolometer was usually square, with an area of

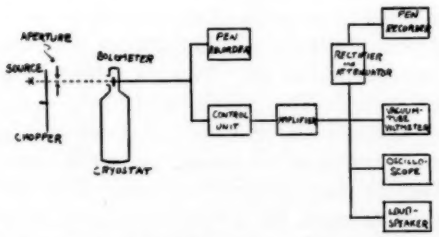

FIG. 2. Block diagram of apparatus used in testing sensitivity of bolometers.

0.5 cm². The radiation source, rotating disk, and aperture were all close together, and the bolometer was usually placed about 30 cm from the aperture.

The radiation signal power, ΔJ, in watts, was computed by the expression

$$\Delta J = Aa\phi(T)/d^2, \tag{1}$$

where A is the area of the source aperture, a the area of the bolometer, d the distance between source aperture and bolometer, and

$$\phi(T) = (\sigma/\pi)(\alpha_1\beta_1 T_1^4 - \alpha_2\beta_2 T_2^4) \times 10^{-7}, \tag{2}$$

where α_1 is the blackbody coefficient of the source, β_1 the rocksalt window transmission coefficient for radiation going from source to receiver, and T_1 the temperature of the source; α_2, β_2, and T_2 are the same quantities for the rotating disk shutter, and σ is the Stefan-Boltzmann constant. Using the following values,[5] $\alpha_1 = 0.79$, $\alpha_2 = 0.10$, $\beta_1 = 0.70$, $\beta_2 = 0.56$, and $T_2 = 300°\text{K}$, Eq. (2) reduces to

$$\phi(T_1) = 1.02 \times 10^{-12}(T_1^4 - 8.1 \times 10^8). \tag{2a}$$

The cryostat used (see Fig. 3) was of the same general type used previously in this laboratory,[3] but with improved materials, better thermal insulation, and different bolometer support and shielding design. The "heat leak" to the inner pot which contains the liquid hydrogen was about 0.25 watt under static conditions for this modified cryostat. A single filling with 500 cc of liquid hydrogen maintained operating conditions for 24 hours, although it was necessary to refill the outer pot with liquid nitrogen at about 10-hour intervals. The equilibrium temperature of the bolometer support base or "sink" was regulated by adjusting the pressure of the vapor over the liquid hydrogen, and was computed by using the vapor tension curve for hydrogen. The pressure control rig is illustrated in Fig. 4. It was possible with this control system to cause the pressure, and accordingly the "sink" temperature, to rise or fall at a uniform rate through the transition interval. For these particular experiments this method of control of temperature proved more flexible than the method[3,4] in which the liquid hydrogen is maintained at the triple point and the bolometer transition temperature

[5] These values, together with the form of Eq. (2), are taken from pages 427–8 of reference 4.

adjusted by using a heater coil located on the copper support between the liquid hydrogen and the bolometer.

The current control unit (see Fig. 2) contained a source of d.c. power for the bolometer circuit as well as connections for checking the potential drop across, and the current through the bolometer. The amplifier used was a 2-tube, wide-band (100–4000 c.p.s.) amplifier with a gain of about 20,000. It was fed by an input transformer which matched 2.5 ohms to 1.1 megohms with a theoretical gain of 666. The over-all gain at 360 c.p.s. was about 8×10^6. Departures from linearity were corrected for in computing bolometer level outputs. The noise level of the apparatus computed at the bolometer level was about 0.01 microvolt. The amplified bolometer a.c. signal was observed on a vacuum-tube voltmeter and an oscilloscope; a rectified portion of the amplifier output was fed to a potentiometer pen recorder. Proper shielding eliminated any noise of a modulated radiofrequency nature.[6]

For time constant measurements a thyratron controlled, variable speed motor driven, perforated disk radiation chopper was employed, the radiation source being a 6-volt auto headlight bulb. This source gave sufficient intensity to produce a measurable output over the wide frequency range of 15 to 3000 c.p.s. For this work a 2-tube amplifier, without input transformer, was used. It had an over-all gain of about 18,000 and was fairly flat over the range studied.

RECORDS

Two types of records were obtained simultaneously during most of this work. The first type (hereafter called the transition curve) was a record of bolometer resistance as a function of "sink" temperature. It was obtained with a potentiometer pen recorder connected directly across the bolometer. Figure 5 shows a transition record for bolometer No. 13. For this type of record the ordinate, the d.c. potential drop across the bolometer, is proportional to the bolometer resistance; the abscissa, time, is proportional to the bolometer "sink" temperature. From the transition curve for very small bolometer currents the dR/dT can be computed.

[6] D. H. Andrews and C. W. Clark, Nature **158**, 945 (1946); Phys. Rev. **72**, 161 (1947).

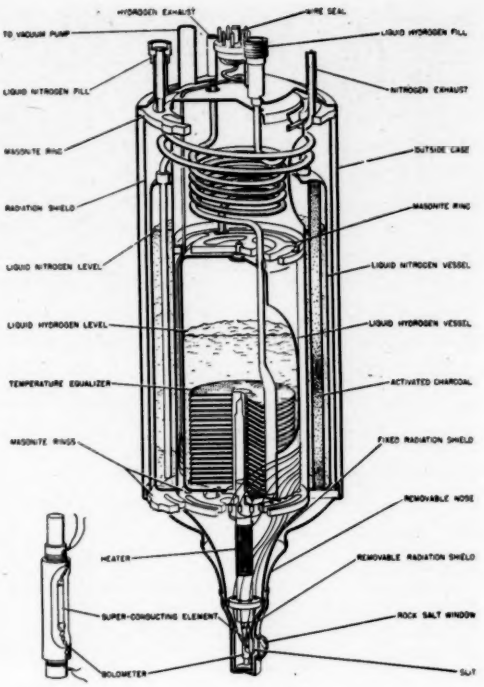

FIG. 3. Diagram of cryostat designed to accommodate the short thick base type of bolometer.

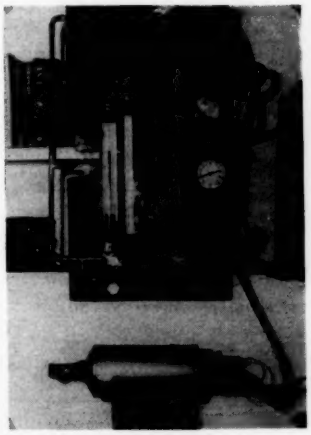

FIG. 4. Photograph of the pressure control rig. The gauges include a dial-type pressure gauge, a closed tube mercury manometer, and a pressure differential oil manometer. The small valve in the lower left is a fine adjustment bypass valve. The lowest tube leading off to the right goes to a vacuum pump; the one immediately above it opens to the air; the tube at the top right of the board is attached to the hydrogen pot of the cryostat by means of the rubber pressure tubing.

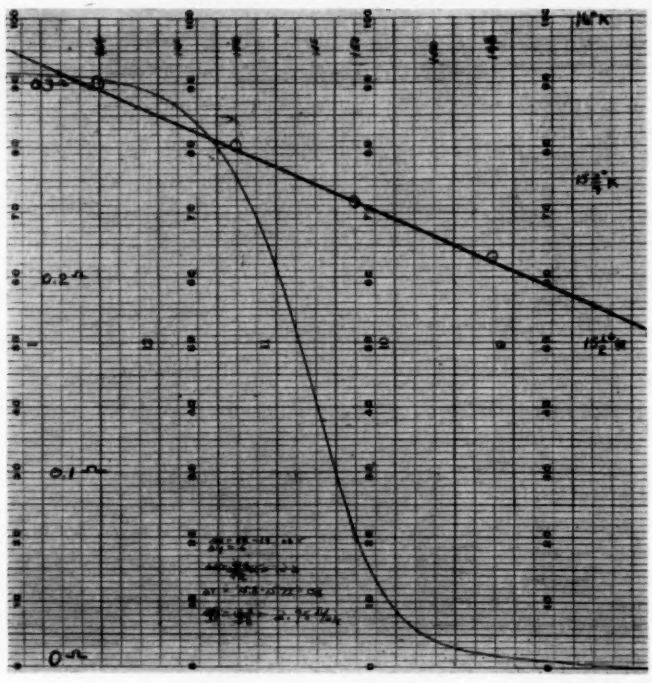

FIG. 5. Photograph of transition curve for bolometer No. 13 for a bolometer current of 31 ma. The slanting straight line indicates the steady rise in "sink" temperature from 15½°K to 16°K as the bolometer resistance changes along the "transition" curve from zero to 0.3 ohm.

If the bolometer No. 13 is exposed to a very slow (⅓ c.p.s.) modulated radiation beam of high infra-red intensity (100 microwatts/mm²) the transition curve appears as in Fig. 6. Here the bolometer resistance varies periodically with fluctuations of bolometer temperature (but not of "sink" temperature) and these variations are seen to be the greatest in the steepest part of the transition, disappearing gradually as the bolometer becomes either superconducting or normally conducting, i.e., where the dR/dT approaches zero. As the signal modulation becomes more rapid and the radiation less intense, these fluctuations become very small and finally cannot even be seen in mid-transition because of the limitations of both speed and sensitivity of the pen recorder (see Fig. 5). It is therefore necessary to amplify and rectify this fluctuating component and to record it upon another potentiometer pen recorder. For this second type of record (called the bolometer response record) shown in Fig. 7, the ordinate, the rectified amplifier output potential, ΔE_{out}, is proportional to the radiation signal intensity, ΔJ; the abscissa, time, is proportional to the "sink" temperature.

EXPERIMENTAL PROCEDURE

A few hours before a bolometer test was to be made, the vacuum jacket of the cryostat in which the bolometer had been installed was connected to a mechanical vacuum pump and evacuation begun. An hour before the test, the vacuum jacket was sealed off with a pinch clamp on the rubber connecting hose. The outer pot was then filled with liquid nitrogen, an operation taking about 10 minutes. A half-hour before the test the inner pot was filled with liquid hydrogen, another 10-minute operation. The filling in each case was done by blowing the liquid out of its container into the cryostat pot under several pounds' pressure of hydrogen or helium gas. The evolution rate of gas from both the inner and outer pots was then determined (by simply timing the displacement of water from a graduated container) in order to check the respective heat leaks and to assure that the cryostat would keep the bolometer cooled the desired length of time. An evolution of 400 cc/min. of hydrogen gas from the inner pot indicated good working conditions. Evolution rates more than twice as great warned of the necessity to examine the

cryostat for possible vacuum leaks or for metallic contacts between the inner pot, bolometer, or radiation shields and the outer case.

Heat leak tests having appeared satisfactory, the cryostat's inner pot exhaust tube was attached to the pressure control rig and the liquid hydrogen container evacuated until its vapor pressure was about 5 to 10 cm Hg, corresponding to a temperature of 14° to 16°K, the region within which the average CbN bolometer will "go super" unless it is faulty in some way. If the bolometer's superconducting transition was satisfactory, the bolometer was exposed to the standard intensity of infra-red modulated radiation (0.1 microwatt/mm²) and lined up for maximum signal response in mid-transition. After proper lineup the bolometer current was adjusted to give maximum signal as the bolometer was first cooled down then warmed up through the transition region by raising and lowering the "sink" temperature. Upon obtaining the best optical lineup and current setting, simultaneous records of the transition curve and the infra-red response were made with the bolometer both cooling and warming through transition.

A second pair of simultaneous records were then made under identical circumstances, save that an opaque shutter was inserted to shield the bolometer from the modulated radiation. The bolometer response record in this case is just a record of the background noise, ΔE_{noise}(out), through transition. In both pairs of records the maximum bolometer responses (response to radiation signal and to noise, respectively) were noted on the vacuum-tube voltmeter and written in on the potentiometer records for use in signal-to-noise ratio calculations.

Finally, with the bolometer current unchanged, data was taken from which the time constant could be calculated.

THE RESULTS

Having obtained the best signal-to-noise ratio for the bolometer for a known intensity of infra-red radiation, the minimum detectable signal, ΔJ_{min}, and the sensitivity ratio, ϵ, could be calculated from

$$\Delta J_{\text{min}} = \Delta J/(\Delta E_b/\Delta E_n) \tag{3}$$

and

$$\epsilon = \Delta E_b/\Delta J. \tag{4}$$

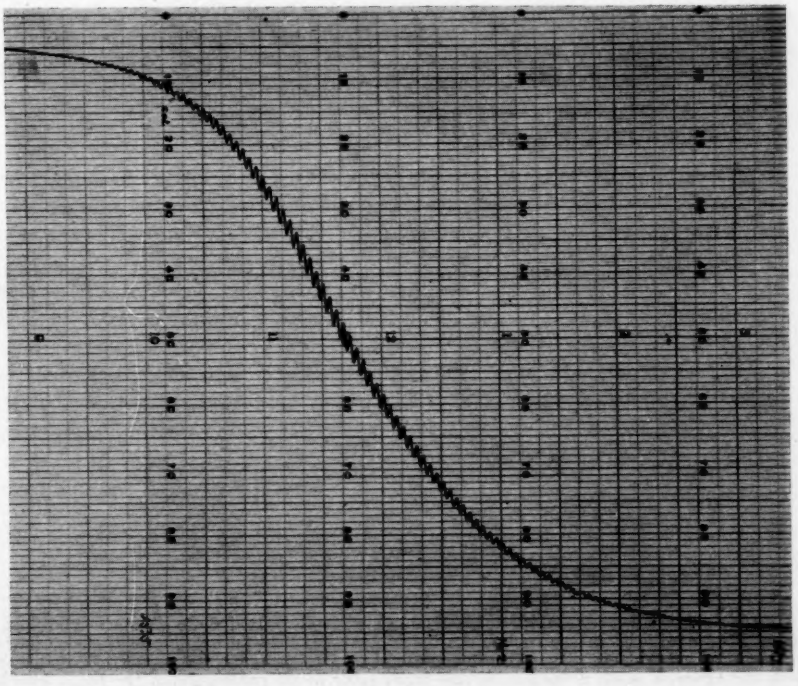

FIG. 6. Photograph of transition curve for bolometer No. 13 with current of 31 ma. Intense radiation (100 microwatt/mm²) modulated at ½ c.p.s. causes the fluctuations which are the greatest in the steepest part of the transition curve.

Table I summarizes the results on the CbN superconducting bolometers. Column 1 gives the number identifying each bolometer. The letter following each number refers to the sample of CbN ribbon from which the bolometer was made. The final number is 1 or ¼, depending upon whether the bolometer flake thickness is 1 mil or ¼ mil. Column 2 gives the bolometer current for maximum sensitivity. Column 3 is the bolometer resistance and column 4 is the bolometer dR/dT, both obtained at point of maximum sensitivity. Column 5 is the total radiant power incident upon the bolometer. Column 6 gives the calculated Johnson noise of the bolometer at temperature of 300°K while column 7 lists the experimentally obtained noise at the bolometer level and is greater than the calculated value, partly because of the amplifier noise and possible 60-c.p.s. hum pick-up, and in some cases because of particularly "noisy" bolometers. Column 8 is the bolometer signal output, column 9 gives the signal-to-noise ratio (using the experimentally obtained noise voltage from column 7), column 10 lists the sensitivity ratio as defined by Eq. (4), and column 11 gives the minimum detectable power as defined by Eq. (3).

COMPARISON OF SENSITIVITY OF DETECTORS AT "REFERENCE CONDITIONS"

In order to compare the sensitivity of these superconducting bolometers among themselves and with that of other detectors, it is necessary to take into consideration not only the area and time constant of the detector but also the modulation frequency and the amplifier's noise equivalent band width. For such an over-all comparison use has been made of the "reference conditions" suggested by R. Clark Jones,[7] which can be summarized as follows: under reference conditions the detector is irradiated with a steady signal; the amplifier used has a flat frequency characteristic except for a simple high frequency RC cut-off whose time constant, RC, is equal to

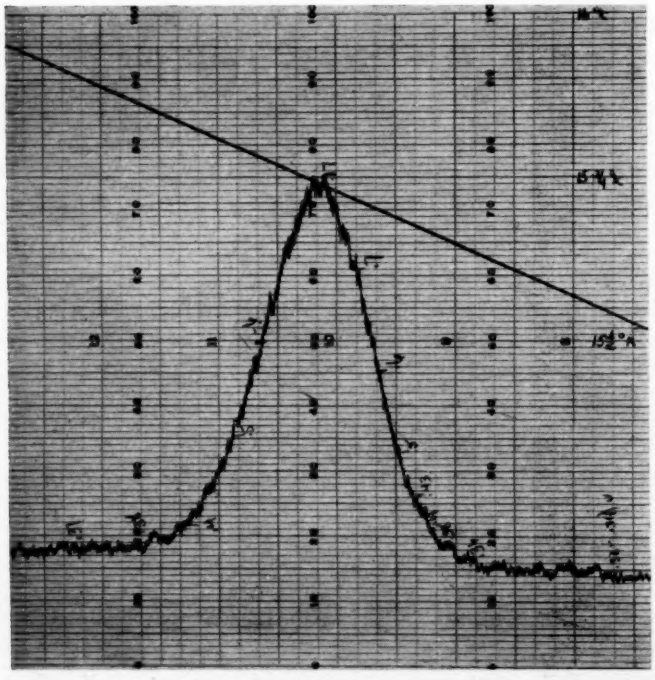

FIG. 7. Photograph of an infrared response curve for bolometer No. 13 with bolometer current of 31 ma. This record was taken simultaneously with the transition curve shown in Fig. 5.

[7] In his published paper (see footnote 1) Jones originally stated these reference conditions for a sinusoidal radiation signal. However, in a private communication of May 13, 1948 he has informed the author of certain changes which he plans to publish soon. The author is grateful to Dr. Jones for permission to employ this revised form, together with the figure of merit definition, in this paper prior to the publication of Dr. Jones' own paper.

TABLE I. Comparison of superconducting bolometer parameters and sensitivities.

1. Bolometer No. and CbN Sample No.	2. I ma	3. R ohm	4. dR/dT_b ohm/°K	5. ΔJ 10^{-10} watt	6. Calculated ΔE_n 10^{-10} v	7. Experimental ΔE_n 10^{-10} v	8. ΔE_b 10^{-10} v	9. $\Delta E_b/\Delta E_n$ S/N ratio	10. ϵ volt/watt	11. ΔJ_{min} 10^{-10} watt
1–$a\frac{1}{4}$	5	3.5	13	66,000	150	1000	30,000	30	0.46	2200
2–$b\frac{1}{4}$	14	0.15	1.7	930,000	31	40	24,000	600	0.026	1550
3–$c\frac{1}{4}$	15	4.0	75	7500	162	1000	11,200	11	1.5	650
4–$c\frac{1}{4}$	2	5.0	34	120,000	180	196	184,000	1000	1.5	120
5–$d1$	33	0.18	3	1660	34	125	1100	8.8	0.67	185
6–$e1$	10	0.16	0.3	530,000	32	32	5000	155	0.094	3400
7–$e1$	36	0.35	2.0	2250	48	310	1900	6.1	0.85	370
8–$f1$	30	0.14	2.0	1200	30	36	1080	30	0.90	40
9–$f1$	24	0.13	0.2	1300	29	32	100	3.1	0.077	420
10–$f1$	22	0.09	3.2	800	24	43	500	11.7	0.63	68
11–$f1$	34	0.10	1.5	630	26	47	500	10.6	0.80	59
12–$g1$	78	0.10	1.5	3700	26	110	630	6.2	0.18	600
13–$g1$	34	0.16	2.0	9600	32	90	790	8.8	0.082	1100
14–$h1$	30	0.10	0.1	380,000	26	186	660	3.5	0.002	110,000
15–$i1$	30	0.06	0.2	1100	20	100	250	2.5	0.22	450
16–$j1$	14	1.05	1.1	2570	83	350	640	1.8	0.25	1450
17–$k\frac{1}{4}$	40	0.70	5.0	4100	68	190	1880	9.9	0.46	410
18–$k\frac{1}{4}$	20	0.70	6.0	3000	68	70	1120	16.0	0.37	190
19–$k\frac{1}{4}$	10	0.95	12.0	2100	79	48	890	18.5	0.43	115
20–$k\frac{1}{4}$	32	0.60	10.0	1430	63	138	1760	12.7	1.23	115
21–$k\frac{1}{4}$	30	0.38	8.6	1950	50	84	2800	33.5	1.43	58
22–$k\frac{1}{4}$	15	0.57	25	1280	61	80	1125	13.5	1.00	83
23–$k\frac{1}{4}$	30	1.3	24	1850	92	1430	3700	2.6	2.00	710
24–$k\frac{1}{4}$	20	0.52	4.0	875	58	133	1780	13.4	2.00	66
25–$k\frac{1}{4}$	43	0.73	4.5	1470	69	110	4300	35	2.90	42

the detector time constant, τ; the noise equivalent band width of such an amplifier, $1/4RC$, is therefore equal to $1/4\tau$; the detector's minimum detectable power under these reference conditions, ΔJ_0, is defined as that value of the steady incident power which produces a steady output voltage equal to the r.m.s. Johnson noise voltage. It can be shown[8] that if, as before, ΔJ_{min} is the minimum detectable power of the detector of known time constant, τ, and area, a, and if ΔJ_{min} is obtained under normal experimental conditions of sinusoidally modulated radiation,[9] modulation frequency, f, falling on the detector, the resulting voltage signal being amplified by the usual type amplifier of band width, $\Delta\nu$, then the reference condition minimum detectable power, ΔJ_0, of this detector can be computed by the following relationship:

$$\Delta J_0=\Delta J_{min}/(4\tau\Delta\nu(1+\omega^2\tau^2))^{\frac{1}{2}}, \qquad (5)$$

where τ is in seconds, $\Delta\nu$ is in c.p.s., and $\omega=2\pi f$, where f is also in c.p.s.

To compare detectors of different areas an arbitrary area of 1 mm² will be chosen as the standard, and any ΔJ_0 may be reduced to that for the standard area on the well-known basis that the minimum detectable power is proportional to the square root of the receiving area, i.e.,

$$\Delta J_{0,1}=\Delta J_0/a^{\frac{1}{2}}, \qquad (6)$$

where a is a number equal to the area of the bolometer in square millimeters.

Until detectors are available whose sensitivity is limited by the temperature noise rather than by Johnson noise, the $\Delta J_{0,1}$ for detectors with different time constants can be intercompared on the basis, as suggested by Havens,[10] that they

[8] Equation (5) and its proof are implicit, but do not appear explicitly in R. Clark Jones' published paper (see footnote 1).

[9] The wave form of the radiation falling on the superconducting bolometers was approximately square wave, or, more accurately, a truncated saw-tooth wave. No correction has been made for this deviation from the sinusoidal wave form called for here.

[10] R. Havens, J. Opt. Soc. Am. **36**, 355A (1946).

TABLE II. Comparison of superconducting bolometers and other detectors as to sensitivity, time constant, figure of merit, etc.

Type of detector	Name or number	τ millisec.	a mm²	f c.p.s.	$\Delta\nu$ c.p.s.	$\Delta J_{\min}$ 10^{-10} watt	ΔJ_0 10^{-10} watt	$\Delta J_{0,1}$ 10^{-10} watt	M
Superconducting bolometer	22–$k\frac{1}{4}$	10	1.8	360	4000	83	0.29	0.22	14
Superconducting bolometer	25–$k\frac{1}{4}$	1.2	1.2	360	4000	42	3.3	3.0	8.3
Superconducting bolometer	8–$f1$	0.9	0.7	360	4000	42	4.9	5.9	5.9
Superconducting bolometer	11–$f1$	1.7	0.4	360	4000	58	2.7	4.3	4.0
Superconducting bolometer	24–$k\frac{1}{4}$	0.7	0.7	360	4000	66	10.5	12.5	3.3
Superconducting bolometer	10–$f1$	1.5	0.4	360	4000	73	4.2	6.3	3.1
Superconducting bolometer	5–$d1$	0.8	1.6	360	4000	186	25.5	20	1.9
Superconducting bolometer	9–$f1$	17	0.4	360	4000	430	0.7	1.1	1.7
Superconducting bolometer	13–$g1$	4.2	6.4	360	4000	1100	14	5.5	1.3
Superconducting bolometer	Milton K-10[a]	0.3	0.8	—	5000	10	3.4	3.8	25
Superconducting bolometer	Nielsen (OSU)[b]	1.8	0.8	27	3	3.5	23	26	0.65
Platinum strip bolometer	Baird[c]	50	3.6	10	—	14.7	1.9	1.0	0.60
Platinum strip bolometer	Baird	4.1	0.2	10	—	16.2	7.2	16	0.46
Semiconductor bolometer	BTL thermistor[d]	3.0	0.6	53	30	200	167	216	0.05
Evaporated Ni bolometer	Polaroid[e]	4.0	6.0	30	100	330	209	85	0.09
B_i-S_b, B_i-S_a thermocouple	Hornig and O'Keefe[f]	36	0.5	5	1	0.5	1.16	1.65	0.51
B_i-S_b, B_i-S_a thermocouple	Hornig and O'Keefe[f]	36	1.0	5	1	0.7	1.63	1.63	0.51
B_i-S_b, B_i-S_a thermocouple	Hornig and O'Keefe[f]	41	4.0	5	1	1.4	2.85	1.42	0.50
Pneumatic detector (Golay cell)	Eppley Labs[g]	5.0	7.0	10	1	0.5	3.3	1.3	4.8

[a] R. M. Milton, Chem. Rev. **39**, 419 (1946). Results for this bolometer were obtained from isolated radiation pulses instead of modulated radiation so no frequency can be given.
[b] E. E. Bell, R. F. Buhl, A. H. Nielsen, and H. H. Nielsen, J. Opt. Soc. Am. **36**, 355A (1946), supplemented by unpublished data. (The superconducting bolometer of this study was made in the Johns Hopkins University Cryogeny Laboratory by R. M. Milton.)
[c] These values are given in R. Clark Jones, J. Opt. Soc. Am. **37**, 897 (1947), coming to him by private communication from W. G. Langton. See Jones' article for explanation of band width used.
[d] W. H. Brattain and J. A. Becker, J. Opt. Soc. Am. **36**, 354A (1946). These results are worked up in Jones' paper mentioned in reference c.
[e] B. H. Billings, W. L. Hyde, and E. E. Barr, J. Opt. Soc. Am. **37**, 123 (1947). These reference conditions values are also obtained from Jones' paper mentioned in reference c.
[f] D. F. Hornig and B. J. O'Keefe, Rev. Sci. Inst. **18**, 474 (1947).
[g] Private communication of 4/26/48 from Mr. Roy Anderson, Manager, The Eppley Laboratory, Inc., Newport, Rhode Island.

are inversely proportional to the time constant. In order to include this intercomparison between detectors with different time constants a factor of merit, M, may be defined[7] as the ratio of Havens' suggested best minimum detectable power for a given time constant, H_τ, to the $\Delta J_{0,1}$ of the detector for which this is the time constant, i.e.,

$$M = H_\tau / \Delta J_{0,1}, \tag{7}$$

where

$$H_\tau = (3\times 10^{-12})/\tau, \tag{8}$$

where H_τ is in watts and τ is in seconds.

Of the 12 superconducting bolometers for which time constants were obtained, the 9 best ones have factors of merit ranging from 14.0 to 1.3. In Table II these 9 bolometers are compared with a number of other rapid response infra-red detectors whose experimentally determined minimum detectable powers have likewise been reduced to reference conditions for the sake of comparison. Figure 8, a graphical representation of the results of Table II, shows the $\Delta J_{0,1}$ *vs.* τ-points on a log-log plot.[11] The perpendicular distance from the points to the Havens' limit line are a measure of the figure of merit, M, those above the line having M greater than unity and those below the line having fractional values of M.

CONCLUSIONS

Study of Table II suggests at first sight that the superconducting bolometer at its best may be two or three times better than the pneumatic detector and perhaps 10 or 20 times better than the best thermopiles and room temperature

[11] Four points on this graph and the two limit lines were obtained from Fig. 1, p. 886, of reference 1. Dr. Jones suggested the inversion of the form of the figure from that given in his published paper. It should be noted that the Havens' limit is based upon a test set-up using a single pulse of radiation of a duration equal to that of the time constant of the detector. The thermodynamic limit, as well as the plotted points, refers to testing with a single infinitely long radiation pulse.

bolometers. However, several important cautions must be underlined in evaluating these comparative results. In the first place the radiation source and filters used in obtaining the sensitivity measurements tabulated in Table II have not been specified, in most cases, in the literature.[12] Therefore, the parameter of spectral distribution in the radiation falling on the detector has not been held constant.[13] In the second place detectors whose noise level is not due to Johnson noise must have due allowance made for this in calculating reference condition sensitivity. This is a particularly serious consideration for the superconducting bolometer, for its noise level sometimes increases when it is maintained at its most advantageous sensitivity ratio condition. All the work reported here for superconducting bolometers has been done using wide-band amplifiers (with the exception of that of Nielsen, in which the figure of merit is perhaps significantly lower than those obtained with wide-band amplifiers). Until a comprehensive study of CbN bolometers is made using a good narrow-band, high gain amplifier, the extent of this particular limitation upon the figure of merit of superconducting bolometers cannot be fairly judged.[14] There may be still other cautions to mention. Certainly spectroscopists will immediately realize that in contrast to this comparison of sensitivity in which the radiation flux is not limited to a slit image focus, the results may be quite different in a spectrometer, where the *shape* as well as the area of the detector is an important concern. Within certain limits previously indicated, the superconducting bolometer receiver shape can be adjusted to the needs of a spectrometer.

Of particular interest will be the investigation of the usefulness of the superconducting bolometer in the study of emission spectra from sources at room temperature, a field as yet unexplored.

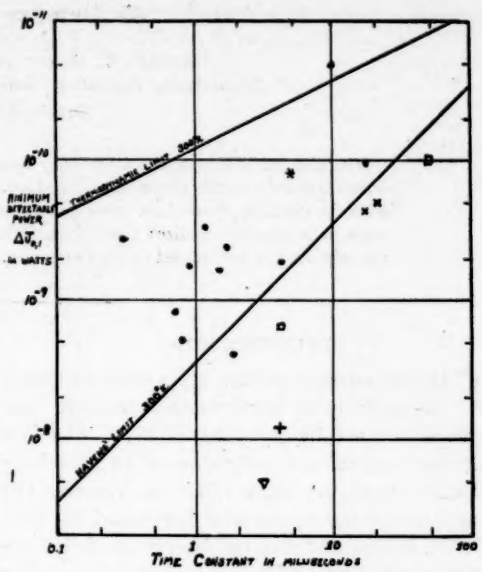

FIG. 8. Graph of $\Delta J_{0,1}$ *vs.* τ-values taken from Table II. The shapes of the points have the following significance:

●=superconducting bolometer,
□=platinum strip bolometer,
△=semiconductor bolometer,
+=evaporated nickel bolometer,
×=Bi-Sb, Bi-Sn thermopile,
*=pneumatic detector.

ACKNOWLEDGMENTS

The results reported in this paper were obtained in connection with an experimental program, supported by the Rockefeller Foundation, to make use of the radiation detecting properties of the superconducting bolometer to explore the possibilities of infra-red emission spectroscopy as an analytical tool for biological research.

Grateful recognition is made of the many helpful discussions with Dr. Donald H. Andrews, Director of the Cryogeny Laboratory, without whose keen interest and generous cooperation this work could not have been undertaken. The author is also much indebted to Miss Mary Camilla Williams, who constructed all the bolometers reported on in this paper, to Mr. William R. Asher and his assistants for the cryostat construction, to Mr. Gilbert Bushong for help on the electronics problems involved in this study, and to all the other members of the Cryogeny Laboratory staff for their cooperation in this work.

[12] The superconducting bolometers were irradiated by an approximately blackbody source held at a temperature of near 100°C, so that the energy peak was close to 7½ microns, the radiation passing through one thin rocksalt window and 30 cm of rather humid air before reaching the bolometer.

[13] Van Zandt Williams, Rev. Sci. Inst. **19**, 135 (1948). See particularly p. 161.

[14] Preliminary tests on 2 CbN bolometers with a narrow-band pass amplifier still under development in this laboratory have indicated figures of merit several times smaller than those tabulated in Table II, which were obtained from the wide-band pass amplifier data.

JOURNAL OF THE OPTICAL SOCIETY OF AMERICA VOLUME 38, NUMBER 10 OCTOBER, 1948

In Defense of Beer's Law

ARTHUR C. HARDY AND F. MANSFIELD YOUNG
Massachusetts Institute of Technology, Cambridge 39, Massachusetts
(Received April 23, 1948)

To state that a substance fails to obey Beer's Law is an injustice, since it is the investigator who has failed to make proper use of the Law. If the substance becomes a mixture of substances when in solution, Beer's Law must be applied to each component of the mixture. It does not seem to be generally realized that this can often be done, even when none of the components of the mixture can be isolated in the pure state.

INTRODUCTION

THE dependence of light absorption on length of path in a homogeneous medium was correctly stated by Bouguer in 1729. The fact that varying the concentration of an absorbing substance has the same effect as varying the length of the light path was discovered by Beer in 1852. Either law may be observed to fail if the light is not sufficiently monochromatic, if the blank cell does not properly compensate for reflection losses, etc. Even with flawless techniques, however, Beer's Law may appear to fail if two or more substances are present in varying proportions. This paper is concerned with the latter type of failure.

STATEMENT OF PROBLEM

Let D_1 be a function of wave-length representing the optical density of a solution containing two substances, A and B. This optical density is the sum of the densities of the components, and, by application of Beer's Law to each,

$$D_1 = a_1 D_a + b_1 D_b, \tag{1}$$

where a_1 and b_1 are the concentrations of the components, and D_a and D_b are functions of wave-length representing their optical densities at unit concentrations in a cell of unit thickness.

Now let the concentrations of A and B be altered in some manner. At the new concentrations a_2 and b_2, the optical density D_2 of this new mixture is

$$D_2 = a_2 D_a + b_2 D_b. \tag{2}$$

The constants a_2 and b_2, like the constants a_1 and b_1, are assumed to be unknown. The problem is to find the functions D_a and D_b, given only the spectral density curves D_1 and D_2. The fact that the two equations contain four unknown constants in addition to the two unknown functions may account in part for the prevailing impression that this problem can never have a unique solution.

GENERAL METHOD OF SOLUTION

From inspection of the above equations, it is evident that D_a and D_b must be linear functions of D_1 and D_2. Consider therefore a new function $F = D_2 - kD_1$, where k is an arbitrary constant. Then, by substitution,

$$\begin{aligned} F &= D_2 - kD_1 \\ &= (a_2 - ka_1)D_a + (b_2 - kb_1)D_b. \end{aligned} \tag{3}$$

When k is assigned a value such that $(a_2 - ka_1) > 0$, F corresponds to a mixture in which a positive amount of substance A is present. On the other hand, for any value of k such that $(a_2 - ka_1) < 0$, F corresponds to an imaginary mixture in which the amount of A is negative. In general, the function F is characteristically different in these two cases. Thus, if F shows evidence of an absorption band caused by A in the one case, it will show evidence of a transmission band in the other. Hence, when the function F is plotted for various values of k, it is frequently possible to recognize the transition case for which $(a_2 - ka_1) = 0$. For this case, the unknown function D_b is proportional to F. By a similar procedure, a value of k can be found for which $(b_2 - kb_1) = 0$. The unknown function D_a is then proportional to the new function F. The determination of the values of the proportionality constants will be illustrated by the following example.

APPLICATION OF THE METHOD

The usefulness of the method just outlined would be best illustrated by determining the ab-

sorption characteristics of two substances that always occur in some sort of equilibrium with one another. The difficulty is that, if the substances cannot be obtained in the pure state, the calculated characteristics cannot be compared with those determined by direct measurement. Since it seemed desirable to provide a validation of the method and an indication of its accuracy, the case of two substances in equilibrium was simulated by the following procedure. Two dyestuffs, A and B, were dissolved in distilled water to make two stock solutions, assumed for convenience to represent unit concentrations of A and B. An unmeasured volume of solution A was then mixed with an unmeasured volume of solution B to produce a mixture M_1, whose spectral transmittance characteristics are shown by curve M_1 in Fig. 1. A second mixture M_2 was then prepared in the same way, and it was found to have the spectral transmittance characteristics shown by curve M_2 in this figure. The problem is to determine the spectral transmittance characteristics of the two stock solutions, given only these spectral transmittance curves; or better, given only the spectral density curve D_1 of mixture M_1 and the spectral density curve D_2 of mixture M_2. (See Fig. 2.)

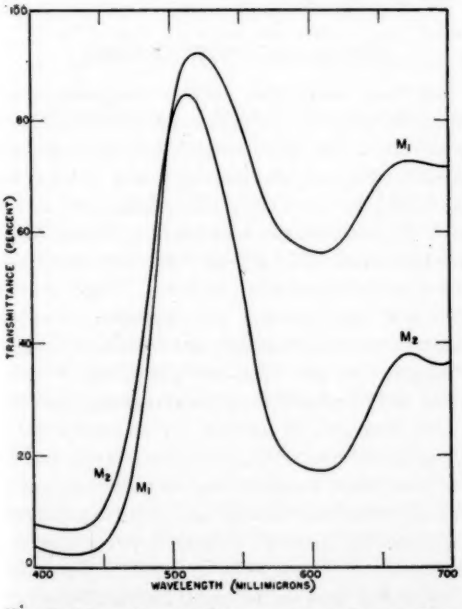

FIG. 1. Spectral transmittance curves of two mixtures, M_1 and M_2, of dyestuffs A and B in different proportions.

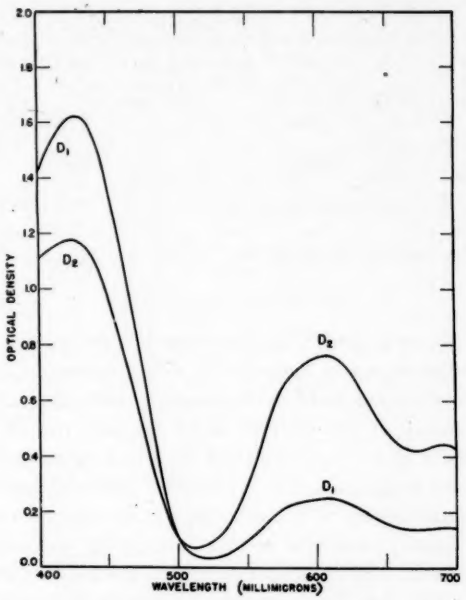

FIG. 2. Spectral density curves of the mixtures whose spectral transmittance curves are shown in Fig. 1.

If the function F is plotted for $k=0.60$, it is found that the curvature is negative in the spectral region from 400 mμ to 450 mμ. On the other hand, the curvature is positive in this region when $k=0.75$; and inspection of the curves for $k=0.60$ and $k=0.75$ suggests that the substance A possesses an absorption band in this spectral region, the effect of which would be eliminated if F were plotted for some intermediate value of k. Actually, it is less laborious to determine k by making use of the fact that

$$d^2F/d\lambda^2=d^2D_2/d\lambda^2-kd^2D_1/d\lambda^2.$$

Since the curvature of the function F is zero when its second derivative is zero, the desired value of k can be found from

$$k=\frac{d^2D_2}{d\lambda^2}\Big/\frac{d^2D_1}{d\lambda^2},$$

which can be approximated by the method of second differences that is illustrated in Table I. From this it follows that, to make $(a_2-ka_1)=0$,

TABLE I.

λ	D_1	ΔD_1	$\Delta^2 D_1$	D_2	ΔD_2	$\Delta^2 D_2$
416	1.581			1.168		
		0.041			0.009	
428	1.622		0.113	1.177		0.076
		−0.072			−0.067	
440	1.550			1.110		

the value of k should be

$$k=0.076/0.113=0.675.$$

When $k=0.675$, the function F is proportional to the unknown function D_b. The proportionality constant need not be determined when the only purpose of the analysis is to identify the substance B, since, by plotting $\log F$ as a function of wave-length, a curve is obtained whose shape is characteristic of the substance B at any concentration. In the case of this illustration, the mixtures M_1 and M_2 were made from stock solutions, so that $a_1+b_1=a_2+b_2=1$. It follows from this that the proportionality constant (b_2-kb_1) $=1-k$. In other words,

$$D_b=\frac{F}{1-k}=\frac{F}{1-0.675}=3.08F.$$

It is therefore possible to plot the spectral density curve of stock solution B, or to plot the spectral transmittance curve of this stock solution, as is done in Fig. 3. The circled points in this figure were calculated by the method just outlined, and the smooth curve was determined by direct measurement with a spectrophotometer.

The spectral transmittance curve of stock solution A was found by following the same procedure, step by step, using the critical region from 580 $m\mu$ to 640 mμ. The circled points in Fig. 4 are the result of this calculation, and the smooth curve was obtained by direct measurement of stock solution A with a spectrophotometer. It will be evident that, having found the unknown functions D_a and D_b, the concentrations of each in any mixture can now be calculated from the density values of the mixture at any two wave-lengths. Thus, mixture M_1 is found to have been composed of 86 parts of A and 14 parts of B; and mixture M_2 to have been composed of 58 parts of A and 42 parts of B.

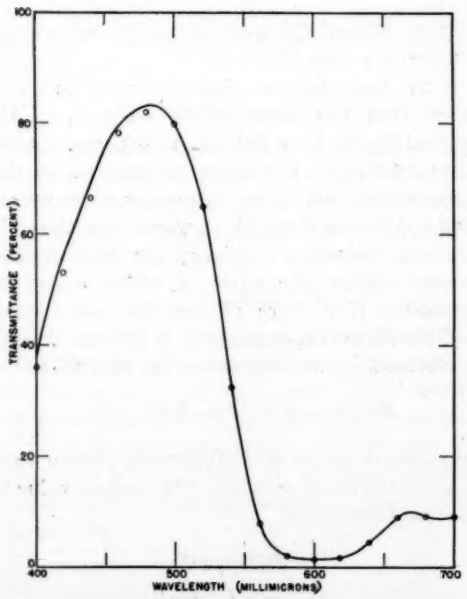

FIG. 3. Spectral transmittance curve of a solution of dyestuff B. The circled points at wave-length intervals of 20 mμ were calculated from the spectral density curves of Fig. 2. The slight disparity in the region of short wave-lengths may be due to the fact that dyestuff B does not form a true solution.

MULTICOMPONENT SYSTEMS

The two-component system discussed above contained a blue dye (Heliogen Blue BWS Extra) and a yellow dye (Tartrazine C Extra) in aqueous solution. Since the log density curve of each dye was found to be invariant in shape over a wide range of concentrations, there was reason to believe that each could be regarded as a single substance for the purpose at hand. That no new substance was present in mixtures of these dyestuffs was ascertained in the following manner. An absorption cell filled with solution A and a similar cell filled with an equal volume of solution B were arranged in tandem for measurement of their spectral transmittance. The contents of the cells were then emptied into another container, the cells were refilled with the resulting mixture, and a second spectral transmittance curve was determined with the cells in tandem. Since the second curve was found to be identical with the first, it was concluded that no new substance was present in the mixture. This conclusion might

have been reached by calculations based on Beer's Law, but the two-cell method avoids the necessity of making these computations and is likely to be more accurate.

It should be emphasized again that, although it is convenient for the purpose of illustration to employ mixtures of substances which are pure in the above sense, the method can be used as an analytical procedure when the nature and amounts of the substances present are unknown and the substances themselves are not available for measurement in the pure state. We use the term *substance* here in the connotation given in Webster's Unabridged Dictionary because we wish to imply that each substance is "being considered as an existant entity." In other words, the product of any chemical process (dissociation, association, etc.) known to the chemist or yet to be discovered can legitimately be regarded as a substance when it displays identifiable optical characteristics.

When a material "fails" to obey Beer's Law, the simplest interpretation is that it consists of a mixture of two substances in an equilibrium that depends on the concentration. Proceeding on this assumption, it is often possible to determine the optical characteristics of each substance from the behavior of two mixtures, as was shown above. Then, knowing the characteristics of each substance, ability to predict the optical characteristics of a third mixture is evidence that only two substances were present. Conversely, inability to predict the characteristics of a third mixture shows that the system contained more than two substances. Extension of the analysis to a three-component system requires three equations of the form of Eq. (1), with an additional term in each. However, regardless of the number of components that may be present, the spectral density curve of each component will always be a linear function of the spectral density curves of the mixtures.

Because the analysis of multicomponent systems becomes rapidly more complex with increase in the number of substances present, it has occurred to us that the laborious computations might be avoided by the following procedure. Let a monochromator be arranged in such a way that the wave-length of the emergent light can be varied rapidly, and let the horizontal sweep

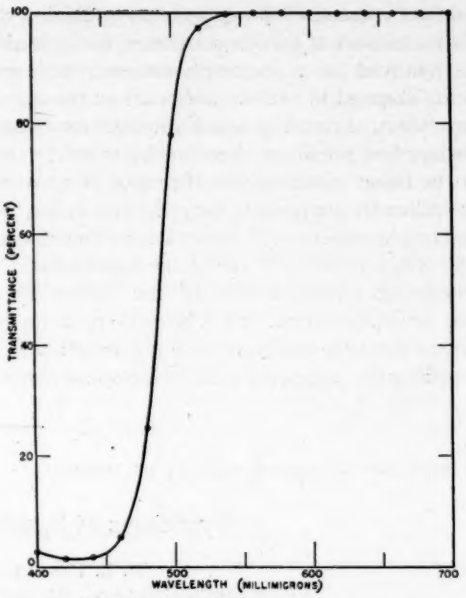

FIG. 4. Spectral transmittance curve of a solution of dyestuff *A*. The circled points at wave-length intervals of 20 mμ were calculated from the spectral density curves of Fig. 2.

circuit of a cathode-ray tube be arranged to follow the cyclical variations in wave-length. In the case of a three-component system, for example, the emergent beam can be split into three beams, each being caused to pass through a cell containing one of the three mixtures. Three similar photo-multiplier tubes giving logarithmic responses can indicate the optical densities of the three mixtures, and additive or subtractive combinations of their output signals can be applied to the vertical sweep of the cathode-ray tube.

It will be evident that the curve appearing on the cathode-ray screen is then a function of wave-length representing some linear combination of the spectral density curves of the three mixtures. The algebraic sign of each term depends upon whether the output of the corresponding photo-multiplier tube is connected additively or subtractively; and the coefficient of each term depends upon the thickness of the corresponding absorption cell. Hence, by varying the modes of connection and the thickness of the absorption cells, every possible linear combination of the mixture curves can be explored. When the curve

on the cathode-ray screen appears to display the characteristics of a single substance, the cells may be removed to a spectrophotometer, each cell being inserted in the sample beam or the standard beam, depending upon whether its optical density had previously been added or subtracted in the linear combination. If proper precautions are taken to compensate for reflection losses, the spectrophotometer will then measure the absorption characteristics of one of the substances, the absorption characteristics of the others being exactly compensated. It will be evident that a device of this type need not have the accuracy that is ordinarily associated with spectrophotometric measurements, since its only function is to determine when the characteristic features of all of the absorbing substances but one have been compensated.

ACKNOWLEDGMENT

We gratefully acknowledge the assistance of Dr. I. H. Godlove of the Central Research Laboratory of the General Aniline & Film Corporation, who suggested that Heliogen blue and Tartrazine would probably serve satisfactorily as an example of a two-component mixture. We are also indebted to him for the samples of the dyes that were used.

JOURNAL OF THE OPTICAL SOCIETY OF AMERICA VOLUME 38, NUMBER 10 OCTOBER, 1948

Syntheses of Spectral-Distribution Curves

W. L. BREWER AND F. R. HOLLY, JR.
Color Control Department, Eastman Kodak Company, Rochester 4, New York

(Received May 3, 1948)

A method is presented for obtaining spectral distributions having colorimetric characteristics which have been pre-specified in terms of a set of tristimulus values or trichromatic coefficients. The distributions may be chosen to correspond to energy radiated from light sources, or to the transmittances or reflectances of materials acting on such energy. Tables and figures are included to facilitate a rapid solution to any given problem. Several examples are given which illustrate the method and indicate the kinds of applications possible.

SINCE the adoption of a standard set of color-mixture curves in 1931 by the International Commission on Illumination,[1] it has been possible to determine a colorimetric specification for any energy distribution in terms of three tristimulus values. Such determinations have proven useful in many fields of applied color because, for the "standard observer" at least, any two sources of light with the same tristimulus values visually match each other, regardless of their comparative spectral-energy distributions. The actual calculation of these values for various energy distributions, or for transmitting media or reflecting surfaces provided one of the three I.C.I. standard illuminants A, B, or C is used, has been made possible through the publication of tables such as those in the *Handbook of Colorimetry*[2] and elsewhere.[3,4]

The interesting converse problem, that of determining one or more of the spectral-energy, transmittance, or reflectance distributions corresponding to a particular set of tristimulus values, or trichromatic coefficients, has received little attention. The necessity of solving this problem confronted the writers recently, and a solution was found which is accurate and capable of fairly rapid application. It is believed that the procedures developed might be of use in studies of energy distributions of theoretical light sources, absorptions of theoretical dyes, and in devising

[1] T. Smith and J. Guild, "The C.I.E. colorimetric standards and their use," Trans. Opt. Soc. **33**, 73–130 (1931–32).

[2] Massachusetts Institute of Technology, the Color Measurement Laboratory, *Handbook of Colorimetry* (The Technology Press, Cambridge, Massachusetts, 1936), 87 pp.

[3] Committee on Colorimetry, "Quantitative data and methods for colorimetry," J. Opt. Soc. Am. **34**, 633–688 (1944).

[4] W. D. Wright, *The Measurement of Colour* (Adam Hilger, Ltd., London, 1944), 223 pp.

illustrative examples of colorimetric principles. Undoubtedly, there are other possible applications.

To be sure, ways are known for finding curves of the type described. One commonly employed is the "cut and try," or calculate for a given distribution, modify, and calculate again. By judicious handling and sufficient repetitions, this method can be made to yield fairly satisfactory results. Other solutions which are more direct have been described.[5-7] The methods given here, however, are believed to be more complete, simpler to handle, and capable of wider usage than any yet described. A graphical type of solution is included which greatly reduces the time necessary to obtain an approximate answer, thus making possible advance determinations of the general shapes of curves that finally will be obtained. Through the use of figures and tables which are included, a minimum amount of time need be spent on computations, and there is little wasted effort through repetitions or because of meaningless results.

ENERGY DISTRIBUTIONS

The I.C.I. tristimulus values X, Y, and Z for any source radiating energy of spectral distribution P are evaluated according to the definitions (see reference 3, p. 646):

$$X=K_m\int_0^\infty \bar{x}P d\lambda, \quad Y=K_m\int_0^\infty \bar{y}P d\lambda, \quad Z=K_m\int_0^\infty \bar{z}P d\lambda, \tag{1}$$

where K_m is the maximum luminous efficiency of radiant flux and $\bar{x}$, $\bar{y}$, and $\bar{z}$ are the tristimulus values for unit amounts of energy per second. Numerical values of $\bar{x}$, $\bar{y}$, and $\bar{z}$ at the various wave-lengths are given in the tables already mentioned.[2-4] The Committee on Colorimetry has accepted 650 lumens per watt as the value of K_m, although other values ranging from about 625 to 675 have been recommended.[8]

For the type of problem under consideration it is assumed that X, Y, and Z are known, and an energy-flux distribution P (as a function of λ) is to be determined. There are, of course, in general, an unlimited number of different spectral distributions which would calculate to give a particular set of tristimulus values. Let it be assumed that one such distribution is given by

$$P=a_1f_1+a_2f_2+a_3f_3, \tag{2}$$

where the f's are known functions of the wavelength, λ, and the a's are constants, independent of λ, whose values for the specific distribution, P, must be determined. Letting

$$X_1=K_m\int_0^\infty \bar{x}f_1 d\lambda, \quad Y_1=K_m\int_0^\infty \bar{y}f_1 d\lambda, \quad Z_1=K_m\int_0^\infty \bar{z}f_1 d\lambda, \tag{3}$$

with corresponding definitions for X_2, Y_2, Z_2, and X_3, Y_3, Z_3, Eqs. (1) can be written as:

$$\begin{aligned} X&=a_1X_1+a_2X_2+a_3X_3,\\ Y&=a_1Y_1+a_2Y_2+a_3Y_3,\\ Z&=a_1Z_1+a_2Z_2+a_3Z_3. \end{aligned} \tag{4}$$

While these equations can be used directly, more convenient forms may be obtained as follows. Let:

$$m=X+Y+Z; \quad m_i=X_i+Y_i+Z_i; \tag{5a}$$

$$x=X/m, \quad y=Y/m, \quad z=Z/m;$$

$$x_i=X_i/m_i, \quad y_i=Y_i/m_i, \quad z_i=Z_i/m_i; \tag{5b}$$

$$\alpha_i=a_im_i/m; \tag{5c}$$

where i is used to designate the terms numbered 1, 2, and 3. Equations (4) now become

$$\begin{aligned} x&=\alpha_1x_1+\alpha_2x_2+\alpha_3x_3,\\ y&=\alpha_1y_1+\alpha_2y_2+\alpha_3y_3,\\ z&=\alpha_1z_1+\alpha_2z_2+\alpha_3z_3, \end{aligned} \tag{6}$$

where

$$x+y+z=1, \quad x_i+y_i+z_i=1, \quad \alpha_1+\alpha_2+\alpha_3=1. \tag{7}$$

Making use of Eqs. (7), the α's of Eqs. (6) are given by:

$$\begin{aligned} \alpha_1&=\frac{x(y_2-y_3)+x_2(y_3-y)+x_3(y-y_2)}{x_1(y_2-y_3)+x_2(y_3-y_1)+x_3(y_1-y_2)},\\ \alpha_2&=\frac{x_1(y-y_3)+x(y_3-y_1)+x_3(y_1-y)}{x_1(y_2-y_3)+x_2(y_3-y_1)+x_3(y_1-y_2)},\\ \alpha_3&=\frac{x_1(y_2-y)+x_2(y-y_1)+x(y_1-y_2)}{x_1(y_2-y_3)+x_2(y_3-y_1)+x_3(y_1-y_2)}. \end{aligned} \tag{8}$$

[5] Ronald H. Bingham and Herman Hoerlin, "Optimum spectral sensitivities for a reversible color film process," J. Opt. Soc. Am. **37**, 199–210 (1947).

[6] Robert H. Morris, "Metameric formulation," J. Opt. Soc. Am. **37**, 669 (1947).

[7] R. H. Park and E. I. Stearns, "Spectrophotometric formulation," J. Opt. Soc. Am. **34**, 112–113 (1944).

[8] Committee on Colorimetry, "The psychophysics of color," J. Opt. Soc. Am. **34**, 245–266 (1944), p. 252.

Once the values of the α's have been computed, the values of the a's can be obtained by use of Eq. (5c). When the values of the a's are substituted into Eq. (2), the spectral-energy distribution, P, as a function of wave-length, λ, is obtained.

It should be noted that, as defined in Eqs. (5a) and (5b), x_i and y_i are the trichromatic coefficients of the corresponding f_i, and m_i is the sum of its tristimulus values or its number of trichromatic units. Likewise, x and y are the trichromatic coefficients of the spectral-energy distribution being synthesized, and m is the number of its trichromatic units. From this last consideration it is evident that if only the trichromatic coefficients of the spectral-energy distribution are of interest, m may be assigned any value.

One other relationship of interest and importance follows from Eq. (8). If the trichromatic coefficients of the three f's and of the spectral distribution to be synthesized are plotted in rectangular coordinates (chromaticity diagram), and lines drawn connecting each point to each of the others, four triangles with these points as vertices will be formed. Two such sets of these triangles are illustrated in Fig. 1, where in (a) the chromaticity point corresponding to the spectral-energy distribution, P, lies inside the triangle formed by the three f's, and in (b) it is outside. For each of these sets of triangles let the areas of triangles Pf_2f_3, f_1Pf_3, f_1f_2P, and $f_1f_2f_3$ be given by A_1, A_2, A_3, and A, respectively. As can easily be established by analytical geometry, one-half of the absolute values of the numerators of Eqs. (8) equal, respectively, A_1, A_2, and A_3, and one-half of the absolute value of the denominator common to the three equations equals A. Therefore, neglecting signs,

$$\alpha_1 = A_1/A, \quad \alpha_2 = A_2/A, \quad \alpha_3 = A_3/A. \qquad (9)$$

While the proof will not be given here, it can also be shown that if the point P lies within the triangle formed by $f_1f_2f_3$, as in (a) of Fig. 1, all the α's will be positive; if P lies outside the triangle, as in (b), either one or two of them will be negative. Inspection of the triangles will indicate which of the α's are negative. In (b) it would be α_2. The choice in signs can be checked readily by use of the fact that the algebraic sum of the three α's must equal unity.

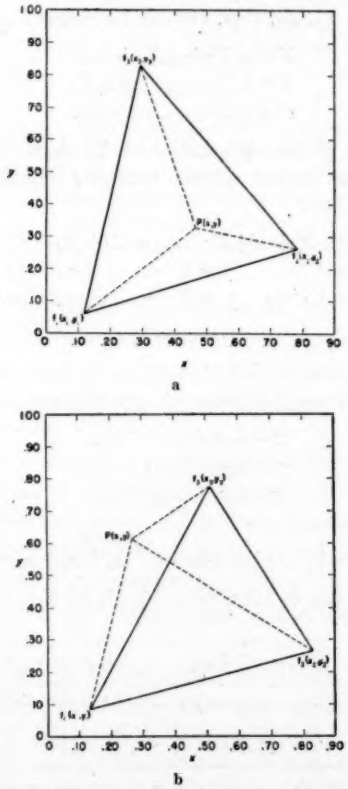

FIG. 1. Graphical representations illustrating the combining of three f's to produce a distribution with a given set of trichromatic coefficients.

CHOICE OF f's

As previously stated, the f's are known function of wave-length, λ, and may be arbitrarily selected. There are, however, considerations involved in their selection, the most important of which being that there must be no negative values in the final spectral-energy distribution and that, for any given set of tristimulus values, it should be possible to obtain a number of energy distributions having wide variations in curve shape.

The first consideration is of importance because negative portions in a spectral-energy distribution have no physical meaning. Two sufficient, though not always necessary, conditions for avoiding such distributions are (1) that the f's used have no negative values and (2) that none of the a's for a particular solution come out negative. These two conditions are easily applied

and in general should be adhered to, although an example illustrating an exception to the second will be given later.

With respect to the second consideration, it has already been indicated that there are an unlimited number of different energy distributions which will yield any particular set of tristimulus values. While it is unreasonable to expect to be able to obtain *all* the varieties of curve shapes with any given set of f's, a considerable amount of variation should be possible.

Taking into account these and other considerations, such as the mathematical ease and convenience of handling, the f's listed in Table I were selected. The f's are given as function of i, where i is defined as:

$$i=(\lambda-400)/10, \qquad (10)$$

with the wave-length, λ, measured in millimicrons. Included in most of the f's is a parameter, i_0. It may be assigned any value from 0 to 60, or from 0 to some other maximum value less than 60, depending upon the particular function. A second parameter, a, is included in one of the f's.

The numerical values of any f at 10 mμ intervals between 400 mμ and 700 mμ may be obtained from Table II. This is done by first assigning i_0 its value, and then, for each value of $(i-i_0)$, as i varies in integral steps from 0 to 30, finding the value of f in the appropriate column.

In Fig. 2 a through h are given the graphical representations of the families of curves corresponding to each type of f. The various member of each family correspond to different values of the parameters i_0 and a.

In Table III are given the values of x, y, and m for each f. These values were obtained by the weighted ordinate method, summing at 10 mμ intervals between 400 mμ and 700 mμ. The values of $\bar{x}$, $\bar{y}$, and $\bar{z}$ were taken from the *Handbook of Colorimetry*. The setting of the summation limits at 400 mμ and 700 mμ introduces slight errors, but for most purposes the accuracy should be more than sufficient. Calculations were made to yield six or more significant figures, and the answers rounded off to give five.

In making up Table III the value of K_m was arbitrarily set equal to unity. This was done because usually the energy distribution to be synthesized need be described only in terms of relative units. If and when an absolute system of units is to be employed, the m's in Table III must be multiplied by 650 or, depending upon the particular system and other considerations as previously discussed, whatever value K_m is assumed to have.

TABLE I. List of f's.

(a)	1	(g)	$\left[\sin\frac{i-i_0}{30}\pi\right]^2$
(b)	i		
(c)	$30-i$	(h)	$1+\left[\sin\frac{i-i_0}{15}\pi\right]^2$
(d)	$(i-i_0)^2$		
(e)	$1+\sin\frac{i-i_0}{10}\pi$	(i)	$1+\left[\sin\frac{i-i_0}{30}\pi\right]^3$
(f)	$1+\sin\frac{i-i_0}{30}\pi$	(j)	$e^{\frac{-(i-i_0)^2}{2a^2}}$

Chromaticity plots of the various f's are given in Fig. 3. It is seen that rather complete coverage is given the entire area within the spectral locus. Combinations of the f's can be used to obtain a wide variety of curve shapes for almost any set of tristimulus values.

APPLICATIONS; GRAPHICAL SOLUTIONS

The use of the f's described in the preceding section in synthesizing spectral-energy curves can be shown best by means of an example.

Example No. 1.—Problem: To find several relative energy distributions which match colorimetrically the white fluorescent light with the relative energy-distribution curve (*a*) in Fig. 4.[9]

The tristimulus values of this light as given in the figure are $X=1125$, $Y=1000$, and $Z=375$. From these it is found that $m=2500$, $x=0.45000$, and $y=0.40000$. The chromaticity point corresponding to these values of x and y plot to give P in Fig. 5. With the help of Fig. 3, the points surrounding p which corresponded to different f's may be located. From these, three sets were selected to yield three different energy distributions. For the first of these, P_1,

$$f_{11}=\left(\sin\frac{i-8}{30}\pi\right)^2, \quad f_{12}=1+\left(\sin\frac{i-20}{30}\pi\right)^3,$$

$$f_{13}=1+\left(\sin\frac{i-56}{30}\pi\right)^3.$$

[9] This curve was taken from G. E. Inman, "Characteristics of fluorescent lamps," Trans. Illum. Eng. Soc. **34**, 65–86 (1939), p. 72.

TABLE II. Numerical values of the f's as functions of $(i-i_0)$.

$(i-i_0)$	1	i	$30-i$	$(i-i_0)^2$	$1+\sin\frac{i-i_0}{10}\pi$	$1+\sin\frac{i-i_0}{30}\pi$	$\left[\sin\frac{i-i_0}{30}\pi\right]^2$	$1+\left[\sin\frac{i-i_0}{15}\pi\right]^2$	$1+\left[\sin\frac{i-i_0}{30}\pi\right]^3$	$e^{\frac{-(i-i_0)^2}{2a^2}}$ $a=1$	$a=2$	$a=3$	$a=5$	$(i-i_0)$
−56	—	—	—	—	—	—	—	—	1.06729	—	—	—	—	−56
−55	—	—	—	—	—	1.50000	—	—	1.12500	—	—	—	—	−55
−54	—	—	—	—	—	1.58779	—	—	1.20307	—	—	—	—	−54
−53	—	—	—	—	—	1.66913	—	—	1.29959	—	—	—	—	−53
−52	—	—	—	—	—	1.74314	—	—	1.41041	—	—	—	—	−52
−51	—	—	—	—	—	1.80902	—	—	1.52951	—	—	—	—	−51
−50	—	—	—	—	—	1.86603	—	—	1.64952	—	—	—	—	−50
−49	—	—	—	—	—	1.91355	—	—	1.76241	—	—	—	—	−49
−48	—	—	—	—	—	1.95106	—	—	1.86024	—	—	—	—	−48
−47	—	—	—	—	—	1.97815	—	—	1.93586	—	—	—	—	−47
−46	—	—	—	—	—	1.99452	—	—	1.98366	—	—	—	—	−46
−45	—	—	—	—	—	2.00000	—	—	2.00000	—	—	—	—	−45
−44	—	—	—	—	—	1.99452	—	—	1.98366	—	—	—	—	−44
−43	—	—	—	—	—	1.97815	—	—	1.93586	—	—	—	—	−43
−42	—	—	—	—	—	1.95106	—	—	1.86024	—	—	—	—	−42
−41	—	—	—	—	—	1.91355	—	—	1.76241	—	—	—	—	−41
−40	—	—	—	—	—	1.86603	—	—	1.64952	—	—	—	—	−40
−39	—	—	—	—	—	1.80902	—	—	1.52951	—	—	—	—	−39
−38	—	—	—	—	—	1.74314	—	—	1.41041	—	—	—	—	−38
−37	—	—	—	—	—	1.66913	—	—	1.29959	—	—	—	—	−37
−36	—	—	—	—	—	1.58779	—	—	1.20307	—	—	—	—	−36
−35	—	—	—	—	—	1.50000	—	—	1.12500	—	—	—	—	−35
−34	—	—	—	—	—	1.40674	—	—	1.06729	—	—	—	—	−34
−33	—	—	—	—	—	1.30902	—	—	1.02951	—	—	—	—	−33
−32	—	—	—	—	—	1.00000	—	—	1.00889	—	—	—	—	−32
−31	—	—	—	—	—	1.20791	—	—	1.00114	—	—	—	—	−31
−30	—	—	—	900	—	1.10453	—	—	1.00000	0.00000	0.00000	0.00000	0.00000	−30
−29	—	—	—	841	—	0.89547	—	—	0.99886	0.00000	0.00000	0.00000	0.00000	−29
−28	—	—	—	784	—	0.79209	0.04323	1.06729	0.99101	0.00000	0.00000	0.00000	0.00000	−28
−27	—	—	—	729	—	0.69098	0.09549	1.20307	0.97049	0.00000	0.00000	0.00000	0.00000	−27
−26	—	—	—	676	—	0.59326	0.16543	1.41041	0.93271	0.00000	0.00000	0.00000	0.00000	−26
−25	—	—	—	625	—	0.50000	0.25000	1.64952	0.87500	0.00000	0.00000	0.00000	0.00000	−25
−24	—	—	—	576	—	0.41221	0.34549	1.86024	0.79693	0.00000	0.00000	0.00000	0.00001	−24
−23	—	—	—	529	—	0.33087	0.44774	1.98366	0.70041	0.00000	0.00000	0.00000	0.00003	−23
−22	—	—	—	484	—	0.25686	0.55226	1.98366	0.58959	0.00000	0.00000	0.00000	0.00006	−22
−21	—	—	—	441	—	0.19098	0.65451	1.86024	0.47049	0.00000	0.00000	0.00000	0.00015	−21
−20	—	—	—	400	—	0.13397	0.75000	1.64952	0.35048	0.00000	0.00000	0.00000	0.00034	−20
−19	—	—	—	361	—	0.08645	0.83457	1.41041	0.23759	0.00000	0.00000	0.00000	0.00073	−19
−18	—	—	—	324	1.58779	0.04894	0.90451	1.20307	0.13976	0.00000	0.00000	0.00000	0.00153	−18
−17	—	—	—	289	1.80902	0.02185	0.95677	1.06729	0.06414	0.00000	0.00000	0.00000	0.00309	−17
−16	—	—	—	256	1.95106	0.00548	0.98907	1.00899	0.01634	0.00000	0.00000	0.00000	0.00598	−16
−15	—	—	—	225	2.00000	0.00000	1.00000	1.00000	0.00000	0.00000	0.00000	0.00000	0.01111	−15
−14	—	—	—	196	1.95106	0.00548	0.98907	0.99101	0.01634	0.00000	0.00000	0.00002	0.01984	−14
−13	—	—	—	169	1.80902	0.02185	0.95677	0.93271	0.06414	0.00000	0.00000	0.00008	0.03405	−13
−12	—	—	—	144	1.58779	0.04894	0.90451	0.79693	0.13976	0.00000	0.00000	0.00034	0.05613	−12
−11	—	—	—	121	1.30902	0.08645	0.83457	0.58959	0.23759	0.00000	0.00000	0.00120	0.08892	−11

From Table III the values of x and y for each of these f's were found:

$$x_{11}=0.51158,\quad x_{12}=0.47876,\quad x_{13}=0.29761,$$
$$y_{11}=0.39694,\quad y_{12}=0.47322,\quad y_{13}=0.35483.$$

With these values, and with those of x and y as already given, α_{11}, α_{12}, and α_{13} become, from Eqs. (8):

$$\alpha_{11}=0.55688,\quad \alpha_{12}=0.18346,\quad \alpha_{13}=0.25966.$$

Then, using Eq. (5c) and the values of m_{11}, m_{12}, and m_{13} found in Table III,

$$a_{11}=9.6666,\quad a_{12}=2.4641,\quad a_{13}=1.3547.$$

The equation for the energy distribution can therefore be written as

$$P_1=9.6666\left(\sin\frac{i-8}{30}\pi\right)^2+2.4641\left[1+\left(\sin\frac{i-20}{30}\pi\right)^3\right]+1.3547\left[1+\left(\sin\frac{i-56}{30}\pi\right)^3\right].$$

While this expression for P_1 can be simplified, its numerical values may be determined more readily without a change of form through the use of Table II. With values found in this table and the sums of the products with the constants for

TABLE II.—*Continued.*

$(i-i_0)$	1	i	$30-i$	$(i-i_0)^2$	$1+\sin\frac{i-i_0}{10}\pi$	$1+\sin\frac{i-i_0}{30}\pi$	$\left[\sin\frac{i-i_0}{30}\pi\right]^2$	$1+\left[\sin\frac{i-i_0}{15}\pi\right]^2$	$1+\left[\sin\frac{i-i_0}{30}\pi\right]^3$	$\epsilon^{\frac{-(i-i_0)^2}{2a^2}}$ $a=1$	$\epsilon^{\frac{-(i-i_0)^2}{2a^2}}$ $a=2$	$\epsilon^{\frac{-(i-i_0)^2}{2a^2}}$ $a=3$	$\epsilon^{\frac{-(i-i_0)^2}{2a^2}}$ $a=5$	$(i-i_0)$
−10	—	—	—	100	1.00000	0.13397	0.75000	0.35048	0.35048	0.00000	0.00000	0.00387	0.13534	−10
−9	—	—	—	81	0.69098	0.19098	0.65451	0.13976	0.47049	0.00000	0.00004	0.01111	0.19790	−9
−8	—	—	—	64	0.41221	0.25686	0.55226	0.01634	0.58959	0.00000	0.00034	0.02856	0.27804	−8
−7	—	—	—	49	0.19098	0.33087	0.44774	0.01634	0.70041	0.00000	0.00219	0.06573	0.37531	−7
−6	—	—	—	36	0.04894	0.41221	0.34549	0.13976	0.79693	0.00000	0.01111	0.13534	0.48657	−6
−5	—	—	—	25	0.00000	0.50000	0.25000	0.35048	0.87500	0.00000	0.04394	0.24935	0.60653	−5
−4	—	—	—	16	0.04894	0.59326	0.16543	0.58959	0.93271	0.00034	0.13534	0.41111	0.72615	−4
−3	—	—	—	9	0.19098	0.69098	0.09549	0.79693	0.97049	0.01111	0.32465	0.60653	0.83527	−3
−2	—	—	—	4	0.41221	0 79209	0.04323	0.93271	0.99101	0.13534	0.60653	0.80076	0.92312	−2
−1	—	—	—	1	0.69098	0.89547	0.01093	0.99101	0.99886	0.60653	0.88250	0.94592	0.98020	−1
0	1	0	30	0	1.00000	1.00000	0.00000	1.00000	1.00000	1.00000	1.00000	1.00000	1.00000	0
1	1	1	29	1	1.30902	1.10453	0.01093	1.00899	1.00114	0.60653	0.88250	0.94592	0.98020	1
2	1	2	28	4	1.58779	1.20791	0.04323	1.06729	1.00899	0.13534	0.60653	0.80076	0.92312	2
3	1	3	27	9	1.80902	1 30902	0.09549	1.20307	1.02951	0.01111	0.32465	0.60653	0.83527	3
4	1	4	26	16	1.95106	1.40674	0.16543	1.41041	1.06729	0.00034	0.13534	0.41111	0.72615	4
5	1	5	25	25	2.00000	1.50000	0.25000	1.64952	1.12500	0.00000	0.04394	0.24935	0.60653	5
6	1	6	24	36	1.95106	1.58779	0.34549	1.86024	1.20307	0.00000	0.01111	0.13534	0.48657	6
7	1	7	23	49	1.80902	1.66913	0.44774	1.98366	1.29959	0.00000	0.00219	0.06573	0.37531	7
8	1	8	22	64	1.58779	1.74314	0.55226	1.98366	1.41041	0.00000	0.00034	0.02856	0.27804	8
9	1	9	21	81	1.30902	1.80902	0.65451	1.86024	1.52951	0.00000	0.00004	0.01111	0.19790	9
10	1	10	20	100	1.00000	1.86603	0.75000	1.64952	1.64952	0.00000	0.00000	0.00387	0.13534	10
11	1	11	19	121	0.69098	1.91355	0.83457	1.41041	1.76241	0.00000	0.00000	0.00120	0.08892	11
12	1	12	18	144	0.41221	1.95106	0.90451	1.20307	1.86024	0.00000	0.00000	0.00034	0.05613	12
13	1	13	17	169	0.19098	1.97815	0.95677	1.06729	1.93586	0.00000	0.00000	0.00008	0.03405	13
14	1	14	16	196	0.04894	1.99452	0.98907	1.00899	1.98366	0.00000	0.00000	0.00002	0.01984	14
15	1	15	15	225	0.00000	2.00000	1.00000	1.00000	2.00000	0.00000	0.00000	0.00000	0.01111	15
16	1	16	14	256	0.04894	1.99452	0.98907	0.99101	1.98366	0.00000	0.00000	0.00000	0.00598	16
17	1	17	13	289	0.19098	1.97815	0.95677	0.93271	1.93586	0.00000	0.00000	0.00000	0.00309	17
18	1	18	12	324	0.41221	1.95106	0.90451	0.79693	1.86024	0.00000	0.00000	0.00000	0.00153	18
19	1	19	11	361	0.69098	1.91355	0.83457	0.58959	1.76241	0.00000	0.00000	0.00000	0.00073	19
20	1	20	10	400	1.00000	1.86603	0.75000	0.35048	1.64952	0.00000	0.00000	0.00000	0.00034	20
21	1	21	9	441	1.30902	1.80902	0.65451	0.13976	1.52951	0.00000	0.00000	0.00000	0.00015	21
22	1	22	8	484	1.58779	1.74314	0.55226	0.01634	1.41041	0.00000	0.00000	0.00000	0.00006	22
23	1	23	7	529	1.80902	1.66913	0.44774	0.01634	1.29959	0.00000	0.00000	0.00000	0.00003	23
24	1	24	6	576	1.95106	1.58779	0.34549	0.13976	1.20307	0.00000	0.00000	0.00000	0.00001	24
25	1	25	5	625	2.00000	1.50000	0.25000	0.35048	1.12500	0.00000	0.00000	0.00000	0.00000	25
26	1	26	4	676	1.95106	1.40674	0.16543	0 58959	1 06729	0.00000	0.00000	0.00000	0.00000	26
27	1	27	3	729	1.80902	1 30902	0.09549	0.79693	1.02951	0.00000	0.00000	0 00000	0.00000	27
28	1	28	2	784	1.58779	1.20791	0.04323	0.93271	1.00899	0.00000	0.00000	0.00000	0.00000	28
29	1	29	1	841	1.30902	1.10453	0.01093	0.99101	1.00114	0.00000	0.00000	0.00000	0.00000	29
30	1	30	0	900	1.00000	1.00000	0.00000	1.00000	1.00000	0.00000	0.00000	0.00000	0.00000	30

integral values of i from 0 to 30, curve (b) of Fig. 4 can be obtained.

In a like manner, the distributions P_2 and P_3 illustrated by curves (c) and (d) of Fig. 4 were obtained:

$$P_2=4.5145\left[1+\left(\sin\frac{i-16}{15}\pi\right)^3\right]+4.9675\left[1+\left(\sin\frac{i-20}{30}\pi\right)^3\right]+0.7121,$$

$$P_3=1.8819+0.20170i+0.015516i^2.$$

A direct graphical solution may also be made for these energy distributions. As an illustration, an enlarged portion of Fig. 5 is given in Fig. 6, with the points P and those corresponding to f_{11}, f_{12}, and f_{13} shown. Lines connecting the various points were drawn, and the areas indicated by A_1, A_2, and A_3 found to be (using an arbitrary scale):

$$A_1=23.3,\quad A_2=7.6,\quad A_3=11.2,\quad A=42.1.$$

The α's are therefore given by

$$\alpha_1=\frac{23.3}{42.1}=0.55,\quad \alpha_2=\frac{7.6}{42.1}=0.18,$$

$$\alpha_3=\frac{11.2}{42.1}=0.26,$$

which, to the number of places given, correspond to those of example No. 1. As P is inside the triangle formed by f_{11}, f_{12}, and f_{13}, the α's are all known to be positive.

On the basis of the preceding example, the steps to be followed in determining any energy

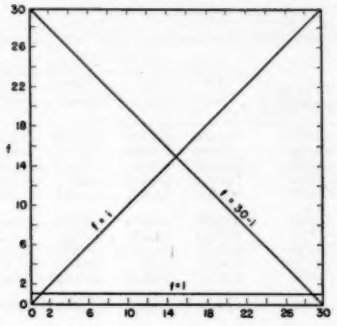

a

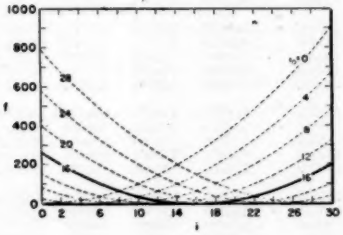

$f=(i-i_0)^2$

b

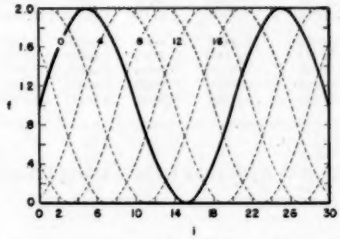

$f=1+\sin\frac{i-i_0}{10}\pi$

c

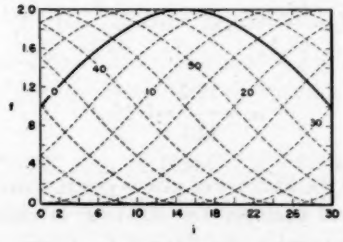

$f=1+\sin\frac{i-i_0}{30}\pi$

d

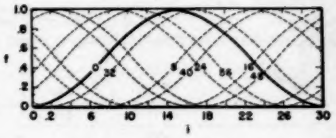

$f=\left[\sin\frac{i-i_0}{30}\pi\right]^2$

e

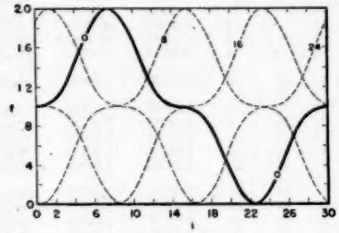

$f=1+\left[\sin\frac{i-i_0}{15}\pi\right]^2$

f

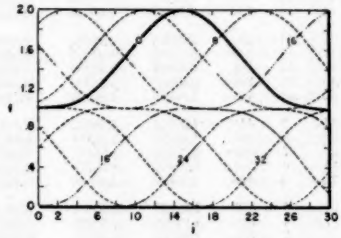

$f=1+\left[\sin\frac{i-i_0}{30}\pi\right]^3$

g

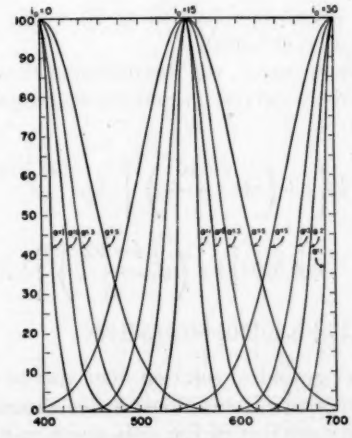

$f=e^{-\frac{(i-i_0)^2}{2a^2}}$

h

FIG. 2. Families of curves of the f's.

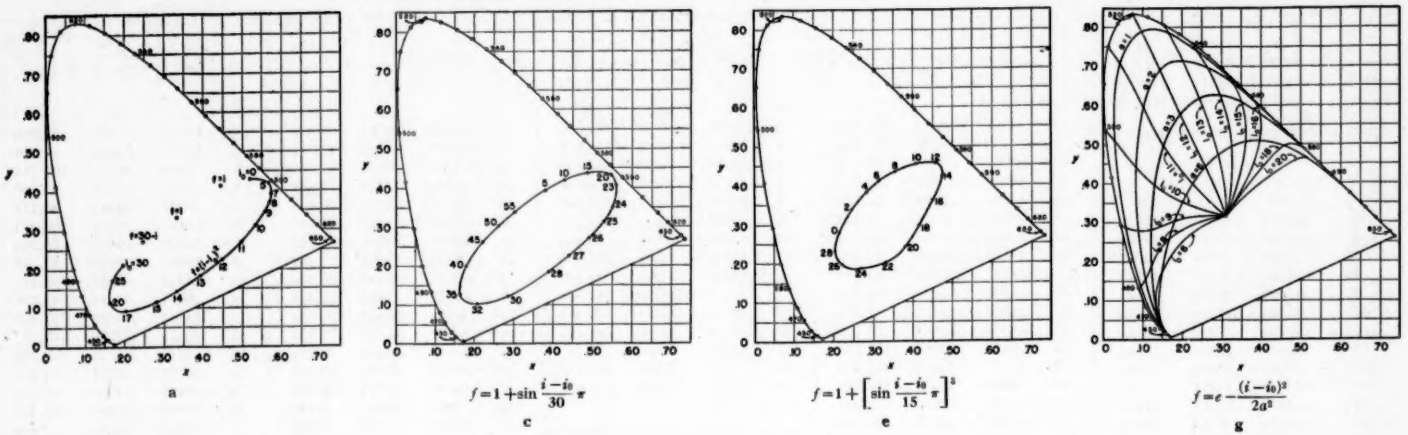

FIG. 3. Chromaticity loci of the f's used as energy distributions.

TABLE III. Values of the x's, y's, and m's for the f's taken as energy distributions.

	x	y	m
$f=1$	.33335	.33381	319.99
$f=i$	.44460	.41519	4119.67
$f=30-i$	.24971	.27263	5479.89

$f=(i-i_0)^2$

i_0	x	y	m
0	.52005	.42553	68755
5	.56547	.41687	35558
7	.57328	.39406	26759
8	.56936	.37419	23319
9	.55689	.34700	20520
10	.53326	.31206	18360
11	.49688	.27028	16841
12	.44846	.22477	15961
13	.39191	.18045	15721
14	.33360	.14267	16122
15	.28017	.11518	17162
17	.20359	.09314	21162
20	.16140	.11153	31962
25	.17276	.16720	62762
30	.19952	.20777	109562

$f=1+\sin\frac{i-i_0}{10}\pi$

i_0	x	y	m
0	.31498	.17360	366.344
2	.25602	.19845	323.130
4	.21244	.29048	278.715
5	.20622	.35818	261.528
6	.21522	.43058	250.064
7	.23988	.49538	245.444
8	.27653	.54029	248.120
10	.35794	.54832	273.626
11	.39007	.51701	293.959
12	.41221	.47186	316.840
13	.42408	.42011	340.028
14	.42663	.36724	361.255
15	.42120	.31697	378.442
16	.40911	.27175	389.906
18	.36932	.20307	391.850

$f=1+\sin\frac{i-i_0}{30}\pi$

i_0	x	y	m
0	.34108	.36684	554.262
5	.38269	.39388	496.388
10	.43081	.41903	391.248
15	.48898	.43841	267.013
20	.54896	.42959	156.972
23	.55628	.37985	110.438
24	.54437	.34999	99.315
25	.52168	.31296	90.609
26	.48717	.27027	84.417
27	.44180	.22516	80.805
28	.38905	.18222	79.814
30	.28332	.12022	85.708
32	.20732	.10097	101.841
35	.16277	.12614	143.582
40	.18003	.19976	248.722
45	.22192	.25893	372.957
50	.26327	.30269	482.998
55	.30228	.33725	549.361

$f=\left[\sin\frac{i-i_0}{30}\pi\right]^2$

i_0	x	y	m
0	.36021	.46729	190.520
2	.41762	.48731	182.654
4	.46798	.48478	170.870
6	.50281	.45528	157.205
8	.51158	.39694	144.022
10	.48499	.31522	133.600
12	.42217	.22712	127.742
14	.33705	.15792	127.460
16	.25440	.12801	132.804
18	.19594	.14117	142.848
20	.17052	.18658	155.857
22	.17567	.24885	169.581
24	.20410	.31522	181.647
26	.24830	.37717	189.969
28	.30206	.42924	193.107

$f=1+\left[\sin\frac{i-i_0}{15}\pi\right]^2$

i_0	x	y	m
0	.21693	.28087	338.626
2	.24817	.33856	345.737
4	.28168	.38402	361.068
6	.31433	.41219	376.361
8	.35555	.43377	373.601
10	.40923	.45314	349.371
12	.45809	.45561	320.826
14	.47225	.42208	304.808
16	.44999	.36095	298.480
18	.41677	.29720	287.566
20	.38227	.24353	270.057
22	.33346	.20490	261.948
24	.27032	.18875	276.547
26	.22084	.19803	305.722
28	.20358	.23003	329.058

$f=1+\left[\sin\frac{i-i_0}{30}\pi\right]^2$

i_0	x	y	m
0	.34347	.39248	484.103
4	.38399	.38455	474.660
8	.40104	.36186	425.998
12	.40566	.37304	337.283
16	.42850	.43783	244.627
20	.47876	.47322	186.135
22	.49172	.43442	172.103
24	.47984	.35944	164.800
26	.43985	.27117	160.789
28	.37680	.19516	157.823
30	.30192	.15158	155.867
32	.23235	.15108	157.164
34	.18792	.18813	165.310
36	.17926	.23926	183.706
40	.22777	.29329	254.948
44	.26816	.27904	351.447
48	.27492	.26757	430.032
52	.27509	.29681	467.867
56	.29761	.35483	479.181

$e^{\frac{-(i-i_0)^2}{2a^2}},\ a=1$

i_0	x	y	m
0	.17220	.00501	3.605
4	.16210	.01300	48.321
6	.14303	.03439	47.316
8	.09854	.13435	28.169
9	.06115	.28292	20.411
10	.03235	.51115	17.217
11	.04506	.70795	18.177
12	.09829	.78960	21.840
13	.16775	.78428	26.636
14	.23909	.74048	31.434
15	.30938	.68213	35.779
16	.37872	.61776	39.517
18	.51068	.48836	43.896
20	.61723	.38230	41.289
22	.68190	.31791	30.380
26	.72697	.27302	6.390
30	.73421	.26579	0.442

$e^{\frac{-(i-i_0)^2}{2a^2}},\ a=2$

i_0	x	y	m
0	.16843	.00771	17.316
4	.15626	.02113	79.741
6	.14007	.05099	82.351
8	.10949	.15734	61.117
9	.09172	.27663	50.770
10	.08503	.44042	44.756
11	.10325	.59693	43.975
12	.14684	.69030	47.679
13	.20449	.71487	54.267
14	.26676	.69503	62.057
15	.32943	.65281	69.696
16	.39066	.60110	76.191
18	.50328	.49477	82.710
20	.59364	.50569	76.833
22	.65604	.34365	58.524
26	.71488	.28505	16.560
30	.73109	.26891	1.773

$e^{\frac{-(i-i_0)^2}{2a^2}},\ a=3$

i_0	x	y	m
0	.16285	.01406	37.885
4	.14947	.04035	98.939
6	.13698	.08527	105.725
8	.12345	.19347	93.790
9	.12223	.28315	86.315
10	.13147	.39084	80.993
11	.15569	.49664	79.204
12	.19477	.57660	81.235
13	.24378	.61833	86.441
14	.29677	.62511	93.576
15	.34963	.60784	101.165
16	.40025	.57710	107.772
18	.49119	.50245	113.469
20	.56558	.43249	105.036
22	.62235	.38298	83.524
26	.69059	.30924	31.423
30	.71982	.28014	5.639

$e^{\frac{-(i-i_0)^2}{2a^2}},\ a=5$

i_0	x	y	m
0	.15189	.05231	75.815
4	.14765	.11674	127.356
6	.15178	.17644	142.228
8	.16739	.25876	148.958
9	.18182	.30626	150.470
10	.20156	.35484	151.571
11	.22666	.40108	152.764
12	.25646	.44145	154.338
13	.28970	.47315	156.309
14	.32481	.49472	158.428
15	.36023	.50618	160.227
16	.39472	.50869	161.114
18	.45794	.49420	157.822
20	.51175	.46561	145.263
22	.55650	.43302	123.519
26	.62352	.37419	67.810
30	.66771	.33170	24.979

distribution P corresponding to a given set of tristimulus values are:

(i) Find the trichromatic coefficients for the given set of tristimulus values, and plot the point corresponding to them on a chromaticity diagram.

(ii) Select three f's with trichromatic values which, when plotted on the same diagram, include within the triangle formed by them the point to be matched. By examining the graphs of the f's being selected, the approximate curve shape can be determined in advance. In making this determination, the area relationships and the influence of the m values on the sizes of the a's as indicated by Eq. (5c) must also be kept in mind.

(iii) Secure from Table III the values of the x's and y's corresponding to each f, and determine the α's by substituting in Eqs. (8).

(iv) From the α's, determine the a's from Eq. (5c). The values of m_1, m_2, and m_3 are taken from Table III for f_1, f_2, and f_3, while m is the sum of the tristimulus values being matched.

(v) Insert the constants (a's) in the equation for P in the form given by Eq. (2). By assigning the i in this equation successive integral values from 0 to 30, and by use of Table II, the plot of P as a function of wave-length, λ, can be obtained.

TRANSMITTANCE AND REFLECTANCE DISTRIBUTIONS

So far the data presented have applied to energy distributions only. Transmittance and reflectance distributions can be obtained by using the same procedures, provided corrections are made for the illuminant. It is often convenient, however, to be able to determine such distributions directly. This may be done by an extension of the methods already outlined. The essential elements of the theory are as follows.

The tristimulus values of the radiation from the light source with a spectral-energy distribution P, as a function of wave-length, λ, as seen through a medium of transmittance T, also a function of wave-length, λ, is defined by the Committee on Colorimetry (reference 3, p. 646) as:

$$X=\int_0^\infty \bar{x}TPd\lambda \Big/ \int_0^\infty \bar{y}Pd\lambda,$$

$$Y=\int_0^\infty \bar{y}TPd\lambda \Big/ \int_0^\infty \bar{y}Pd\lambda, \qquad (11)$$

$$Z=\int_0^\infty \bar{z}TPd\lambda \Big/ \int_0^\infty \bar{y}Pd\lambda,$$

when all the other symbols are the same as those given in Eqs. (1). Let:

$$T=a_1f_1+a_2f_2+a_3f_3. \qquad (12)$$

Then:

$$\begin{aligned} X&=a_1X_1+a_2X_2+a_3X_3,\\ Y&=a_1Y_1+a_2Y_2+a_3Y_3,\\ Z&=a_1Z_1+a_2Z_2+a_3Z_3, \end{aligned} \qquad (13)$$

where

$$X_i=\int_0^\infty \bar{x}f_iPd\lambda \Big/ \int_0^\infty \bar{y}Pd\lambda,$$

$$Y_i=\int_0^\infty \bar{y}f_iPd\lambda \Big/ \int_0^\infty \bar{y}Pd\lambda, \qquad (14)$$

$$Z_i=\int_0^\infty \bar{z}f_iPd\lambda \Big/ \int_0^\infty \bar{y}Pd\lambda.$$

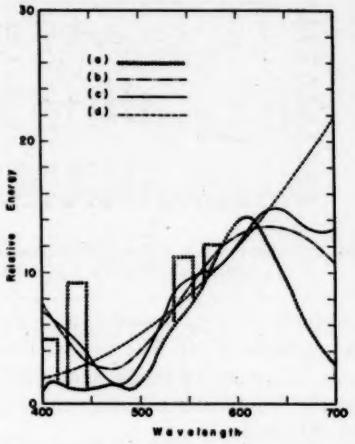

FIG. 4. Spectral-energy distribution of the white fluorescent light indicated in Fig. 5 and three calculated distributions which yield the same tristimulus values.

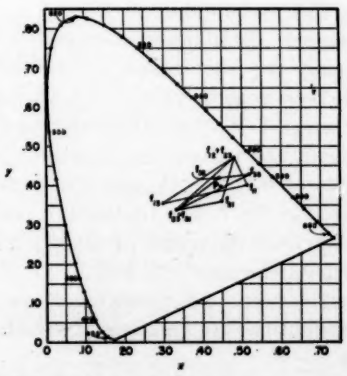

FIG. 5. Chromaticity plots of white fluorescent light and of f's used as energy distributions which can be combined to match it.

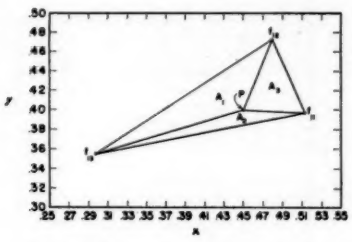

FIG. 6. Portion of Fig. 5 enlarged to illustrate graphical solution.

The equations of (13), however, are exactly the same as are those of (4). The same definitions as in (5) can therefore be made and, through the same series of transformations, the results of Eqs. (8) obtained.

From these considerations it is evident that the method for securing transmittance distributions is exactly the same as that for energy distributions, except for the difference in defining X_i, Y_i, and Z_i. These differences may be seen by comparing Eqs. (3) with those of (14). Reflectance distributions depend upon exactly the same definitions as transmittance distributions, although it is convenient to distinguish between the two types of problems by use of the letter R in place of the letter T in equations such as (11) and (12).

In dealing with transmittances and reflectances, the same f's were used. These are listed in Table I, their values given in Table II, and their plots in Fig. 2. While the f's are the same, however, the integrals are not, although they would be the same, except for a constant factor, if a source with equal amounts of energy at all wavelengths were to be assumed. If such a source is not assumed, the illuminant must be decided upon before the integrations can be performed. This has been done by using I.C.I. Illuminant C, and the integrals of the type indicated by Eqs. (14) determined. The values of x, y, and m for each f are tabulated in Table IV, and the chromaticity plots given in Fig. 7. The tristimulus values used were taken from the report of the committee on colorimetry (reference 3, p. 643).

Determinations of transmittance and reflectance distributions are illustrated in the following example.

Example No. 2.—Problem: To determine colorimetric matches for the green paint with the spectrophotometric curve given as (a) in Fig. 8,[10] using I.C.I. Illuminant C.

The tristimulus values are 0.1550, 0.2419, and 0.2264. From these $m=0.6233$, $x=0.24868$, and $y=0.38810$. The chromaticity plot is given as P in Fig. 9. By the procedures already shown, the equations were found to be

$$R_1=0.08800\left[1+\sin\frac{i-7}{10}\pi\right]+0.07073\left[1+\sin\frac{i-5}{10}\pi\right]+0.03923\left[1+\sin\frac{i}{30}\pi\right],$$

$$R_2=0.16819\left[1+\sin\frac{i-6}{10}\pi\right]+0.003069i+0.001308(30-i),$$

$$R_3=0.19593\left[e^{\frac{-(i-11)^2}{50}}\right]+0.28548\left[e^{\frac{-(i-12)^2}{50}}\right]-0.15784\left[e^{\frac{-(i-11)^2}{18}}\right].$$

The distributions of R_1, R_2, and R_3 are given as b, c, and d, respectively, of Fig. 8.

In determining transmittance or reflectance distributions, ordinate values greater than 100 percent may sometimes be obtained. This can usually be avoided by means of an advance rough graphical solution using the combination of f's being considered, with the rejection of those sets which do not appear to be satisfactory. If, however, such a result is obtained, an entirely new solution must be found. Exception to this rule may be taken if a trichromatic rather than a tristimulus match is required. In this case all the ordinate values can be multiplied by any arbitrary constant to reduce the maximum point to the desired level.

NEGATIVE CONSTANTS

Negative portions of either an energy, transmittance, or reflectance distribution have no

[10] Taken from the *Handbook of Colorimetry* (reference 2), p. 2.

TABLE IV. Values of the x's, y's, and m's for the f's taken as transmittance or reflectance distributions with I.C.I. Illuminant C.

	x	y	m
$f=1$	.31004	.31646	3.1600
$f=i$	.42154	.40953	38.4113
$f=30-i$	.23408	.25306	56.3876

$f=(i-i_0)^2$

i_0	x	y	m
0	.50276	.42948	616.83
5	.55401	.42541	311.72
7	.56192	.40052	233.91
8	.55627	.37765	204.49
9	.54040	.34602	181.38
10	.51185	.30560	164.60
11	.46998	.25847	154.14
12	.41728	.20920	149.99
13	.35946	.16374	152.17
14	.30353	.12731	160.67
15	.25526	.10254	175.48
17	.19068	.08511	224.08
20	.15775	.10363	344.36
25	.16810	.15401	671.24
30	.19058	.19122	1156.12

$f=1+\sin\frac{i-i_0}{10}\pi$

i_0	x	y	m
0	.28353	.15574	3.73776
2	.23074	.18007	3.37098
4	.19599	.26748	2.92360
5	.19313	.33284	2.72370
6	.20397	.40532	2.56650
7	.22933	.47439	2.46740
8	.26611	.52672	2.43609
10	.34841	.54910	2.58217
11	.38020	.51955	2.74526
12	.40068	.47237	2.94895
13	.40957	.41636	3.17329
14	.40821	.35862	3.39633
15	.39858	.30405	3.59623
16	.38256	.25570	3.75343
18	.33759	.18457	3.88384

$f=1+\sin\frac{i-i_0}{30}\pi$

i_0	x	y	m
0	.31846	.35020	5.44303
5	.35917	.38130	4.77163
10	.40824	.41249	3.66838
15	.47039	.44028	2.42890
20	.53697	.43819	1.38531
23	.54258	.38295	.97414
24	.52723	.34840	.88321
25	.49972	.30586	.81724
26	.46001	.25798	.77693
27	.41064	.20933	.76273
28	.35665	.16533	.77479
30	.25773	.10705	.87689
32	.19338	.09200	1.07878
35	.15860	.11663	1.54830
40	.17418	.18361	2.65155
45	.20994	.23917	3.89102
50	.24633	.28229	4.93462
55	.28187	.31803	5.50269

$f=\left[\sin\frac{i-i_0}{30}\pi\right]^2$

i_0	x	y	m
0	.34180	.45659	1.83452
2	.40056	.48588	1.70705
4	.45390	.49066	1.55762
6	.49055	.46274	1.41205
8	.49654	.39831	1.29551
10	.46195	.30604	1.22817
12	.39129	.21052	1.22165
14	.30596	.14132	1.27710
16	.23149	.11482	1.38491
18	.18325	.12875	1.52646
20	.16406	.17082	1.67726
22	.16991	.22824	1.81124
24	.19515	.29144	1.90523
26	.23484	.35388	1.94298
28	.28497	.41057	1.91797

$f=1+\left[\sin\frac{i-i_0}{15}\pi\right]^3$

i_0	x	y	m
0	.20529	.25920	3.56352
2	.23281	.31683	3.53984
4	.26420	.36442	3.60852
6	.29588	.39450	3.71500
8	.33581	.41941	3.63878
10	.38943	.44652	3.31079
12	.44138	.45816	2.93903
14	.45597	.42390	2.76350
16	.42802	.35292	2.77190
18	.38926	.28230	2.76066
20	.35211	.22690	2.64949
22	.30411	.18808	2.60888
24	.24663	.17185	2.82161
26	.20556	.18069	3.20820
28	.19316	.21079	3.49972

$f=1+\left[\sin\frac{i-i_0}{30}\pi\right]^2$

i_0	x	y	m
0	.32255	.37736	4.72782
4	.36126	.37202	4.56031
8	.37545	.34875	4.07922
12	.37885	.36059	3.22039
16	.40572	.43316	2.28732
20	.46471	.48069	1.68453
22	.47792	.43899	1.55399
24	.46037	.35414	1.51149
26	.41223	.25657	1.52105
28	.34472	.17737	1.55205
30	.27287	.13563	1.59211
32	.21244	.13693	1.65183
34	.17728	.17247	1.75962
36	.17272	.22050	1.94860
40	.21687	.27318	2.63420
44	.25126	.25986	3.58536
48	.25529	.24814	4.39152
52	.25530	.27651	4.76593
56	.27765	.33544	4.79887

$e^{\frac{-(i-i_0)^2}{2a^2}}$, $a=1$

i_0	x	y	m
0	.17192	.00491	0.02832
4	.16197	.01313	0.54481
6	.14303	.03437	0.54844
8	.09868	.13299	0.32525
9	.06247	.27466	0.22933
10	.03351	.49436	0.18102
11	.04337	.69712	0.17674
12	.09743	.78795	0.20387
13	.16921	.78260	0.24956
14	.24090	.73913	0.30165
15	.31004	.68161	0.34965
16	.37775	.61869	0.38539
18	.50801	.49096	0.40280
20	.61593	.38359	0.35220
22	.68175	.31808	0.25206
26	.72694	.27306	0.05268
30	.73540	.26460	0.00332

$e^{\frac{-(i-i_0)^2}{2a^2}}$, $a=2$

i_0	x	y	m
0	.16784	.00810	0.16996
4	.15577	.02158	0.89183
6	.14002	.05021	0.94322
8	.11067	.14729	0.69409
9	.09319	.25583	0.56172
10	.08522	.41160	0.47355
11	.10173	.57261	0.44263
12	.14575	.67736	0.46365
13	.20494	.70960	0.52134
14	.26746	.69330	0.59558
15	.32860	.65352	0.66828
16	.38746	.60424	0.72486
18	.49710	.50085	0.75622
20	.58900	.41029	0.66837
22	.65420	.34550	0.49242
26	.71480	.28517	0.13654
30	.73126	.26874	0.01408

$e^{\frac{-(i-i_0)^2}{2a^2}}$, $a=3$

i_0	x	y	m
0	.16201	.01481	0.39863
4	.14897	.03978	1.10268
6	.13702	.08033	1.19080
8	.12378	.17654	1.04340
9	.12188	.25829	0.94214
10	.12961	.36106	0.85999
11	.15213	.46843	0.81468
12	.19025	.55594	0.81145
13	.23909	.60683	0.84424
14	.29193	.62106	0.89938
15	.34413	.60891	0.96009
16	.39367	.58154	1.01035
18	.48298	.51013	1.03381
20	.55810	.43981	0.92683
22	.61729	.38195	0.71664
26	.68942	.31043	0.26112
30	.71961	.28036	0.04595

$e^{\frac{-(i-i_0)^2}{2a^2}}$, $a=5$

i_0	x	y	m
0	.15102	.05060	0.82581
4	.14645	.10788	1.39868
6	.14944	.16118	1.55264
8	.16248	.23660	1.59991
9	.17503	.28162	1.59621
10	.19265	.32918	1.58386
11	.21563	.37631	1.56927
12	.24361	.41950	1.55673
13	.27554	.45556	1.54776
14	.30993	.48231	1.54102
15	.34519	.49899	1.53287
16	.37993	.50619	1.51826
18	.44435	.49841	1.44929
20	.49973	.47303	1.30584
22	.54619	.44121	1.09040
26	.61678	.38053	0.58134
30	.66401	.33534	0.20963

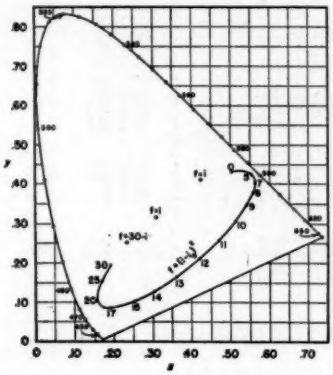

a

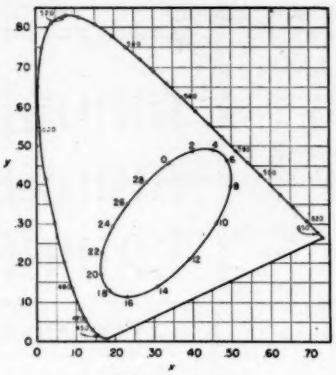

$f=\left[\sin\frac{i-i_0}{30}\pi\right]^3$

d

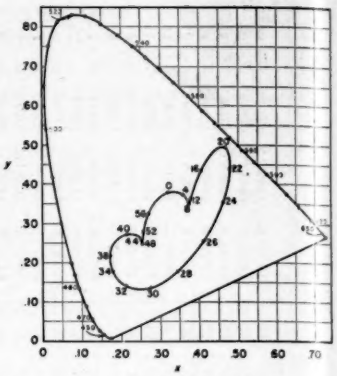

$f=1+\left[\sin\frac{i-i_0}{30}\pi\right]^3$

f

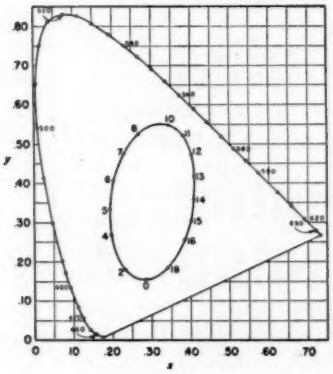

$f=1+\sin\frac{i-i_0}{10}\pi$

b

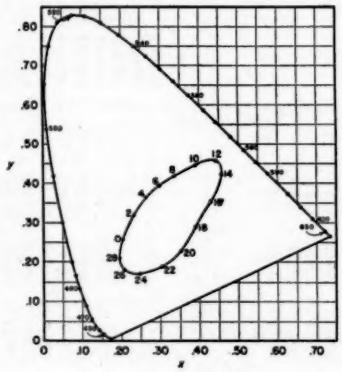

$f=1+\left[\sin\frac{i-i_0}{15}\pi\right]^3$

e

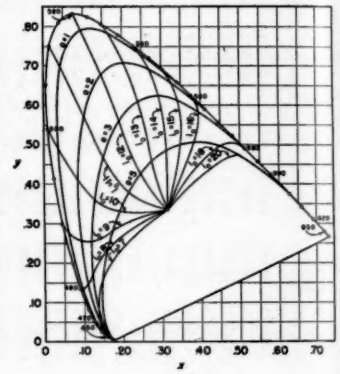

$f=e-\frac{(i-i_0)^2}{2a^2}$

g

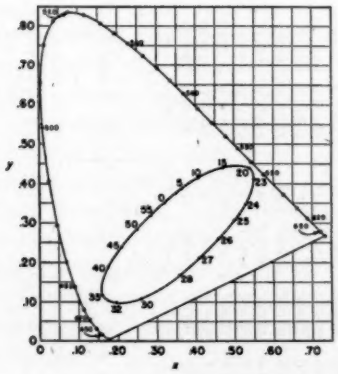

$f=1+\sin\frac{i-i_0}{30}\pi$

c

FIG. 7. Chromaticity loci of the f's used as transmittance or reflectance distributions with Illuminant C.

physical significance. As was pointed out earlier, these may be avoided, provided the f's are positive throughout the spectral region and provided the a's come out to be positive. All the f's selected and listed in Table I are positive throughout the interval of $\lambda = 400$ mμ to 700 mμ. As has been indicated, the necessary and sufficient condition that the a's be positive is that the points corresponding to the given tristimulus values be located within the triangle on the chromaticity diagram formed by the three f's.

It is sometimes convenient, however, to violate the rule that the a's shall all be positive. This was illustrated in Example No. 2, in which a_{33} for R_3 was found to be negative. The only guide that can be followed in such cases is that the value of such an a shall be small enough so that, when multiplied by its f, the product is not greater at any wave-length than that obtained at the same wave-length from the other two sets of a's and f's. In this way, the distribution curve may be kept positive, even though one of the a's is negative.

CHROMATICITY MATCHES

In synthesizing a spectral distribution, it is sometimes sufficient that the curve obtained correspond to a given chromaticity, without requiring that it correspond to any particular set of tristimulus values. This means that in the equations

$$\begin{aligned} X &= mx = a_1X_1 + a_2X_2 + a_3X_3, \\ Y &= my = a_1Y_1 + a_2Y_2 + a_3Y_3, \\ Z &= mz = a_1Z_1 + a_2Z_2 + a_3Z_3, \end{aligned} \tag{15}$$

which may be obtained from Eqs. (4) and (5), the values of x, y, and z would be specified, but that those of X, Y, and Z would not be. This condition is attained if it is assumed that the value of m is arbitrary, or free to be determined on the basis of some other consideration.

In Eqs. (15) it is assumed that, in accordance with definitions already given, X_i, Y_i, and Z_i are the tristimulus values of the f's, and are therefore known. If an energy distribution is being synthesized, they would be defined by Eqs. (3); if a transmittance or reflectance distribution, by Eqs. (14). If x, y, and z are also known, then this gives (considering only the parts of the equations *not* including X, Y, and Z) three equations with four unknowns. These equations do not define, therefore, a unique solution.

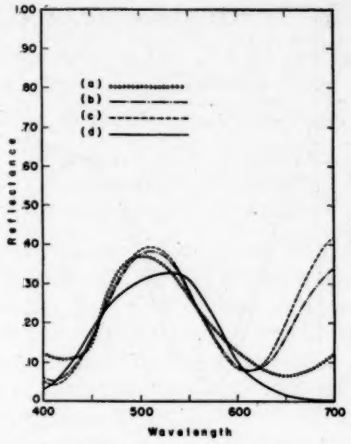

FIG. 8. Spectral-reflectance distributions of the green paint of Fig. 9 and the calculated distributions which yield matches with it when all are used with Illuminant C.

To obtain a unique solution, either the m or one of the a's may be assigned an arbitrary value. Usually it is most convenient to let $m = 1$ and determine α_1, α_2, and α_3, using the Eqs. (8). In determining the a's, using Eq. (5c), the m may then be given any other desired value, without affecting the trichromatic match. This value may be chosen to fulfill some other conditions, such as to give the distribution a particular ordinate value at some wave-length. This is done in the following example.

Example No. 3.—Problem: To determine three

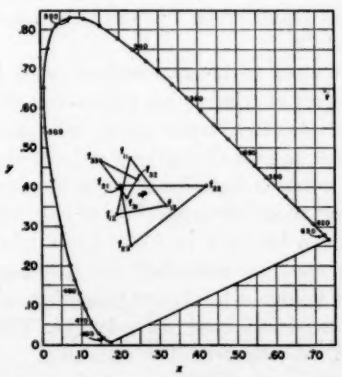

FIG. 9. Chromaticity plot of a green paint under Illuminant C and plots of f's used as reflectance distributions with the same illuminant which can be combined to match it.

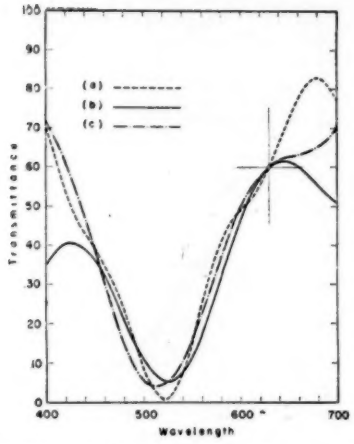

FIG. 10. Spectral-transmittance distributions which, with Illuminant *C*, are of the same chromaticities and which have transmittances of 0.60 at 630 mμ.

spectral-transmittance distributions of the chromaticity $x=0.37790$ and $y=0.23781$, all of which have a transmittance of 0.60 at 630 mμ.

Using the method just described, these curves were found and are given in Fig. 10.

USE OF MORE THAN THREE *f*'s

Through the use of three *f*'s it is possible to obtain spectral-distribution curves having a given set of tristimulus values, or curves having given trichromatic coefficients and which meet some other condition, as was described in the preceding section. If, in addition, other conditions are to be applied, use must, in general, be made of more than three *f*'s. Also, the number of these conditions must equal or be less than the number of additional *f*'s.

If the curve to be synthesized is to have a particular set of tristimulus values and also is to meet some one other requirement, one approach is to make use of four *f*'s and proceed as before, except that a fourth equation must be introduced to supplement those corresponding to Eqs. (4). This equation can be used to fulfill some additional condition such as assigning the distribution a particular value, or a relative maximum or minimum, at some selected wave-length. This procedure is, mathematically speaking, easy to handle, but in practice presents the major difficulty that it provides no simple way of predicting in advance what sort of solution will result. Negative values for a distribution will often be obtained, as well as transmittance and reflectance values above 100 percent.

Another, and better, procedure by which the same results can be accomplished is apparent from the following consideration: Let P_1 and P_2 be two energy distributions which have the same tristimulus values. If a third distribution, P, is defined as

$$P=\theta P_1+\eta P_2, \tag{16}$$

where

$$\theta+\eta=1, \tag{17}$$

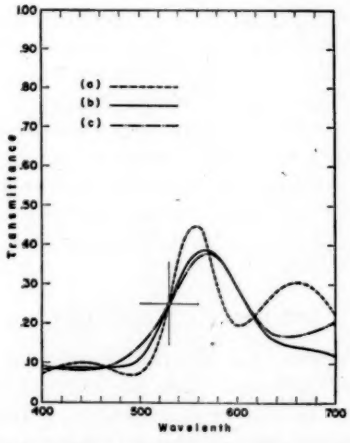

FIG. 11. Spectral-transmittance distributions which, with Illuminant *C*, have the same tristimulus values and which have transmittances of 0.25 at 530 mμ.

then the distribution P will have the same tristimulus values as P_1 and P_2.

The following examples will illustrate the manner in which combinations can be made which fulfill conditions of the type described.

Example No. 4.—Problem: To synthesize spectral-transmittance curves which with I.C.I. Illuminant *C* have the same tristimulus value as Wratten light filter No. 3N5[11] and which have transmittances of 0.25 at 530 mμ.

The tristimulus values for the filter are $X=0.2423$, $Y=0.2784$, $Z=0.1094$.[12] In synthesizing the curves meeting the requirements given,

[11] The spectral transmittances for this filter is given in Eastman Kodak Company, *Wratten Light Filters* (Eastman Kodak Company, Rochester, New York, 1945), 17th edition, p. 72.

[12] David L. MacAdam, "Colorimetric specifications of Wratten light filters," J. Opt. Soc. Am. **35**, 670–675 (1945), p. 671.

curves having these same tristimulus values were first obtained by the method given earlier. The equations were

$$T_1=0.09523e^{\frac{-(i-4)^2}{50}}+0.40229e^{\frac{-(i-14)^2}{8}}+0.44264e^{\frac{-(i-26)^2}{50}},$$

$$T_2=0.47755e^{\frac{-(i-16)^2}{8}}+0.10179e^{\frac{-(i-4)^2}{50}}+0.24356e^{\frac{-(i-26)^2}{50}},$$

$$T_3=0.08831+0.15258e^{\frac{-(i-16)^2}{18}}+0.19046e^{\frac{-(i-18)^2}{18}},$$

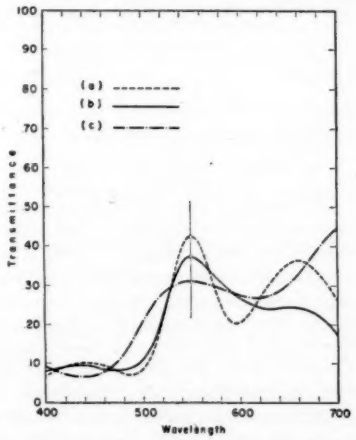

FIG. 12. Spectral-transmittance distributions which, with Illuminant *C*, have the same tristimulus values and which have maxima at 550 mμ.

$$T_4=0.03460+0.0012576(i-7)^2+0.27928e^{\frac{-(i-12)^2}{18}}.$$

The ordinate values of these four curves for $\lambda=530$ were

$$T_1=0.38894,\quad T_2=0.18347,$$
$$T_3=0.22837,\quad T_4=0.34405.$$

Using these values and value of 0.25 for T_a, T_b, and T_c, in the following equation

$$T_a=\theta_aT_1+\eta_aT_2,\quad T_b=\theta_bT_1+\eta_bT_3,$$
$$T_c=\theta_cT_3+\eta_cT_4.$$

The values of the θ's and η's were found, giving:

$$T_a=0.32379T_1+0.67621T_2;$$
$$T_b=0.13473T_1+0.86527T_3;$$
$$T_c=0.81300T_3+0.18700T_4.$$

The curves are plotted in Fig. 11, where *a*, *b*, and *c* correspond to T_a, T_b, and T_c, respectively.

Example No. 5.—Problem: To synthesize spectral-transmittance curves which with I.C.I. Illuminant *C* have the same tristimulus values as Wratten light filter No. 3N5 and which have relative maxima at 550 mμ.

In this problem, let

$$T=\theta T'+\eta T'';$$

then

$$dT/di=\theta(dT'/di)+\eta(dT''/di).$$

If the curve is to have a maximum at 550 mμ, then

$$(dT/di)_{i=15}=0$$

and

$$\theta(dT'/di)_{i=15}+\eta(dT''/di)_{i=15}=0.$$

Using the same distributions as were first obtained in Example No. 4, three curves were obtained with the equations

$$T_a=0.59605T_1+0.40395T_2,$$
$$T_b=0.42051T_1+0.57949T_3,$$
$$T_c=0.39987T_3+0.60013T_4,$$

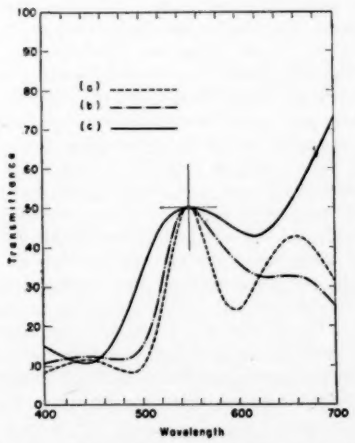

FIG. 13. Spectral-transmittance distributions which, with Illuminant *C*, have the same chromaticities, and which have maxima of 0.50 at 550 mμ.

These curves are plotted as a, b, and c, respectively, in Fig. 12.

In this last example it will be noted that if θ and η are both to be positive that $(dT'/di)_{i=1b}$ and $(dT''/di)_{i=1b}$ must have opposite signs. Furthermore, if the point is to be a relative maximum, then the second derivative must be negative, or

$$d^2T/di^2=\theta(d^2T'/di^2)+\eta(d^2T''/di^2)<0.$$

From these two relationships it is evident that a maximum in a combination curve (T) can best be obtained between the maxima of the component curves (T' and T''), preferably in the region in which both have negative second derivatives, or, in other words, are concave downward.

Example No. 6.—Problem: To obtain spectral-transmittance curves which with I.C.I. Illuminant *C* have the same chromaticity as Wratten light filter No. 3N5, and which have relative maxima of 0.50 at 550 mμ.

The three curves of the preceding example have relative maxima at 550 mμ. At this wave-length their ordinates are $T_a=0.42276$, $T_b=0.37116$, and $T_c=0.30994$. The new curves, T_a', T_b', and T_c', will therefore be given by:

$$T_a'=(0.50/0.42276)T_a \quad T_b'=(0.50/0.37116)T_b$$
$$=1.1827T_a \qquad =1.3471T_b,$$

$$T_c'=(0.50/0.30994)T_c$$
$$=1.6132T_c.$$

Their plots are shown as a, b, and c, respectively, in Fig. 13.

The writers are indebted to Mr. James W. Watts for drawing the figures, to Mr. Howard Smith for preparing most of the examples, and to Miss Nancy Allison for much of the computational work. They wish also to thank Mr. R. H. Morris, Dr. D. L. MacAdam, and Dr. C. F. J. Overhage for detailed criticisms on preliminary drafts of the paper, and Mr. R. M. Evans, Dr. W. T. Hanson, Jr., Dr. C. A. Horton, and Mr. R. A. Morris for many helpful suggestions.

Book Review

An Introduction to Color

RALPH M. EVANS. John Wiley and Sons, Inc., New York, and Chapman and Hall, Limited, London, 1948. Price $6.00.

It was Lord Kelvin who said, "I often say that when you can measure what you are speaking about, and express it in numbers, you know something about it; but when you cannot measure it, when you cannot express it in numbers, your knowledge is of a meagre and unsatisfactory kind; it may be the beginning of knowledge, but you have scarcely, in your thoughts, advanced to the stage of *Science*, whatever the matter may be." By this criterion, color has become a science during modern times; and the metamorphosis has made available a new and concise terminology. Evans employs this modern terminology to good advantage in his excellent survey of color phenomena, but he skillfully avoids the use of mathematics that would be an obstacle for many readers. His style appears to be elementary enough for the beginner who is willing to read carefully, but is nevertheless accurate enough to satisfy the expert.

One receives the impression on reading this volume that it must have been a long time in preparation. The subject matter is well organized, the copious figures and plates are well selected, and there are remarkably few errors.

The context may be surmised from the titles of the twenty-one chapters: Color and Light, Color Perception, The Physical Nature of Light, The Measurement of Color, Light Sources, The Specification of Color, Illumination, Color Differences and Color Names, Colored Objects, Mixtures of Colored Lights, The Physics of Everyday Color, Effects of Illuminants, Color Vision, Transparent Colorant Mixtures, The Visual Variables of Color, Paints and Pigments, Perception and Illusion, Color in Photography, Brightness Perception, Color in Art, Design and Abstraction.

The author is in charge of the Color Control Department of the Eastman Kodak Company, and this close association with color photography has made him a keen observer of perceptual phenomena. His excellent treatment of these phenomena should appeal especially to the artist, who is generally more interested in what he sees than in the object colors that Newton called "The permanent colours of natural bodies."

ARTHUR C. HARDY,
Massachusetts Institute of Technology

JOURNAL OF THE OPTICAL SOCIETY OF AMERICA VOLUME 38, NUMBER 10 OCTOBER, 1948

A Recording Photometer and its Use in Studies of Cathode-Ray Screen Displays

FERDINAND HAMBURGER, JR. AND ELLWOOD J. KING
The Johns Hopkins University, Baltimore, Maryland

(Received February 6, 1948)

In studies involving the performance of operators of radar indicators it became necessary to provide data concerning the transient light patterns generated on the screens of cathode-ray tubes. This paper describes a photometer which permits the determination of brightness at any instant at a selected point on the radar screen.

A 931-A photo-multiplier tube combined with suitable optical and electronic auxiliaries provides a photometer that will respond faithfully to rapid light transients for peak brightness determinations, and will also provide data for slow brightness changes associated with phosphor decay characteristics.

The photometer described is useful down to 0.005 footlamberts when examining a circular area 0.025 inch in diameter. It will measure much greater brightness levels by incorporated sensitivity controls. Its usefulness is not limited to radar screen measurements but it is applicable to many photometric problems.

INTRODUCTION

A SPECIAL photometer has been designed and constructed to provide data describing the transient light patterns generated by radar indicators. The photometer permits the determination of brightness at any instant, at a selected point on the radar screen, as the sweep turns through its azimuthal cycle. Since the area to be examined must be quite small the design required a compromise between sensitivity and areal resolution.

The photometer will respond faithfully to rapid light transients for peak brightness determinations, and will also provide data concerning the slower changes of light after the radar sweep has moved through the examination area. Recording techniques have been incorporated in the design to provide for the large quantity of data necessary for complete studies of radar screens.

The device described is not limited to radar screen measurements but is applicable to many photometric problems such as the response of glow modulator tubes, light valves, and television screen presentations.

PHOTOMETER DESIGN

A 931-A photomultiplier tube is used in the photometer, which combined with an optical system incorporating a Wratten No. 15 yellow filter, produces a spectral response characteristic approximately matching that of the human eye (Fig. 1). Although it is apparent that the matching is not perfect it was considered sufficient for the present purpose. The photomultiplier tube is supplied from a well regulated power supply shown schematically in Fig. 2. No appreciable change in photometer output was noted as the alternating voltage input to the power supply was varied between 95 and 130 volts.

The details of the photo-tube mounting are shown in Fig. 3. An f 1.9 anastigmat photographic objective lens is mounted at one end of a long tube and focuses an image of the radar sweep on a mask located immediately in front of the photo-tube. The arrangement provides a fixed magnification of 10, thus a 0.25 inch diameter hole in the mask limits examination to a 0.025 inch diameter spot on the screen. Preliminary measurements of sweep line widths for normal radar indicator operating conditions indicated that this definition was adequate, providing a sensitivity of 0.005 footlambert. Variation in sensitivity may be obtained by the use of the attenuating diaphragm which is part of the lens assembly, by variation of the applied dynode potentials, and by the insertion of neutral filters in a compartment located in front of the photo-tube. This same compartment contains the spectral correction filter. The photo-tube is housed in a compartment at the end of the vertical lens tube. This same compartment also contains the photo-tube voltage divider (135,000 ohms total) and provides for introduction of the

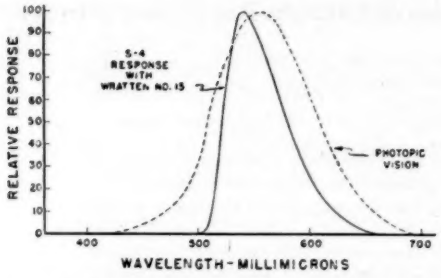

FIG. 1. Adjustment of the photometer's spectral characteristic to simulate the human visibility function.

high voltage by a standard RG-8/U coaxial cable. The entire unit is raised or lowered for focusing as indicated by the position of maximum response. Ordinary laboratory style clamps and fixtures are used for mounting.

To measure rapid light variations associated with peak brightness the photo-multiplier anode (Fig. 4a) is coupled to a frequency compensating load (Fig. 4b) and then to the vertical deflection amplifier of an oscilloscope having an essentially flat frequency characteristic from 20 cycles to 2 megacycles. The response was checked by the use of a rotating mirror unit providing pulses of constant amplitude with durations from one microsecond to 10,000 microseconds.

To measure slow light variations the photo-multiplier anode is coupled to a resistive load (Fig. 4c) and then to a direct current amplifier whose output controls the vertical deflection of an oscilloscope. By means of a mechanically operated cam switch on the radar indicator a slow horizontal time sweep is initiated and a plot of brightness *versus* time appears on the oscilloscope screen (a type P5 phosphor). This plot on the oscilloscope screen is recorded by a 16 mm motion picture camera adjusted for a single frame time exposure. The camera operation is synchronized with the sweep as is a counter which is photographed simultaneously with the oscilloscope screen for identification purposes.

The interconnections of the equipment are shown functionally in Fig. 5. The solid lines shown in the diagram indicate circuits used normally for automatic recording of data. The dotted lines indicate circuits used for manual control during adjustments. The control box circuits are shown schematically in Fig. 6.

The trigger voltage delivered to the radar indicator is provided by either a radar or target simulating equipment and is permanently connected. Under manual operation this trigger voltage is grounded to prevent illumination of the screen. This permits darkening the screen without disturbing previously adjusted controls on the radar indicator. The d.c. amplifier shown on the right side of Fig. 7 amplifies the sweep voltage developed by charging either one, two, or three 10-microfarad capacitors as selected by the sweep selector. Fine adjustment of the sweep time is controlled by the sweep adjusting rheostat. The

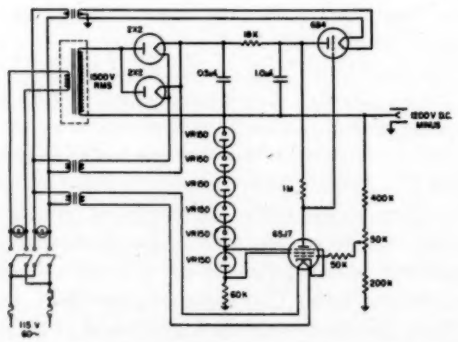

FIG. 2. Regulated high voltage power supply.

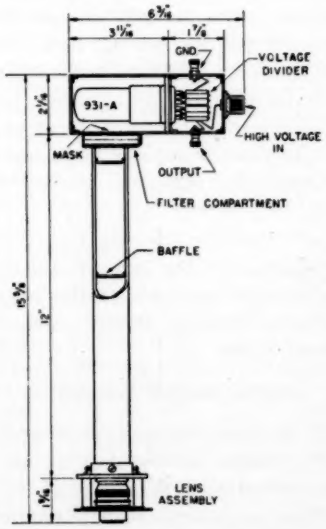

FIG. 3. Details of the photometer head.

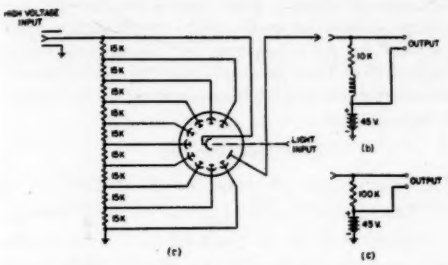

FIG. 4. Schematic of the photo-multiplier (a), load circuit for high speed phenomena (b), load circuit for low speed phenomena (c).

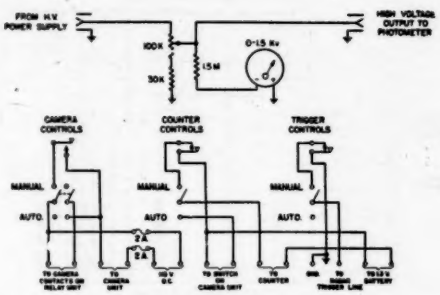

FIG. 6. Schematic of control box.

synchronous motor driving a contactor produces voltage pulses used as timing markers.

The complete sequence of operation for the recording of data from the radar indicator screen is initiated by a cam switch mounted on the radar indicator. This switch through its operation controls the relay unit shown in Fig. 8. With switch S1 in the "part cycle" position, relay K1 is operated by the closing of the cam switch on the radar indicator. The operation of K1 initiates the sweep and opens the camera shutter. The shutter will then remain open through approximately sixty degrees of radar sweep travel when the cam switch opens. When switch S1 is in the "full cycle" position relays K2 and K3 are operated also, and in such sequence that K1 is held energized for approximately four hundred and twenty degrees of radar sweep travel.

CALIBRATION AND STABILITY OF PHOTOMETER

Calibration was accomplished by comparison with a Macbeth Illuminometer. Direct comparisons were possible for the slow speed system which permits evaluation of constant brightnesses. For the high speed system, resorting to light chopping permitted calibration.

Stability was checked by calibrating both before and after a series of measurements. The maximum drift in calibration over a one hour test period was five percent for the first 931A tube used. Six other 931A tubes were installed in the photometer and each was checked for stability over a one hour period. The best tube in this group of six drifted seven percent and the poorest drifted twelve percent. All the calibration drifts were in the direction of decreasing sensitivity.

An examination of the seven tubes used showed a difference in the characteristic appearance of the cathode surface as between the first tube used (most stable) and the other six tubes. The cathode surface of the first tube was grayish and presented a crystalline appearance similar to frost on a window pane. The remaining six tubes' cathodes were evenly grayed. There is reason to believe that the first tube was much older (shelf life) than the other six tubes. It is

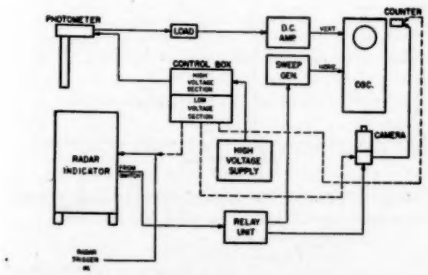

FIG. 5. Functional plan of equipment for recording slow speed phenomena.

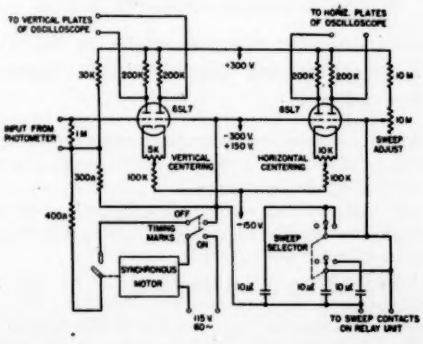

FIG. 7. Schematic of d.c. amplifier and sweep generator.

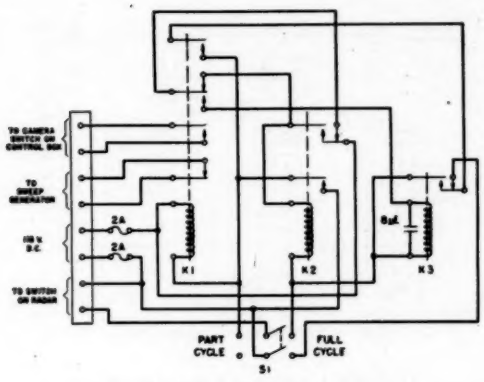

FIG. 8. Schematic of relay unit.

self-evident that stability is largely a function of the condition of the particular photo-multiplier tube.

RADAR INDICATOR BRIGHTNESS MEASUREMENTS

Representative data showing peak brightness as a function of cathode-ray tube bias are shown in Fig. 9. These data were obtained on a 7BP7 cathode-ray tube operated under the following conditions:

Heater voltage—6.05 volts
First anoded gated to +272 volts
Second anode—+5200 volts
Sweep rotation rate—10 r.p.m.
Trigger rate—600 pulses per second
Area scanned at half-radius.

Figure 10 presents a composite set of data for several bias values for the tube operating as described above and indicates the capability of the photometer.

POSSIBLE DESIGN IMPROVEMENTS

Experience with the photometer as described has indicated several possible design improvements as follows:

1. Sensitivity increases could be obtained by providing for operation of the tube at reduced temperatures and by a more efficient optical system.
2. A built-in incandescent lamp calibration unit and a more elaborate and readily adjustable mounting would result in economies in time and labor.
3. By incorporating a light chopping unit, the a.c. amplifier could be used for both fast and slow light changes, thereby reducing the time involved in rearranging the equipment for the two conditions of operation.
4. The neutral density filters could be replaced by an optical attenuating wedge, and a simple device could be provided for easily engaging and disengaging the color balance filter. Both these modifications would reduce the time required in making measurements over a wide range of light values.

CONCLUSIONS

The recording photometer described in this paper has proven to be of great value in studying the characteristics of cathode-ray screen phosphors, and is applicable to many photometric problems involving steady-state or transient illuminations at low brightness levels.

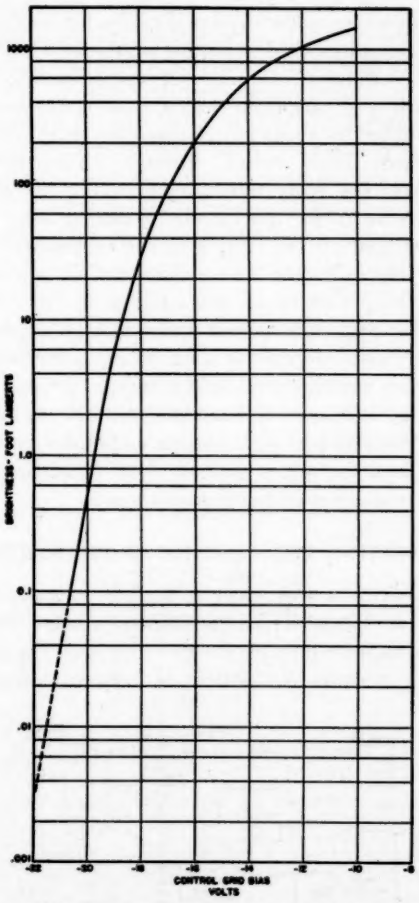

FIG. 9. Peak brightness of a radar P.P.I. sweep over a normal range of indicator tube bias values.

Conditions:
Indicator tube; type 7BP7
Heater: 6.05 volts, 60 c.p.s.
1st anode: +272 volts (gated)
2nd anode: +5200 volts
Sweep length: 20 miles (3 inches)

The present photometer is useful down to 0.005 footlambert when examining a circular area 0.025 inch in diameter. It is adapted to the measurement of much greater brightness levels by reducing its sensitivity with a dynode voltage control, a light attenuating diaphragm, and neutral density filters.

As a result of experience with the photometer certain improvements have been suggested to provide a more convenient instrument.

ACKNOWLEDGMENTS

The development described in this paper was carried out in the Systems Research Laboratory of The Johns Hopkins University under Contract N5ori-166 between The Johns Hopkins University and Special Devices Center, Office of Naval Research.

The authors particularly wish to express their appreciation of contributions to the development on the part of Messrs. C. E. Woollen, Jr., D. J. Healey, 3rd, and James Faran, formerly associated with Systems Research.

BIBLIOGRAPHY

G. H. Dieke, H. Y. Loh, and H. Crosswhite, "Spectral intensity measurements with phototubes and the oscillograph," J. Opt. Soc. Am. **36**, 185 (1946).

David L. Drabkin, "Photometry and spectrophotometry," Medical Physics, pp. 967–1008 (1944).

Monroe H. Sweet, "Logarithmic photometer," Electronics, pp. 105–109 (Nov. 1946).

Parry Moon, *Scientific Basis of Illuminating Engineering*, First Edition (McGraw-Hill Book Company, New York, 1936).

"RCA Tube Handbook HB-3," Vols. **3–4**, Phototube Section.

"Wratten Light Filters," Eastman Kodak Company.

"Photographic Lenses and Shutters," Richard W. St. Clair (Ziff-Davis Publishing Company, New York, 1940).

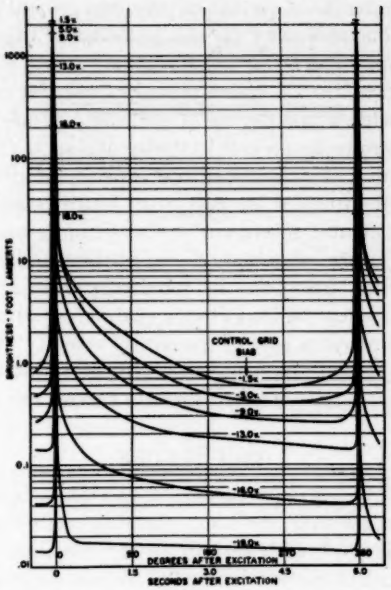

FIG. 10. Family of brightness rise and decay functions determined at a single location on an operating radar plan position indicator.

Conditions:
Same as those listed under caption for Fig. 9.

JOURNAL OF THE OPTICAL SOCIETY OF AMERICA VOLUME 38, NUMBER 10 OCTOBER, 1948

The Measurement of the Velocity of Light by Signals Sent in One Direction

HERBERT E. IVES
Upper Montclair, New Jersey

(Received July 7, 1948)

The problem of measuring the velocity of light by signals sent in one direction, instead of the usual method, by signals sent out and back, is studied. This requires two clocks, and the necessary steps to set the two clocks are discussed. It is found desirable to distinguish between "velocity" in its elementary and traditional sense, and the "rod-clock-quotient" directly obtained by measurement with rods and clocks experiencing the Fitzgerald-Larmor-Lorentz contractions. The precise formula derived for the one-way measurement of the velocity of light involves two rod-clock-quotients. The use of one-way light signal measurements in the Lorentz transformations and the Special Theory of Relativity is discussed.

INTRODUCTION

SINCE the time of Galileo terrestrial measurements of the velocity of light have been made by out-and-back signals, whereby the time of transit is measured by a single "fixed" clock. This has been a tacit recognition of the difficulty of insuring the exact uniformity of rate and identity of setting of two separated clocks.

With the development of precision crystal clocks the measurement of the velocity of light by sending signals in one direction, timed by two separate clocks, could probably now be carried out with a fair degree of accuracy. While there appears to be no call to undertake such a measurement, the theory of the experiment presents some features of interest, with bearings on some fundamental questions in the defining and nomenclature of physical quantities, and hence deserves attention. In particular the problem emphasizes the importance of differentiating between various uses of the word "velocity" which have caused obscurity and confusion, notably in presentations of the Special Theory of Relativity.

GROUNDWORK

"Light" is here considered as a disturbance in a transmitting medium, traveling at a definite velocity "c" with respect to the medium, independent of the motion of the source with respect to the medium.[1] The term "velocity" is in this paper rigorously restricted to the ratio

$$\frac{\text{distance traveled in the medium}}{\text{time taken to travel the distance}},$$

where distance is measured by material rods *stationary in the medium*, and time is measured by a clock *stationary in the medium*.[2] This is equivalent to the alternative statement that distances and clock rates are measured by rods and clocks unaffected by their motion through the medium. This definition of velocity corresponds to its original meaning in physics before the Fitzgerald-Larmor-Lorentz contractions were postulated or experimentally established.[3] By it velocities are added arithmetically.

The Fitzgerald-Larmor-Lorentz contractions are taken in this paper to be functions of the velocity *with respect to the medium*, where velocity is defined in the above way.[4] Accordingly, a rod of stationary length l_0 becomes, when moving with velocity v (as above defined)

$$l=l_0[1-(v^2/c^2)]^{\frac{1}{2}},$$

and a clock of stationary frequency ν_0, assumes the frequency

$$\nu=\nu_0[1-(v^2/c^2)]^{\frac{1}{2}}.$$

MEASUREMENT OF THE VELOCITY OF LIGHT BY SIGNALS SENT OUT AND BACK

In order to emphasize the characteristics of one-way signal measurement, the theory of two-way or out-and-back measurement in terms of the above "Groundwork" should be reviewed.

In Fig. 1 let ab be the measuring platform; at a is a clock, at b a mirror. Let W be the velocity (in the above defined sense) of the medium past the platform. Let D' be the length of the platform, as measured by rods laid end to end on it. The true length, because of the F.L.L. contraction, is $D'[1-(W^2/c^2)]^{\frac{1}{2}}$. For t_1, the time of transit (by a clock stationary in the medium) of a light signal from a to b, we have

$$t_1=\frac{D'[1-(W^2/c^2)]^{\frac{1}{2}}}{c-W}, \tag{1}$$

and similarly for the return signal,

$$t_2=\frac{D'[1-(W^2/c^2)]^{\frac{1}{2}}}{c+W}, \tag{2}$$

[1] The frequent assertion that "the Michelson-Morley experiment abolished the ether" is a piece of faulty logic. When Maxwell predicted a positive result from the experiment he did so on the basis of *two* assumptions; the first, that the light waves were transmitted through a medium, the second, which was not realized until pointed out by Fitzgerald, that the measuring instruments would not be affected by motion. The nul result of the experiment proved *some* assumption made in predicting a positive result to be wrong. The experimental demonstration of the variation of measuring instruments with motion, in exactly the way to produce a nul result, shows that it was the second assumption alone that was wrong; leaving the evidence for a transmitting medium, as derived from aberrational and rotational phenomena, as strong, if not stronger, than ever.

[2] While more than one clock may be involved in a measurement, all clocks in a stationary medium can be given the same rate and setting by light signals, using for setting one-half the transit time out and back. Hence all clocks, being identical in indication, may be included under the above "a" clock. The question whether it is practically possible to determine that a clock or rod is stationary in the medium is no bar to using such rods and clocks in developing a theoretical argument.

[3] The demonstration of the contraction of clock rates is described in "An Experimental study of the rate of a moving atomic clock," H. E. Ives and G. H. Stilwell, J. Opt. Soc. Am. **28**, 215 (1938), and **31**, 369 (1941). For the proof of the contraction of lengths the Kennedy-Thorndyke experiment (Phys. Rev. **42**, 400 (1932)) serves. This assumed the contractions of length and showed that the nul result of the experiment demanded that clock rates should vary: With the just quoted positive establishment of the clock rate variation, the Kennedy-Thorndyke experiment proves the assumed length contraction.

[4] For the derivation of the F.L.L. contractions in terms of motion through the light transmitting medium from Maxwell's radiation pressure and the conservation laws, see "Derivation of the Lorentz transformations," H. E. Ives, Phil. Mag. **36**, 392 (1945).

so that

$$t_1+t_2=\frac{2cD'[1-(W^2/c^2)]}{c^2-W^2}. \qquad (3)$$

Now if t' is the total elapsed time as read by the clock at a, we have, from the F.L.L. contraction

$$t_1+t_2=\frac{t'}{[1-(W^2/c^2)]^{\frac{1}{2}}} \qquad (4)$$

from which we have finally

$$c=2(D'/t'). \qquad (5)$$

What we have obtained is that, although the velocity of light *relative to the platform* is $c-W$ out, and $c-W$ back, the quotient of rod reading to clock reading gives us the velocity of light *in the medium* where "velocity" has the meaning in the definition above. The F.L.L. contractions have eliminated W.

DISTINCTION BETWEEN VELOCITY AND ROD-CLOCK-QUOTIENT

The result just obtained, that measurements made with clocks experiencing the F.L.L. contractions do not give the velocity of light relative to the platform, brings out the necessity of differentiating between "velocity" as above defined, and the quantity obtained directly by the quotient of length and time measurement.

In order to be free of all ambiguity in further discussion, we shall, while restricting the term "velocity" to the definition above, designate by a new term the quotient of distance, measured by a rod stationary with respect to the platform, to the interval indicated by a clock (or clocks, as in the next section), to be used when rods and clocks are employed which experience the F.L.L. contractions. This we shall call the "*rod-clock-quotient*," and designate by the letter Q, using subscripts and change of type face to indicate the different clocks involved in any measuring operation.

The several Q's we shall need are as follows: Q_1 where a single clock, stationary on the platform, is used, Q_2 where two clocks, stationary on the platform, are used, q where a clock, moving with respect to the platform, is used.

In accordance with the above use of symbols, we have, from the previous section, for the velocity of light, using out-and-back signals and a single fixed clock

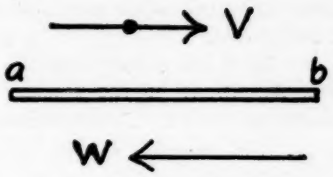

FIG. 1.

$$Q_1=c. \qquad (6)$$

We shall find that this identification of c and Q_1, is not parallelled in the case of one-way signals and the corresponding Q_2.

MEASUREMENT OF THE VELOCITY OF LIGHT BY SIGNALS SENT IN ONE DIRECTION

In order to measure the velocity of light by a signal sent in one direction it is necessary to know its time of emission at one point (a in Fig. 1) and the time of its reception at another (b in Fig. 1). This means that we can no longer use one clock, we must have two, and the second must be set to run at the same rate as the first, and be set in some known relation to the first. Synchronism as to rate can be maintained, when both clocks are stationary on the platform, by periodic signals, assuming that distance of transmission does not alter the frequency of the signals. Similarity of setting cannot, however, be achieved by this means, without knowing the velocity of transmission with respect to the platform, which of course is the ostensible purpose of our measurement. Our only recourse is to set the second clock to agree with the first at the origin (a) and then move it to its stationary position at the far end of the platform (b), (or, what is equivalent, to use a third, moving, clock to carry the setting from one stationary clock to the other). The moved clock will have its rate changed because of its motion, and this will cause a change of setting. It is our next problem to investigate this change.

Consider the clock which is to take up its station, or to be used to set a clock, at b, as moved from a to b at a uniform rate, as measured by the number of divisions moved over, divided by the elapsed interval, *as measured by the clock*

itself—there being no other available criterion for time evaluation.[5]

Designate by Y the velocity (in the sense of the above definition) of the clock. We then have, because of the F.L.L. contractions

$$Y=\frac{D}{\tau}=\frac{D'}{\tau'}\left[1-\frac{W^2}{c^2}\right]^{\frac{1}{2}}\left[1-\frac{(W+Y)^2}{c^2}\right]^{\frac{1}{2}}. \quad (7)$$

In this equation D' is the observed distance between reference points, by rods stationary on the platform; the distance D in the light transmitting medium is less by the factor $[1-(W^2/c^2)]^{\frac{1}{2}}$, where W is the velocity of the medium past the platform. τ' is the interval indicated by the moving clock; it is less than the time by a clock stationary in the medium by the factor $[1-(W+Y)^2/c^2]^{\frac{1}{2}}$.

Now according to the symbols above listed D'/t' is the rod-clock-quotient q for the moving clock. Putting this in (7) and solving for Y we get

$$Y=\frac{q[1-(W^2/c^2)]}{[1+(q^2/c^2)]^{\frac{1}{2}}+(qW/c^2)}, \quad (8)$$

and also

$$\tau'=\frac{\tau[1-(W^2/c^2)]^{\frac{1}{2}}-\dfrac{WD}{c^2[1-(W^2/c^2)]^{\frac{1}{2}}}}{[1+(q^2/c^2)]^{\frac{1}{2}}}, \quad (9)$$

which is the indication of the moved clock when it reaches b, and with which we set the clock fixed at b.

Since the clock left standing at a measures τ, the time taken by the moved clock to reach b, as $\tau[1-(W^2/c^2)]^{\frac{1}{2}}$, the difference in indication of the two clocks, Δ, is

$$\Delta=\tau[1-(W^2/c^2)]^{\frac{1}{2}}-\frac{\tau[1-(W^2/c^2)]^{\frac{1}{2}}-\dfrac{WD}{c^2[1-(W^2/c^2)]^{\frac{1}{2}}}}{\left(1+\dfrac{q^2}{c^2}\right)^{\frac{1}{2}}}$$

$$=\frac{\tau\left(1-\dfrac{W^2}{c^2}\right)^{\frac{1}{2}}\left[\left(1+\dfrac{q^2}{c^2}\right)^{\frac{1}{2}}-1\right]+\dfrac{WD}{c^2[0-(W^2/c^2)]^{\frac{1}{2}}}}{\left(1+\dfrac{q^2}{c^2}\right)^{\frac{1}{2}}}. \quad (10)$$

If we imagine this process carried through for a series of clocks fixed on the platform we end up by having an array of clocks all running with the frequency $\nu_0[1-(W^2/c^2)]^{\frac{1}{2}}$, but each *set back* by an amount which is a function of its distance, the velocity of the platform through the medium, and the rod-clock-quotient of the moved clock.

We can simplify the expression for Δ, by inserting the value of τ from the relation $\tau=D/Y=D'/Y[1-(W^2/c^2)]^{\frac{1}{2}}$, taking the value of Y from (8) which gives

$$\tau=\left[D'\left[\left(1+\frac{q^2}{c^2}\right)^{\frac{1}{2}}+\frac{Wq}{c^2}\right]\right]\Big/\left[q\left(1-\frac{W^2}{c^2}\right)^{\frac{1}{2}}\right], \quad (11)$$

and this in (10) gives

$$\Delta=\frac{D'}{q}\left[\left(\left(1+\frac{q^2}{c^2}\right)^{\frac{1}{2}}-1\right)+\frac{Wq}{c^2}\right]. \quad (12)$$

We now seek the expression for the velocity, V (Fig. 1), of any body moving uniformly with respect to the platform, as measured by two fixed clocks at a and b, set by the above procedure. Since $V=D/t$ we can obtain this by finding D and t. For D we have $D=D'[1-(W^2/c^2)]^{\frac{1}{2}}$. We get t from the time indicated by the clock at b when the moving body passes it, having passed a at the indicated time zero. This is given by the relation

$$t'=t[1-(W^2/c^2)]^{\frac{1}{2}}-\Delta$$

or

$$t=(t'+\Delta)\Big/\left(1-\frac{W^2}{c^2}\right)^{\frac{1}{2}}. \quad (13)$$

[5] This is one of the commonest ways of measuring velocity. It is used by the mariner with his chronometer, by the automobilist in traversing the "measured mile," and by the train traveller who counts telegraph poles passed in the interval given by the watch in his hand. By it the measured velocity of light is infinity.

Substituting the value of Δ from (12) and putting Q_2 for D'/t' we get

$$V=\frac{Q_2\left(1-\frac{W^2}{c^2}\right)}{1+\frac{Q_2W}{c^2}+\frac{Q_2}{q}\left[\left(1+\frac{q^2}{c^2}\right)^{\frac{1}{2}}-1\right]}. \quad (14)$$

We now find the expression for the velocity of light. For the case considered the velocity of light with respect to the platform is $c-W$. Putting this in place of V we get, for the rod-clock-quotient

$$Q_2=(c)\Big/\left[1-\frac{c}{q}\left(\left(1+\frac{q^2}{c^2}\right)^{\frac{1}{2}}-1\right)\right], \quad (15)$$

a constant, independent of W.

This constant, if we had performed the measurement in ignorance of the F.L.L. contractions, *would have been interpreted as the velocity of light.* It is not equal to c.

We get the velocity of light by solving (15) for c. This gives us

$$c=[2Q_2(Q_2-q)]\Big/[2Q_2-q]. \quad (16)$$

This formula is the goal of the present paper. It gives the velocity of light as measured by signals in one direction, in terms of the observed quantities, namely two rod-clock-quotients. These are the rod-clock-quotient Q_2, involving the difference of readings of the two fixed clocks as the light signal passes them, and the rod-clock-quotient q of the moved clock used for setting the fixed clocks.

Again, as with the out-and-back signals, we do not get the velocity of light with respect to the platform ($c\pm W$), but the velocity of light with respect to the medium. Note that if the moved clock is moved so slowly that $q\cong 0$ we approximate to

$$c=Q_2.$$

THE LORENTZ TRANSFORMATIONS

From the preceding section we see that the rod-clock-quotient Q_2, for a unidirectional light signal, has the interesting property of being the same (if a definite q is adhered to) no matter what the velocity of the body on which it is measured. Consequently if we initiate a light signal at a given point in the light transmitting medium at which the initial points of a series of moving platforms are at that instant in coincidence, the spherical wave expanding in the medium will be ascribed the same Q_2 on each platform. That is, the equations describing the wave, as set up for each platform, will have *the same form in terms of* Q_2, as a spherical wave in the stationary medium *in terms of* c. We can thus set up a family of equations, applying to a series of relatively moving bodies, in which Q_2 is expressed in rod and clock measurements peculiar to each body, and thus derive a relationship between these measurements, involving the relative measured motions of the bodies, and Q_2.

This is the procedure used in expositions of the Special Theory of relativity to derive the Lorentz transformations,[6] which are, according to our development, properly expressed in terms of Q_2. By the further step of agreeing to move the clocks used for setting "local times" at infinitesimal rates ($q\cong 0$), Q_2 approximates to c, and the usual form of the Lorentz transformations is obtained. Incidentally, by adopting this convention, we permit, as a practical substitute for the slowly moved clock for setting purposes, the use of light signals ascribed the (false) velocity c.

THE SPECIAL THEORY OF RELATIVITY

The Special Theory of Relativity, the formulae of which are developed from consideration of light signals sent in one direction, is an example of the importance of the precise definition of the measuring processes involved, and of the distinction here drawn between "velocity" and the "rod-clock-quotients." The paradox confronting our elementary and traditional concept of velocity by the proposition that the velocity of light is constant, both with respect to the medium and to a body moving through the medium, is avoided by the analysis and nomenclature here employed.

The "constancy of the velocity of light" which figures in current text-book treatments of the theory, should, according to the present analysis, be more accurately described as *two* "constancies" namely of the two rod-clock-quotients Q_1 and Q_2.

[6] W. H. McCrea, *Relativity Physics* (Methuen, London, and Company, Ltd. 1935), p. 8.

The rod-clock-quotient Q_1, which is obtained in the out-and-back measurement of light signals, using a single clock, has the constant value c, which is the velocity of light measured by rods and clocks stationary in the medium, or by formulae (6) and (16). The rod-clock-quotient Q_2, which is obtained in the one-way measurement of light signals, using two clocks, is a constant for any one choice of the rate of motion (q) of the auxiliary clock used for setting the two fixed clocks, but varies with q, and is not in general equal to c.

The single value for the "velocity of light" which figures in developing the formulae of the theory is due to the specification that the rod-clock-quotient for one-way light signals, Q_2, shall be the same as that for out-and-back signals, Q_1.[7] This specification (sometimes called "the adjustment of constants") turns out to mean that the only measurement of one-way light signals which is to be allowed is one where the clock used for setting is moved at an infinitesimal rate. This reservation on permissible measurements vitiates the claim that the "velocity of light" is an "absolute" factor in the Special Theory of Relativity.

LIGHT SIGNALS IN ONE DIRECTION THROUGH A REFRACTING MEDIUM

In the foregoing we have been concerned solely with light signals in the ether. The case where the light is transmitted through a refracting medium can be handled in the same manner. It is only necessary to insert for V in Eq. (14) the velocity of light in the refracting material, in place of $c-W$, the velocity in the ether, as was done in deriving Eq. (15).

For the velocity of light in a refracting material moving through the ether, two formulae are available, derived from the theory of electrons, one due to Lorentz,[8] the other to Larmor.[9] The formula of Lorentz, aimed at explaining the observed Fresnel drag coefficient, neglects all terms in the second order of v/c, and while adequate for its purpose, is not suited for the present discussion, in which the second order terms are an essential factor. The formula of Larmor, incorporating the F.L.L. contractions and correct to the second order, is expressed in the exact form here needed.

Larmor's formula for the velocity[10] of light in a refracting material, moving with velocity W with respect to the ether, in terms of coordinates fixed in the refracting material, is

$$V=\frac{c}{\mu}\left(1-\frac{W^2}{c^2}\right)\Big/\left(1+\frac{W}{c\mu}\right) \qquad (17)$$

where c/μ is the velocity of light in the material when stationary in the ether.[11]

Putting this for V in (14) we get

$$Q_2=\frac{c}{\mu}\Big/\left[1-\frac{c}{\mu q}\left[\left(1+\frac{q^2}{c^2}\right)^{\frac{1}{2}}-1\right]\right] \qquad (18)$$

a constant independent of W.

[7] In Einstein's original presentation he declared the value "c" for the velocity of light to be "firmly established by experiment." This was not a legitimate citation, for he was discussing the *one-way* transmission of signals, while the only existing experimental values were those from *out-and-back* measurement.

[8] P. Drude, *Lehrbuch der Optik* (Hirzel, Leipzig, 1900) p. 426.

[9] J. Larmor, "Aether and Matter," (Cambridge University Press, 1900) p. 178.

[10] Larmor uses the term "velocity" in exactly the sense adhered to in the present paper.

[11] If we transform our origin of coordinates to the light transmitting medium instead of the refracting material we get the relation

$$V+W=\left[\frac{c}{\mu}\left(1-\frac{W^2}{c^2}\right)\Big/\left(1+\frac{W}{c\mu}\right)\right]+W=\left(\frac{c}{\mu}+W\right)\Big/\left(1+\frac{W}{c\mu}\right).$$

This formula is commonly credited to the Special Theory of Relativity. That the considerably earlier formula of Larmor (17), derived from analysis of the effect of moving charges on the velocity of electromagnetic waves through the surrounding ether, is identical in content, appears to have been generally overlooked.

JOURNAL OF THE OPTICAL SOCIETY OF AMERICA VOLUME 38, NUMBER 10 OCTOBER, 1948

Empirical Relationships between the Partial Dispersions of the Ordinary Types of Optical Glasses*

D. H. RANK
Physics Department, The Pennsylvania State College, State College, Pennsylvania

(Received June 14, 1948)

Three empirical relationships have been derived between reciprocals of pairs of partial dispersions of the ordinary optical glasses. The relationships are of the form $X=a+bY+cY^2$ where X and Y are variable and a, b, and c the empirical constants. a, b, and c were determined by least squares making use of the data on sixteen optical glasses manufactured by The Bausch and Lomb Optical Company. The fit obtained appears to hold within the 5th place experimental error of the index determinations. Determination of N_D and N_h and the use of the three empirical relationships quoted above allows calculation of N_F, N_C, $N_{G'}$, and V in a simple manner. These relationships, however, do not apply to the barium glasses.

IT is well known that the accurate determinition (± 0.1) of V (the dispersion) $V=(N_D-1/N_F-N_C)$ of glasses involves an accuracy of 1 or 2 in the 5th decimal place for the determination of the necessary indices of refraction. It is also necessary to make use of hydrogen discharge tubes to produce light of the requisite purity for the measurement of N_F and N_C. These discharge tubes are not ideal light sources because of their variable characteristics with the age of the tubes.

From a practical standpoint it would be more desirable to define the dispersion of glass in terms of the indices obtained for the mercury radiations and sodium since powerful and easily obtainable stable sources of these radiations are readily available on the market. However, optical engineering practices and custom demand the determination of V as defined above.

It occurred to the author that it might be possible to transform index measurements made by means of sodium and mercury radiations, in an empirical manner, so as to obtain the requisite dispersion as defined above. In order to obtain the best accuracy the experimental measurements should be made over as large a wave-length interval as possible since the accuracy of the index measurement remains approximately constant with wave-length.

Let us define the following quantities;

$$X=\frac{1}{N_h-N_D}, \quad Y=\frac{1}{N_F-N_C},$$

$$Z=\frac{1}{N_{G'}-N_F}, \quad W=\frac{1}{N_F-N_D}.$$

We shall assume that the variables defined above are connected by means of the following power series.

$$Y=A_y+B_yX+C_yX^2. \tag{1}$$

$$Z=A_z+B_zX+C_zX^2. \tag{2}$$

$$W=A_w+B_wX+C_wX^2. \tag{3}$$

The significance of the A, B, and C's above is at once apparent in that they are parameters to be determined from experimental data. Use was made of the Bausch and Lomb optical glass catalogue for obtaining the indices of refraction necessary for the determination of the above parameters. These indices given in the catalogue are spectrometer measurements which are quoted to the 5th decimal place. (It will be seen later that the quoted indices of refraction must have a very small or zero error in the 5th decimal place.) Use was made of the refractive index data of all the glasses listed in the Bausch and Lomb catalogue with the exception of the barium glasses. The parameters A, B, and C were determined by the method of least squares, fitting the 16 types of glasses mentioned above.

The values obtained for the constants were,

$$A_y=1.042, \quad B_y=1.856416, \quad C_y=-0.00257167,$$
$$A_z=0.157, \quad B_z=2.921149, \quad C_z=0.00115970,$$
$$A_w=1.275, \quad B_w=2.571014, \quad C_w=-0.00262692.$$

Results of calculations using Eqs. (1), (2) and (3) and the constants given above are compiled in Table I. The mean of the residuals calculated

* This research was carried out on Contract N6Onr-269 Task V of the Office of Naval Research. Submitted in report March 15, 1948.

TABLE I. Showing residuals calculated from Eqs. (1), (2) and (3) (calculated minus measured values) for sixteen Bausch and Lomb ordinary optical glasses.

Type	N_D	V	Residuals (N_F-N_C) calculated	Residuals $(N_{G'}-N_F)$ calculated	Residuals (N_F-N_D) calculated	Residuals ΔV calculated
B8C-1	1.51100	63.5	$+0.7\times10^{-5}$	$+1.0\times10^{-5}$	$+0.5\times10^{-5}$	−0.06
B8C-2	1.51700	64.5	−1.1	−0.8	−0.7	+0.09
C-1	1.52300	58.6	−1.0	+0.4	−0.7	+0.06
C-2	1.51250	60.5	+1.0	−0.3	+0.4	−0.07
CF-1	1.52860	51.6	+0.9	−0.9	+1.0	−0.04
ELF-1	1.55850	45.5	+0.3	+0.3	0.0	−0.01
ELF-2	1.54970	45.8	+2.8	−0.1	+1.0	−0.11
LF-1	1.57250	42.5	−1.1	−0.2	+0.1	+0.04
LF-2	1.57950	41.0	−3.6	−0.6	−2.7	+0.11
LF-3	1.57500	41.4	−1.5	+2.1	−0.6	+0.04
DF-1	1.60500	38.0	−0.4	+0.5	−1.7	+0.01
DF-2	1.61700	36.6	−0.5	+0.6	+0.7	+0.01
DF-3	1.62100	36.2	+0.3	−1.0	+1.2	−0.01
EDF-1	1.64900	33.8	+1.9	−1.5	+1.5	−0.03
EDF-2	1.68900	30.9	+0.6	+0.6	−0.4	−0.01
EDF-3	1.72000	29.3	+1.1	−0.2	+0.5	−0.01
		Mean	1.2	0.7	0.9	0.044

minus the observed is seen to be 1.2, 0.7 and 0.9×10^{-5} respectively for N_F-N_C, $N_{G'}-N_F$ and N_F-N_D. The maximum deviations are −3.6, +2.1 and -2.7×10^{-5} respectively for the previously mentioned quantities. These maximum deviations probably equal or may slightly exceed the maximum probable experimental error to be expected for the measurements which were used in making the computations. If the author is permitted to be so bold as to hazard a speculation it would not seem improbable to expect that V values obtained from the use of Eq. (1) might be more accurate than V values obtained directly from 5th place measurements.

Inspection of Table I shows that it is possible to determine the indices of refraction of the ordinary types of optical glasses to 5th place accuracy for 5 wave-lengths by the 5th place measurement of N_D and N_h and the use of Eqs. (1), (2) and (3).

It should be stated that the barium glasses cannot be plotted to functions of the form of (1), (2) and (3) and yield small 5th place residuals. However, the residuals when Eq. (1) is used for the barium glasses yield a minimum of −2.7 and a maximum of -17×10^{-5} for $\Delta(N_F-N_C)$. This situation can be greatly improved by determining the parameters A_y, B_y and C_y for the barium glasses. However, even when this is done the fit is not within expected experimental error and the residuals do not appear to deviate from zero in any regular or simple manner.

It might be pertinent to point out the fact that for the ordinary optical glasses, Eqs. (1), (2) and (3) are certainly not the only relationships of this type which can be derived. It should be possible to treat other partial dispersions in the same manner.

JOURNAL OF THE OPTICAL SOCIETY OF AMERICA VOLUME 38, NUMBER 10 OCTOBER, 1948

The Visibility of Stars in the Daylight Sky

R. TOUSEY AND E. O. HULBURT
Naval Research Laboratory, Washington, D. C.

(Received March 23, 1948)

From the theory of the passage of light through a telescope and into the eye, formulas are derived for the improvement in the visual threshold of a point source, as a star, viewed in a field of light, as the sky, in terms of telescope parameters, as magnification, transmission, and entrance and exit pupils. For fields of the brightness of the daylight sky the first parameter is the most important and the others are of less importance. Observations of artificial stars in the laboratory and of real stars in the daylight sky are given, which were in fair accord with the theory.

Charts and tables are presented of the visual thresholds of stars in various parts of a clear daylight sky in terms of the stellar magnitude, the magnification of the telescope, the use of a polarizer, the altitude of the observer above the surface, and the altitude of the sun above the horizon.

New data are given of extra-foveal thresholds of point sources in a field of brightness 360 ft.-c^{-2}.

INTRODUCTION

IN full daylight stars cannot be seen with the unaided eye at sea level because the brightness of the sky masks the little points of light which are the stars. A telescope increases the stellar illumination relative to the brightness of the sky and makes it possible to see the star, although this is by no means easy even with a 20-power

telescope and a first magnitude star. In the following pages the optical features are analyzed and calculations are made based on the thresholds of vision and on the optical characteristics of telescopes, of the eye, of stars, and of the atmosphere. The calculations are compared with observations with various types of telescopes of real stars in the sky and of artificial stars in the laboratory. Charts are presented of star visibilities at various points in the sky at several altitudes above sea level for several altitudes of the sun.

VISUAL THRESHOLDS OF DISKS OF LIGHT

In the present star problem two investigations of the visual thresholds of disks of various brightnesses in fields of various brightnesses are of importance, one by Blackwell at the Tiffany Foundation[1] and one at this Laboratory.[2] The NRL data apply directly to the case of a star in the sky, for they were observed with the luminous disk so small as to appear as a point source and were viewed in effect through a perfectly transparent luminous field, the disk appearing brighter than the field. The observations were made by five young observers and referred to disks of apparent diameter 1 minute of arc, to an approximately 98 percent probability of detection, and to brightnesses of all disks and fields at a color temperature of 2360° Kelvin. Discussion and definition of "probability of detection" is given in reference 1, p. 629, and need not be repeated here. The results are plotted in the dotted curve of Fig. 1 as $\log_{10} i$ against $\log_{10} b$, where i footcandles was the illumination produced by the disk at the eye, not including the field covering the disk, and b candles per square foot was the brightness of the field.

The Tiffany data were obtained from many thousands of observations by nineteen young observers of opaque disks in front of the fields. The disks and fields were at a color temperature of 2850° Kelvin. The results for disks brighter than the fields were listed in Table VIII of reference 1, in which the contrast factor c was tabulated for disk diameters θ from 0.595 to 360.0 minutes of arc for various field brightnesses b in foot-lamberts for a 50 percent probability of detection. θ is the angle which the diameter of the disk subtended at the eye. c was defined by

$$c=(b_d-b)/b, \tag{1}$$

where b_d was the brightness of the opaque disk in front of the field b.

TABLE I. Values of $-\log_{10} i$ footcandles for 98 percent probability threshold.

	$\log_{10} b$ candles per square foot								
θ	2.503	1.503	0.503	−0.497	−1.497	−2.497	−3.497	−4.497	−5.497
360′	1.827	2.817	3.819	4.739	5.533	6.220	6.780	7.366	8.127
121′	2.768	3.768	4.760	5.671	6.419	7.025	7.531	7.174	8.769
55.2′	3.396	4.436	5.427	6.317	7.020	7.555	7.985	8.575	9.128
18.2′	4.313	5.313	6.281	7.129	7.767	8.194	8.467	8.947	9.409
9.68′	4.740	5.729	6.642	7.452	8.073	8.442	8.609	9.005	9.423
3.60′	5.071	5.980	6.828	7.581	8.183	8.559	8.637	9.006	9.422
0.595′	5.208	6.073	6.885	7.629	8.218	8.579	8.646	9.012	9.428

In order to convert c into the illumination i for the case of a disk seen through a luminous field, which corresponds to a star in the sky, one must subtract from the illumination i_d due to the opaque disk the illumination i_f due to the portion of the field obscured by the disk. Then

$$i=i_d-i_f. \tag{2}$$

From photometric relations

$$i_d=b_d(\theta/2)^2 \quad \text{and} \quad i_f=b(\theta/2)^2, \tag{3}$$

where i_d and i_f are in ft.-c, b_d and b are in ft.-c^{-2}, and θ is in radians. From (1)–(3)

$$i=bc(\theta/2)^2. \tag{4}$$

From (4) the values of i were calculated from the Tiffany values of c, b, and θ (keeping note

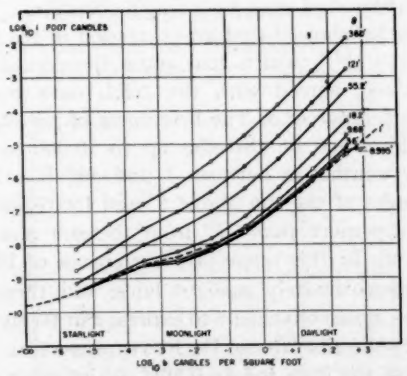

FIG. 1. Threshold illumination i for 98 percent probability of detection; full lines Tiffany data (reference 1), dotted line NRL data (reference 2).

[1] H. R. Blackwell, J. Opt. Soc. Am. 36, 624 (1946).
[2] H. A. Knoll, R. Tousey, and E. O. Hulburt, J. Opt. Soc. Am. 36, 480 (1946).

that Tiffany b was in foot-lamberts and 1 ft.-c^{-2} $=\pi$-ft.-L) and were multiplied by 2 to bring them up to the threshold of about 98 percent probability of detection. The results are listed in Table I as $-\log_{10}i$ and are plotted in the full line curves of Fig. 1. They do not extend to completely dark fields because when $b=0$ from (1) c is infinite and from (4) i is indeterminate.

It is seen from Fig. 1 that the Tiffany and the NRL values differed by less than 0.1 in $\log_{10}i$, or less than about 30 percent in i. For low values of b about half of the difference was ascribable to the different color temperatures used in the two investigations. Although the remaining difference was almost too small to be of significance, the different methods of search employed in the two investigations would account for the fact that the NRL thresholds were slightly below the Tiffany thresholds at the higher field brightness levels; the Tiffany observers were allowed only 6 seconds to search over a circular area of 6° diameter, whereas the NRL observers had all the time they wished and knew closely where to look. There is, of course, no question that the Tiffany data are the most authoritative which are available for the circumstances in which they are valid. However, the agreement between the two investigations indicated that a relatively simple non-statistical procedure gave results close enough for many purposes to those derived from statistical reduction of thousands of measurements. This was an important thing to know, because in the following paragraphs conclusions are reached on the basis of observations by a few observers, and even by a single observer.

Hecht[3] showed that an expression of the form $i=c(1+kb^{\frac{1}{2}})^2$, which had some theoretical significance, agreed with the NRL data over a certain range of b. The brightness of the sky at sea level and at altitudes up to 10,000 feet in clear weather is between 1 and 500 ft.-c^{-2} for altitudes of the sun above 5° and for regions of the sky more than 15° from the sun and the horizon. In this range of b the curves of Fig. 1 are approximately straight lines, and therefore it was more convenient to express i in terms of a power of b than to use Hecht's expression. In the case of the data for $\theta=0.595'$, which refer to a point source, the equation

$$i=kb^{0.84}, \tag{5}$$

where $k=4.85\times10^{-8}$, agrees with the values of Table I within 5 percent for b from about 2 to 400 ft.-c^{-2}. Furthermore, NRL experiments showed that the i,b curve for bluish point sources and fields agreed with the two lower curves of Fig. 1 for b above 5 ft.-c^{-2}, when i and b were measured with correct photometric procedure. Therefore (5) was considered to be valid for the present star problem.

OPTICS OF A TELESCOPE

Let D and d be the diameters of the used portion of the objective lens (more accurately, the "entrance pupil") and the exit pupil of the telescope, respectively, and M the magnification. Then

$$dMD^{-1}=1. \tag{6}$$

Let i and b be the stellar illumination and field brightness, respectively, viewed with the unaided eye, and i_a and b_a the apparent values of the respective quantities viewed through the telescope. Let t be the transmission of the telescope and p the diameter of the pupil of the eye. Assume that the eye pupil is in the same plane and centered with the exit pupil, and is of the same size as when viewing b unaided. From the theory of the passage of light through a telescope and into the eye one derives

$$\text{for } d\geqq p, \quad i_a=tM^2i, \tag{7}$$

$$b_a=tb, \tag{8}$$

$$\text{and for } d\leqq p, \quad i_a=t(D/p)^2i, \tag{9}$$

$$b_a=t(d/p)^2b=t(D/pM)^2b. \tag{10}$$

Now, let i_a be the threshold for the field b_a in the telescope and i' be the unaided i threshold for the field b. Then from (5)

$$i'=kb^{0.84}, \tag{11}$$

$$i_a=kb_a^{0.84}. \tag{12}$$

It is assumed that (12), which was obtained from data for the natural pupil, can be applied to the case in which $d<p$, which in effect is the case of the artificial pupil. The assumption is probably strictly true only in the absence of zonal aberrations and diffraction effects in the

[3] Selig Hecht, J. Opt. Soc. Am. **37**, 59 (1947).

eye and the Stiles-Crawford effect. For $d \geqq p$, one has from (7), (8), and (12)

$$i = kb^{0.84} M^{-2} t^{-0.16}, \tag{13}$$

and substituting (11) in (13) gives

$$i'/i = M^2 t^{0.16}. \tag{14}$$

For $d \leqq p$, one has from (9), (10), and (12)

$$i = kb^{0.84} (D/p)^{-0.32} M^{-1.68} t^{-0.16}, \tag{15}$$

and substituting (11) into (15) gives

$$i'/i = (D/p)^{0.32} M^{1.68} t^{0.16}. \tag{16}$$

By introducing (6) alternative expressions for (15) and (16) can be written in terms of any two of the variables M, D, and d.

Because of the introduction of (5) which refers to point sources, Eqs. (11) to (16) are valid only as long as the stellar images are effective point sources, which means that the angle θ subtended at the eye be less than about 0.8′. Diffraction in the telescope may make θ greater than 0.8′, and therefore the effect of diffraction is considered in a letter paragraph.

Since i is the illumination on the objective lens when the star appears at threshold in the telescope and i' is the unaided eye threshold, the ratio i'/i is the improvement in the threshold due to the telescope. Therefore Eqs. (14) and (16) describe the influence of the several telescope parameters on the improvement in star thresholds due to the telescope. If M is increased by the use of stronger eye pieces, keeping the objective diameter unchanged, (14) shows that the improvement varies as M^2 as long as $d \geqq p$; when, with further increase of M, d becomes less than p, (16) shows that the improvement varies as $M^{1.68}$.

For $d \geqq p$ the improvement is independent of the objective diameter D and exit pupil p, as shown by (14); this is obvious, for in this case the eye is more than filled with light. On the other hand, for $d < p$ the eye is not filled with light and the improvement depends on $D^{0.32}$, as shown by (16); this is a rather small dependence. It is of some interest that the improvement does not depend on the sky brightness, since b does not appear in (14) or (16). The improvement varies as the 0.16 power of t, which is a small variance. For example, for $t = 1$, 0.8, 0.6, 0.4, and 0.2 the improvement is reduced by 0, 4, 8, 16, and 29 percent, respectively. Thus, increasing the transparency of the telescope, as by the use of low reflecting films, produces only a minor improvement in the daylight threshold. Contrariwise, a small amount of stray light due to dust or imperfections does no great harm.

It is hardly necessary to say that the assumption used in (14) and (16), that the eye pupil was the same size with and without the telescope, is rarely strictly true. When the telescope is used the eye pupil is usually slightly enlarged due to the absorption of light in the telescope, the restricted field, and monocular vision if the other eye is dark. From theory the enlarged pupil results in slightly lowered thresholds for $d \geqq p$.

The effects on the threshold of magnification and of stopping down the objective lens of the telescope were determined by laboratory experiments. Measurements were made by an observer whose eye pupil diameter was about 3 mm during the observations. The apparatus of Fig. 2, reference 2, was used. The artificial star subtended about 1 second of arc; b was 360 ft.-c^{-2}. The objective lens of the telescope was achromatic, 82 mm in diameter, and 60 cm in focal length; t was 0.85. For the magnification experiments the objective lens was diaphragmed to $D = 30$ mm, and magnifications from 5.8 to 46.6 were obtained by nine eyepieces. Care was taken to observe along the axis of the telescope where the definition was best. The observed values of $\log_{10} i$ are plotted as dots in Fig. 2 against $\log_{10} M$. The dot for $M = 1$ was obtained without the telescope and corrected by (13) to make it consistent with the other dots.

The same apparatus was used to study the

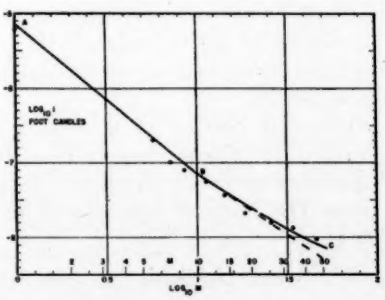

FIG. 2. Telescopic thresholds for various magnifications.

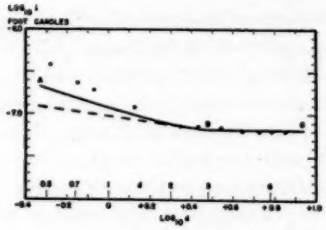

FIG. 3. Telescopic thresholds for various exit pupils.

effect on the threshold of stopping down the objective lens. With the magnification of the telescope set at 11.3, i was measured for D from about 80 to 6 mm, which from (6) corresponded to an exit pupil diameter d from about 7 to 0.5 mm. The observed values of $\log_{10} i$ are plotted as dots in Fig. 3 against $\log_{10} d$ for d in mm. In the experiments of both Figs. 2 and 3 when the eye pupil was nearly equal to the exit pupil, accurate observation was difficult because of the necessity of keeping the eye correctly in line.

In order to calculate i from the threshold of Table I for comparison with the observations of Figs. 2 and 3, two cases are considered.

Case 1, $d \geqq p$.—In this case the Tiffany data for a point source apply directly because they were obtained with the natural pupil. Hence one uses (13), which when the numerical values were introduced gave the straight line portion AB of the curves of Figs. 2 and 3, of slopes -2 and zero, respectively, B being at $M=10$ in Fig. 2 and at $d=3$ mm in Fig. 3.

Case 2, $d \leqq p$.—In this case we begin by using (15) which gave the two dotted straight lines in Figs. 2 and 3 of slopes -1.68 and -0.32, respectively. But since $d<p$, the exit pupil is in effect an aperture at the eye which is smaller than the eye pupil, and corresponds to an artificial pupil. This introduces diffraction effects, which are calculated approximately in the following paragraphs, since there are no threshold data for artificial pupils.

The diffraction pattern of a distant point source imaged by a lens consists of a bright central spot surrounded by alternately dark and bright rings. The diameter δ-radians of the first dark ring is, according to Airy,

$$\delta = 2.44\lambda/d, \tag{17}$$

where d is the diameter of the lens and λ is the wave-length of light. For a telescope d is the diameter of the exit pupil. With $\lambda = 5.5 \times 10^{-5}$ cm, δ in minutes of arc, and d in cm, (17) reduces to

$$\delta = 0.461/d, \tag{18}$$

and from (6) to

$$\delta = 0.461M/D. \tag{19}$$

With $p=0.3$ cm from (18) $\delta = 1.53'$. It was assumed that $1.53'$ was the diameter of the diffraction disk in the eye of the Tiffany observer produced by a point source (i.e., $0.595'$); it was further assumed that the threshold given by the telescope of exit pupil d or of magnification M referred to the curve of Fig. 1 for θ where

$$\theta = \delta - 1.53, \tag{20}$$

δ being given by (19) or (18), respectively. In this way i from (15) was corrected by reading i from the curve of Fig. 1 for θ given by (20). The corrected curves are shown in portions BC of Figs. 2 and 3.

It is seen that the calculated curves ABC and the observed dots of Figs. 2 and 3 are in fair agreement both in trend and in absolute value. It is mainly chance that they agree as well as they do in absolute value, for the curves were based on the average of the thresholds of the nineteen Tiffany observers, whereas the dots were the thresholds of a single observer, and in general people differ in their visual thresholds; however, other experiments, as well as the present one, showed that our observer usually agreed with the Tiffany average. The departure between the dots and the curve for the lower values of d in Fig. 3 may be due both to experimental and theoretical imperfections. Certainly the diffraction calculation should be improved; this will require further experimental threshold data with artificial pupils. The Stiles-Crawford effect may be important, particularly for larger pupil diameters.

STAR VISIBILITY OBSERVATIONS

In Table II are given results of star observations made from the surface at Washington on August 13 with three telescopes of 5, 10, and 20 power. The day was unusually clear, the vertical transmission of the total atmosphere being about 0.70. A polarizing attachment was used to take

advantage of the partial polarization of the skylight and to weaken the sky brightness relative to the illumination from the star. The brightness and polarization of the sky were measured near each star and the illumination of the star at the telescope was calculated, allowing for the atmospheric attenuation. From these data the observed threshold value was computed and compared with the threshold for the telescope as measured in the laboratory. The calculations for the effect of a polarizer are explained in the last section. The numbers in Table II are the ratios of the illumination calculated from the magnitude of the star to the threshold illumination for the specified telescope with the polarizer helping, neutral, or hindering.

Sirius at 8:40 A.M. was 34 times above threshold, with the polarizer aiding, and was very easy to see in the 20-power telescope. In several cases by rotating the polarizer stars could be followed down to threshold, but not below. Spica, magnitude +1.2 and the weakest star seen, was a good example of this. In the 10-power telescope with polarizer helping it was 2.3 times threshold and was visible with difficulty. On rotating the polarizer Spica was barely visible at the neutral position 1.3 times the threshold. With polarizer hindering, Spica was 0.8 times the threshold and could not be seen.

In general, as brought out in Table II, when the illumination of the star was 5 to 10 times the threshold, it was easy to find; when 2.5 to 5 times the threshold it was moderately hard to find. For 2 times the threshold the star could be found with difficulty; usually several minutes of search were necessary even though the star was in the field of the telescope. At threshold it was necessary to know exactly where to look and even then to spend some time in searching. These conclusions refer to extremely favorable conditions, since the observer was comfortable and the telescopes were on a steady mounting and were preset in the correct position.

It was found very important to provide the telescope with cross wires or a reticle at infinity to aid the eye in maintaining accommodation for infinity. Without such aid the eye did not remain focused on infinity, and searching for a star with an unfocused eye was usually a fruitless procedure.

TABLE II. Star visibility observations; the numbers are the ratio of actual to threshold illumination.

Celestial object	Telescope magnification	Polarizer helping	No polarizer	Polarizer hindering
Sirius	20	34, very easy	27, very easy	21, very easy
−1.6	10	8, easy	6, easy	5, easy
8:40 A.M.	5	33, mod. easy	2.2, hard	1.7, hard
Rigel	20	14, very easy	8, easy	4.4, easy
0.3	10	3.2, mod. easy	1.8, hard	1.0, very hard
9:05 A.M.	5	1.1, very hard	0.6, not seen	0.35, not seen
Capella	20	21, very easy	9, easy	4, easy
0.2	10	4.6, easy	2, hard	1.0, very hard
11:30 A.M.	5	1.7, not tried	0.8, not tried	0.35, not tried
Arcturus	20	53, very easy	21, very easy	8, very easy
0.2	10	12, very easy	5, easy	2, hard
2:00 P.M.	5	4.3, not tried	1.7, not tried	0.7, not tried
Vega	20	28, very easy	13, very easy	6, easy
0.1	10	6, easy	3, mod. easy	1.3, very hard
3:35 P.M.	5	2.2, not tried	1.0, not tried	0.5, not tried
Spica	20	10, easy	6, easy	3.4, mod. easy
1.2	10	2.3, hard	1.3, very hard	0.8, not seen
3:15 P.M.	5	0.8, not tried	0.5, not tried	0.3, not tried

Experiments with color filters showed that, in general, the only color that made any improvement in the stellar threshold was orange, and even this was slight; other colors were either harmful or of no noticeable effect. To mention a few of the observations: when Arcturus and Venus, which are reddish celestial objects, were viewed in a blue sky with a 5-power telescope, the Wratten 22 orange filter reduced the threshold about twofold. Wratten 24A red and 48A green were of no help or hindrance. In the case of Sirius, a blue star, viewed in the 5-power telescope, deep red (Wratten 70), red, deep blue, and violet filters were harmful; the best, or rather the least harmful, filters were orange yellow and yellow green, the results with these of several observers indicating no help and no harm.

Frequently it was possible to notice twinkling effects, and it was concluded that, in general, twinkling seemed more prominent in the day than at night. On one occasion twinkling was observed during the afternoon but not after sunset. With the telescope steady the twinkling was not obvious, but when the telescope was moved the star, as a result of persistence of vision, appeared as a streak of light. The streak was sometimes broken into fairly regular segments and sometimes was perceptibly wavy. It was probable that twinkling reduced the effective magnitude of the star.

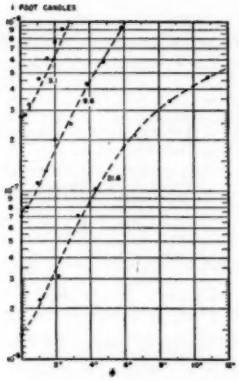

FIG. 4. Extra-foveal thresholds for three telescopes for $b=360$ ft.-c^{-2}.

Experiment showed that the use of a binocular telescope made finding stars a little easier than with a monocular instrument. It was soon found, by throwing one eyepiece of the binocular out of adjustment, that it made no difference whether both eyes actually saw the star. Further, it was observed, when, for example, the right eye was used for search, that the advantage of a binocular instrument was achieved by presenting to the left eye a false field, as by shining a flashlight into the left eye. It was found that the false field in the left eye made the pupil of the right eye contract about 0.5 mm from its value for the left eye in the dark. A satisfactory explanation of the advantage caused by the false field seemed to be that the diminished pupil diameter improved the definition of the telescope, especially off-axis, which more than offset the increase of threshold due to less light.

Some observations were made with a 20-power telescope from a small two-engined airplane at 10,000 feet. Venus and Jupiter were easily seen. Sirius, Arcturus, Vega, and Capella were observed a number of times, always at more than 25 times the threshold. But vibration of the aircraft and instability of the telescope made the work very difficult. A larger airplane would have been better, and would have made possible a better vibrationless mounting of both the telescope and the observer and more convenience in presetting the telescope than was feasible in the small airplane. There was found to be a region of optically disturbed air behind the wings in and near the propeller and exhaust stream through which observation of stars was impossible. However, no more will be said about this here, for the present paper is not concerned with the optical distractions in the vicinity of an airplane in flight.

EXTRA-FOVEAL VISUAL THRESHOLDS

A very noticeable feature about a star in the daytime was the fact that near threshold it was necessary to look almost exactly at it to see it. The effect was investigated in the laboratory by means of a movable fixation point and an artificial star in a field of brightness $b=360$ ft.-c^{-2}. The star was maintained on the axis of the telescope, and the threshold illumination i of the star was observed for various angles ϕ between the star and the fixation point or the fovea. The data for a single observer for three telescopes of magnifications 5.1, 9.6, and 21.6 are plotted as dots in Fig. 4, in which ϕ is the angle in the image space of the telescope. Since $d>p$

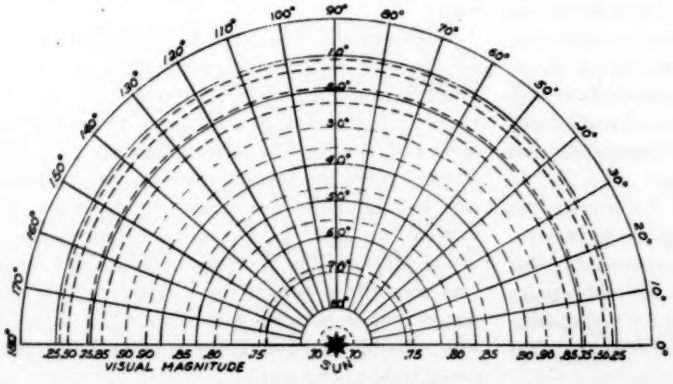

FIG. 5. Star visibility chart, 10,000 feet altitude of sun 90°.

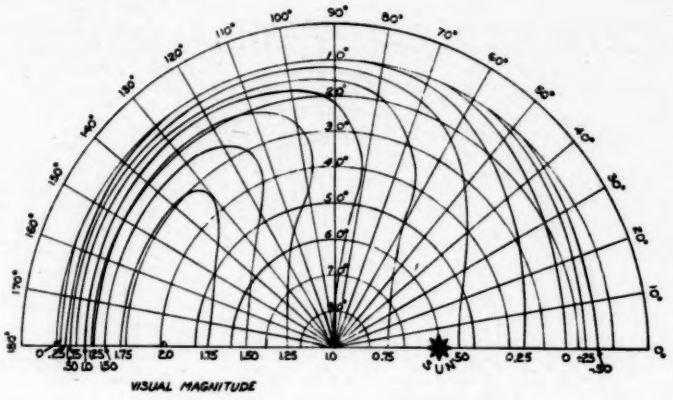

FIG. 6. Star visibility chart, 10,000 feet altitude of sun 60°.

for all the telescopes, the curves drawn through the dots were related to each other by (13), which states that the threshold is proportional to M^{-2}, and at $\phi=0$ passed through the threshold calculated from Table I and (7) and (8).

It is seen from Fig. 4 that increasing ϕ to about 2° increased the threshold about two times the value for $\phi=0$. Thus a star which was two times the foveal threshold would not be seen unless the eye were directed within less than 2° of it. The higher the magnification the wider the area over which the star could be seen and the easier it was to see the star in the area. Since the object space of a telescope is $1/M$ in linear dimensions of the image space, a star that can be seen over only a small area of the image space can be seen over an M times smaller area of the object space. This means that the telescope must be pointed very accurately at the star in order that the star be seen.

Furthermore, the definition of a telescope decreases with the distance from the axis, which causes an increase in the threshold of stars viewed foveally off-axis. In the case of two telescopes of very good quality, measurement showed that the stellar threshold was increased by factors of 2 and 3 for about 10° and 14° respectively, off-axis in the apparent field. This was true for a 10-power and a 20-power telescope. Since both extra-foveal and off-axis viewing occur in searching for a star and since both of these cause degradation of threshold, it is apparent that successful search for stars of brightness near the foveal on-axis threshold is difficult.

DESIGN OF TELESCOPE

From the foregoing considerations one may outline the important characteristics of the design of a telescope for the daylight observation of stars. Obviously, the definition over the entire

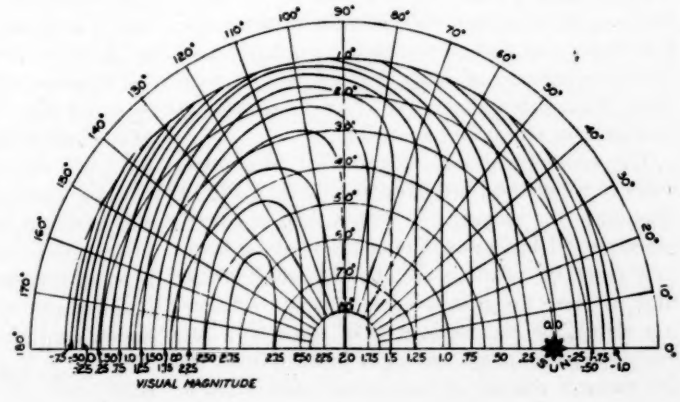

FIG. 7. Star visibility chart, 10,000 feet altitude of sun 30°.

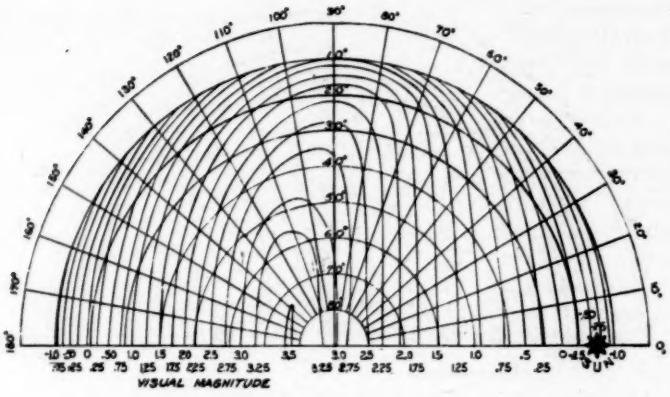

FIG. 8. Star visibility chart, 10,000 feet altitude of sun 15°.

field of the telescope must be as good as possible. High magnification is of great importance. The size of the exit pupil is not especially important. Therefore, if, as is usually the case, there is a size limitation of the telescope, it is better to increase the magnification until the exit pupil is 0.5 mm, or perhaps less, than to use less magnification and an appropriately larger exit pupil.

The choice of the size of the field of view, apart from optical design restrictions, depends on whether the telescope can be accurately preset and on whether it can be readily turned for search. If these things can be done a small field can be used; if not, the field should be as large as possible. In general, there is little advantage in increasing the field of view to the point of deterioration of image definition. Nor is there much advantage in increasing the magnification until the star is more than 10 times the threshold when viewed extra-foveally anywhere in the field. In such a case one would prefer to use a less magnification and thereby gain in useful true field. Vibration and atmospheric turbulence may limit the amount of magnification that can be used. The telescope and the observer should be as free from vibration as possible.

The telescope should be provided with cross wires or reticle and provision should be made to illuminate the unused eye with a field of about the same brightness as that of the working field. Low reflecting coatings are of small effect unless they increase the transmission greatly. A polarizer should be provided; it is of some aid, but not perhaps as much as might be supposed. In the areas of the sky of maximum polarization a perfectly efficient polarizer set for maximum darkening of the sky decreases the stellar threshold about 4 times; however, in many areas of the sky the polarization is such that the polarizer decreases the stellar threshold less than 2 times.

CHARTS OF STAR VISIBILITIES

By means of the threshold data and telescope formulas of the preceding paragraphs, together with the measurements and theory of an earlier paper[4] of the brightness and polarization of the sky at various altitudes above sea level, charts were prepared of the visibilities of stars of various magnitudes. The charts are given in Figs. 5 to 8; they refer to an observer at 10,000 feet using a telescope of 15 power, of $t=1$, and $d>p$, with a polarizer set to maximum darkening of the sky, to a "clear" sky overhead, and to a "working factor" of 7.

A "clear" sky is defined to be an atmosphere for which the attenuation coefficient $\beta=0.017$ km^{-1}, $e^{-\beta}$ being the fractional reduction per km of air at N.T.P. for collimated light of the spectral distribution of sunlight viewed with the light adapted eye. The "working factor" is the ratio of the stellar illumination to the threshold illumination in the telescope.

Each curve on the charts of Figs. 5 to 8 is the locus of points in the sky for which the illumination of the star of visual magnitude marked on the curve is 7 times the threshold illumination. On the side of the curve toward higher magnitudes (less bright stars) stars of the

[4] R. Tousey and E. O. Hulburt, J. Opt. Soc. Am. **37**, 78 (1947).

TABLE III. Correction for magnification of telescope; apply correction to star magnitude before using star visibility charts, Figs. 5 to 8.

Magnification	Correction
1	−5.9
2	−4.4
4	−2.9
6	−2.0
8	−1.4
10	−0.9
12	−0.5
15	0
20	0.6
25	1.1
30	1.5

TABLE IV. Correction for working factor; Apply correction to star magnitude before using star visibility charts, Figs. 5 to 8.

Working factor	Correction
1	−2.11
2	−1.36
4	−0.61
7	0
10	0.39
15	0.83
20	1.14
25	1.39
50	2.14
100	2.83

given magnitude will be increasingly easier to see; on the other side they will be increasingly difficult to see. For example, at Washington, D. C., at noon, December 1, 1941, the sun was at an altitude 29°. Vega, magnitude 0.1, was 99° from the sun in azimuth and was at altitude 66°. Spica, magnitude 1.2, was 52° from the sun in azimuth and was at altitude 23°. From Fig. 7 one finds that a star of magnitude 2.2 at the position of Vega should be visible, and hence one concludes that Vega should be easily seen. At the position of Spica, however, stars weaker than 0.35 magnitude are not visible (according to Fig. 7) and hence one concludes that Spica will be difficult or impossible to see.

The star charts were worked out as follows:

Let m be the visual magnitude of the star outside of the atmosphere. The illumination i_s footcandles at the telescope objective of the star at zenith angle ξ is given by

$$i_s = 10^{-6.555-0.4m} \exp(-(\beta\chi_1+\beta')\sec.\xi), \quad (21)$$

where $\beta=0.017$ km^{-1}, $\chi_1=5.5$ km is the vertical thickness of air above 10,000 feet reduced to N.T.P., and $\beta'=0.023$ is an average value of the visual attenuation of atmospheric ozone. The values of β and β' were those determined for the sun and are probably sufficiently correct for stars whose spectral distributions differ from that of the sun. For the sun $m=-26.72$ and the first factor of (22) gives $i_s=13{,}600$ ft.-c for the illumination of the sun outside the atmosphere. All of these numerical values are discussed in reference 4.

The values of the sky brightness B and the polarization γ as determined by an observer at 10,000 feet were listed in Table I, reference 4, for altitudes of the sun above the horizon from 15° to 90°. γ is the ratio of the sky brightness viewed through the polarizer in the position of maximum darkening to the brightness when the polarizer is at right angles to this position.

Assume that the telescope has no polarizing effects and let T be its transmission. Let the absorption of the polarizer, when set for maximum transmission of plane polarized light, be included in T. Hence, the polarizer reduces unpolarized light to $\frac{1}{2}$, and when set for maximum darkening of the sky reduces B to a brightness b, where

$$b = B\gamma/(1+\gamma). \quad (22)$$

A telescope is assumed of magnification M for which $d>p$; the starlight is assumed to be unpolarized. Then the values of i_a and b_a at the exit pupil of the telescope after passing through the polarizer are, from (7), (8), and (22),

$$i_a = 0.5TM^2i, \quad (23)$$

$$b_a = TB\gamma/(1+\gamma). \quad (24)$$

i_a is assumed to be at threshold and hence is related to b_a by the threshold equation (12) for point sources. From the definition of the working

TABLE V. Correction for transmission T of telescope and polarizer; apply correction to star magnitude before using star visibility charts, Figs. 5 to 8.

Transmission	Correction
1.0	0
0.8	−0.04
0.6	−0.09
0.4	−0.16
0.2	−0.28

TABLE VI. Correction for altitude above the surface; apply correction to star magnitude before using star visibility charts, Figs. 5 to 8.

Altitude feet	Correction
0	(−0.5)
5000	−0.3
10,000	0
15,000	0.4
20,000	0.6
25,000	0.8
30,000	1.0
35,000	1.3
40,000	1.6

factor f, one has

$$i_s = fi. \tag{25}$$

Solving (12), (21), (23)–(25) for m one obtains

$$m = E - F \sec.\xi - 2.10 \log_{10} B\gamma/(1+\gamma), \tag{26}$$

where

$$\left.\begin{aligned} E &= -17.140 - 2.5 \log_{10} k - 2.5 \log_{10} f \\ &\quad + 0.4 \log_{10} T + 5 \log_{10} M, \\ F &= 1.087(\beta\chi_1 + \beta'). \end{aligned}\right\} \tag{27}$$

With $M=15$, $T=1$, and $f=7$, m was calculated from (26) for a specified place in the sky and altitude of the sun. From this the charts of Figs. 5 to 8 were prepared by finding for each altitude of the sun and for each m the locus of points on the celestial sphere for which the stellar illumination was 7 times the threshold. The charts were drawn with sufficient care to be correct within about 0.15 of m.

An interesting table of threshold stellar magnitudes in the zenith daylight sky for an observer at sea level with unaided eyes was prepared by Weaver[5] using the threshold data of Fig. 1 and an equation similar to (21) with suitable constants and values of sky brightness and atmospheric transmission. Weaver found that for the sun above 15° above the horizon the star must be brighter than $m=-2.1$ to be visible, and therefore concluded that since the brightest star is Sirius of magnitude −1.6, no star may be seen from sea level during daylight hours without optical aid, except perhaps in very unusual circumstances.

In order that the star visibility charts may be applied to cases other than those for which they were drawn up, Tables III–VI were calculated, which give corrections to be added to m before referring to the chart. Table III is for telescopes of magnification other than 15, for which $t=1$ and $d>p$. Table IV is for working factors other than 7, and Table V for telescope and polarizer transmissions T other than 1. Table VI, for altitudes of the observer other than 10,000 feet, is based on the approximate relation that the sky brightness is proportional to the atmospheric pressure and that the polarization is independent of the pressure. The approximations are tolerable, and have some experimental support (see reference 4), as long as the air is very clear and β not far from 0.017, but become unsatisfactory for usual conditions at the surface or sea level where due to normal slight haze β usually exceeds 0.05. Hence, the correction for zero altitude should generally be much greater than −0.5, and especially so for stars near the sun because of the rapid increase of the brightness of the sky as the sun is approached due to the forward scattering of haze. Further, the sky brightness is probably greater and the polarization less (see Table IV, reference 4) when there are white clouds or a snow-covered surface below the observer than when there are dark areas beneath him, as forests or the sea. Thus the stellar thresholds are somewhat dependent on the cloud and surface conditions. When used for the planets the charts require correction because of the size of the planet disk; for M less than 30 the corrections are less than 2 stellar magnitudes.

[5] H. F. Weaver, Pub. Ast. Soc. Pac. **59**, 232 (1947).